Diffusion and Equilibrium Measurements in Polymer-Solvent Systems by Inverse Gas Chromatography Method

By

Hülya ESER

A Dissertation Submitted to the Graduate School in Partial Fulfillment of the Requirement for the Degree of

MASTER OF SCIENCE

Department: Chemical Engineering
Major: Chemical Engineering

İzmir Institute of Technology
İzmir, Turkey

July,2004

We approve the thesis of **Hülya ESER**

Date of Signature

..... **20.07.2004**

Assoc.Prof.Dr. Funda TIHMINLIOĞLU
Supervisor

Department of Chemical Engineering

..... **20.07.2004**

Prof. Dr. Devrim BALKÖSE
Department of Chemical Engineering

..... **20.07.2004**

Prof. Dr. Tamerkan ÖZGEN

Department of Chemistry

..... **20.07.2004**

Prof. Dr. Devrim BALKÖSE

Head of Department

ACKNOWLEDGEMENTS

I would like to thank to my thesis advisor Assoc. Prof. Funda Tıhmınlıoğlu for her guidance, encouragement and criticism throughout this work. I would also like to thank to Prof. Devrim Balköse and Prof. Tamerkan Özgen for the time spent serving as members of my thesis commette. The financial support of İzmir Institute of Technology Research Fund (2001 Eng 15) is gratefully acknowledged.

I extend special thanks to Serdar Öztürk for his support, patience and comfort. I present my thanks to Nesrin Tatlıdil and Güler Narin for their valuable discussions and suggestions concerning gas chromatography.

I would like to thank to my friends Sevdiye Atakul, Ayben Top, Dildare Metin, Yılmaz Yürekli, Murat Molva and Tülin Burhanoğlu for their friendship, encouragement and valuable suggestions. Finally, my thanks go to my family for their support and appreciation during this study.

ABSTRACT

In this study, thermodynamic properties, namely retention volume, infinitely dilute weight fraction activity coefficient, Flory- Huggins interaction parameter, solubility parameters of solute and polymer, partition coefficient and diffusion coefficients of the various solvents in poly (methyl methacrylate co butyl methacrylate) (PMMA co BMA) and poly (lactide co glycolide) (PLGA) at infinite dilution of the solvent have been determined by inverse gas chromatography (IGC). In this technique, a small amount of the solvent was injected into the capillary column and its retention time was measured and used to calculate several polymer-solvent interaction parameters which are mentioned above. The solutes used in this study were methanol, ethanol, propanol, butanol, methyl acetate, ethyl acetate, propyl acetate, dichloromethane, trichloromethane, acetone, methyl methacrylate, butyl methacrylate, water for PMMA co BMA and acetone, dichloromethane, trichloromethane, ethyl acetate, ethyl alcohol, tetrahydrofuran, water for PLGA.

The glass transition temperature of the polymers were determined as 106 ^{0}C and 42 ^{0}C for PMMA co BMA and PLGA respectively by differential scanning calorimetry. Experiments were performed in the range of 150-200 ^{0}C for PMMA co BMA and 80-120 ^{0}C for PLGA which are above the glass transition temperature of the polymer.

The thermodynamic results, obtained from the experiments, indicated that trichloromethane and dichloromethane were the most suitable solutes among all the solvents studied for both of the polymers. The partition (K) and diffusion coefficients (D_p) of various solvents at infinite dilution of the solvent were calculated by using the model developed by Pawlisch et al. (1987). The optimum K and D_p values that best fit the data were found and the model predicted experimental data very well. In summary, IGC method is a powerful tool for the determination of thermodynamic and diffusion properties of solvent in polymer at infinite dilution of the solvent. Vrentas- Duda free volume theory was used to correlate the diffusion data and to investigate the effect of solvent size on diffusion process. The theory has shown to correlate diffusion data above the glass transition temperature very well for the PMMA-co-BMA –solvent system.

ÖZ

Bu çalışmada, değişik çözeltilerin poli (metil metakrilat ko bütil metakrilat) (PMMA ko BMA) ve (poli laktid ko glikolid) (PLGA) içindeki termodinamik özellikleri (kalış hacmi, ihmal edilebilecek çözücü konsantrasyonda ağırlık kesri aktivasyon katsayısı, Flory Huggins parametresi, çözücünün ve polimerin çözünürlük parametreleri), çözünürlük katsayısı ve difüzyon katsayısı, çok düşük konsantrasyonda (ihmal edilebilecek düzeyde) ters gaz kromatografisi metoduyla hesaplanmıştır. Çok az miktarda çözücü kolona enjekte edilir ve bu çözücünün çıkış zamanından yaralanarak yukarıdaki parametreler hesaplanır. Bu çalışmada PMMA ko BMA kolonu için metanol, etanol, propanol, butanol, metil asetat, etil asetat, propil asetat, diklorometan, triklorometan, aseton, metil metakrilat, bütil metakrilat, su ve PLGA kolonu için aseton, diklorometan, triklorometan, etil asetat, etil alkol, tetrahydrofuran, su kullanılmıştır.

Polimerlerin camsı geçiş sıcaklığı termal analiz metoduyla PMMA ko BMA için 106 ^{0}C ve PLGA için 42 ^{0}C olarak belirlenmiştir. Bu nedenle çalışma PMMA ko BMA için 150-200 ^{0}C, PLGA için 80-120 ^{0}C sıcaklık aralığında gerçekleştirilmiştir.

Deneylerden elde edilen termodinamik sonuçlar triklorometanın ve diklorometanın her iki polimer için de en uygun çözücüler olduğunu göstermiştir. Çözünürlük (K) ve difüzyon (D_p) katsayıları ihmal edilebilecek çözücü konsantrasyonunda Pawlisch ve ark. (1987) tarafından geliştirilen kapiler kolon ters gaz kromatografisi modeli kullanılarak bulunmuştur. Modeli en iyi fit eden K ve D_p değerleri regresyonla hesaplanmış ve modelin deneysel verilerle uyum içerisinde olduğu gözlemlenmiştir.Kısaca, ters gaz kromatografisi metodunun çözücülerin polimer içindeki termodinamik ve difüzyon özelliklerinin hesaplanması için uygun bir metot olduğu belirlenmiştir. PMMA co BMA kolonu için difüzyon katsayılarının Vrentas ve Duda tarafından geliştirilen free volume teorisiyle korelasyonu gerçekleştirilmiş ve modelin iyi sonuç verdiği saptanmıştır.

TABLE OF CONTENTS

LIST OF FIGURES

LIST OF TABLES

CHAPTER 1

INTRODUCTION

Molecular diffusion of solvents and monomers is important and finds wide range of applications in many areas. These areas include solvent devolatilization, residual monomer stripping, packaging, polymer synthesis, drying of paints and coating processes. These processes rely on transport and thermodynamic data of the polymer solvent system. Various techniques exist to measure these data, including gravimetric sorption, piezoelectric sorption, nuclear magnetic resonance, light scattering and inverse gas chromatography.

Conventional methods like gravimetric sorption rely on bulk equilibration and hence it is slow. Also, these methods are difficult to apply when the solute is present in small amount (ie. at infinite dilution of solvent). So, inverse gas chromatography method is being introduced. It is a fast, simple, accurate and reliable technique, feasible to measure small diffusion coefficients, can be applied both above and below glass transition temperature. Also, the changes in the solute and the temperature can be made readily in a chromatographic experiment. By this method, many parameters like solubility parameters, interaction parameters, degrees of crystallinity, enthalpies of mixing, partition coefficient, diffusion constants can be determined.

Inverse gas chromatography (IGC) is an extension of conventional gas chromatography in which a non-volatile material to be investigated is immobilized within a gas chromatographic column. The term “inverse “ indicates that the stationary phase is under investigation in contrast to conventional gas chromatography. (Kaya et al., 1999) This stationary phase is then characterized by monitoring the passage of volatile probe molecules of known properties as they are carried through the column via an inert gas. While IGC was initially used only in the study of synthetic polymers, today it is used to study of synthetic and biological polymers, copolymers, polymer blends, glass and carbon fibers, coal and solid foods. (Schreiber et al.,1989)

IGC method has been used to determine the diffusion coefficient of solvent in polymers by many researchers using both packed and capillary column chromatography. Packed column models, firstly derived by Gray and Guillet (1973), had disadvantage of having a nonuniform distribution of the polymer. This resulted the

higher diffusion coefficients by almost 2 orders of magnitude than those expected. (Romdhane, 1995). Therefore, the reliability of the calculated diffusivities was clouded by the nonuniformity in the packed column. So; capillary column models were introduced to overcome this problem.. Modeling capillary column chromatography is a well-developed subject, because the simple geometry frequently leads to models described by analytical solutions. (Pawlisch et al., 1987)

The early capillary column models were developed by Golay et al. (1958), Aris et al. (1959) and Khan et al. (1962), taking into account that dispersion occured as a result of coupling between radial diffusion and axial convection in gas phase including mathematical complexity in the resulting differential equations. Edwards and Newman (1977) presented a model that neglects the gas phase transport processes. But they didn't generate moment equations. Noting that further simlifications to the model can be achieved for certain applications, Macris et al. (1979) had developed a model and this model had been improved by Pawlisch et al. (1985). All these models were developed for infinitely dilute case of the solvent. Tıhmınlıoğlu et al. (1998) had derived a capillary column model to determine the diffusion coefficient of solvent for the finite concentration range of the solvent.

The objective of this project is to investigate the equilibrium and diffusion behavior of two polymer solvent systems. In this work, the polymers under investigation include poly (D-L-lactide-co-glycolide) and (poly methyl methacrylate-co-butyl methacrylate). These polymers were coated on the fused silica capillary columns by the static coating technique. Several solvents at different temperatures were used to obtain thermodynamic and diffusion data at infinite dilute case of the solvent. Diffusion coefficients were obtained by the model developed by Pawlisch et. al (1987). Vrentas-Duda free volume diffusion theory was used to correlate the diffusion data and to test its ability to account for the temperature and solvent effects.

The thesis is organized in the following way: Chapter 2 includes the background and modeling of inverse gas chromatography, Chapter 3 deals with background on Vrentas-Duda free volume diffusion theory. Chapter 4 presents the experimental methods & procedure used in this study. In chapter 5 thermodynamic results for two polymer-solvent sytems, the results of diffusion coefficients obtained by capillary column inverse gas chromatography model and also the free volume correlation of the diffusion data are presented. Finally, Chapter 6 provides conclusions and future work.

CHAPTER 2

THE THEORY AND MODELING OF INVERSE GAS CHROMATOGRAPHY

2.1 Background

Chromatography is a separation technique in which the separation of compounds is based on the partition or distribution of the analytes between two phases in a dynamic system.

Modern chromatography has developed almost entirely during the past fifty years and now widely employed for both qualitative and quantitative analysis in virtually every chemical field. Of all of the chromatographic techniques, gas chromatography is the most powerful with regard to its ability to separate very complex mixtures. (Grant, 1995)

Inverse gas chromatography is an extension of conventional gas chromatography in which the species of interest is the stationary phase in contrast to conventional gas chromatography, where the stationary phase is of interest only as far as its ability to separate the injected compounds concerned. (Etxeberria,1992)

Dozens of detectors have been investigated and used during the development of gas chromatography. The most widely used detectors are flame ionization detector (FID), thermal conductivity detector (TCD), electron capture detector (ECD).

The flame ionization detector (FID) is one of the most widely used and generally applicable one. The effluent from the column is mixed with hydrogen and air and then ignited electrically. It is a mass flow sensitive device. The flame ionization detector exhibits high sensitivity, large linear response range and low noise. A disadvantage of the FID is that the destructive of the sample.

Thermal conductivity detector (TCD) is an early detector for gas chromatography, is based upon the changes in the thermal conductivity of the gas stream. The advantage of the thermal conductivity detector is its simplicity, its large linear dynamic range, its general response to both organic and inorganic species, and its

nondestructive character. A disadvantage of this detector type is its relatively low sensitivity.

Electron capture detector (ECD) operates in much the same way as a proportional counter for measurement of X-radiation. The ECD is selective in its response, being highly sensitive toward molecules that contain electronegative functional groups such as halogens, peroxides, quinones, and nitro groups. It is insensitive toward functional groups such as amines, alcohols, and hydrocarbons. ECD detectors are highly sensitive and possess the advantage of not altering the sample significantly. On the other hand, their linear response range is usually limited to about two orders of magnitude.

Gas chromatographs require a supply of carrier gas of sufficient quality and pressure to achieve the desired separations. Carrier gases, usually nitrogen, helium or hydrogen are normally supplied from compressed gas cylinders. Carrier gas should be inert, dry and free of oxygen to prevent degradation of the column. (Skoog, 1991)

Inverse gas chromatography is based on the characteristic equilibrium partitioning of a solute between a mobile phase and a stationary phase. As a solute sample passes through the column via an inert gas, resistances occur. Most important resistances are;

i. The longitudinal diffusion in the gas phase
ii. The mass transfer resistance in the polymeric stationary phase

The longitudinal diffusion occurs because solute molecules tend to move from center of the band to the edges. Since the equilibrium of the solute between the stationary and mobile phase can not be reached instantaneously, mass transfer resistance in the polymeric stationary phase results. Due to the mass transfer resistance in the polymer phase, the material in the mobile phase is swept forward while that in the stationary phase lags behind. The output elution profile of the peak from the gas chromatogram gives the solubility or the partition coefficient and the diffusion coefficient for a polymer solvent system. The outlet elution profile can be used to determine the thermodynamic and transport properties of the system. (Surana et. al,1997 ;Tıhmınlıoğlu , 1998)

IGC is a fast, reliable, accurate simple and available technique which can measure the diffusion coefficients as small as 10^{-13} cm^2/sec.(Huang et. al, 2001 ; Tıhmınlıoğlu et. al,1997 ; Zhao et. al, 2001)

2.2 Thermodynamic Properties

Inverse gas chromatography is a useful method in the study of some of the thermodynamic properties of polymers. Only peak retention time data are needed. Retention time is generally expressed as retention volume (V_g^0)

2.2.1 Retention Volume (V_g^0)

The knowledge of the retention volume due to the dissolution of a substance makes it possible to calculate relevant thermodynamic characteristics of the solution process, namely the partition coefficient, the activity coefficient and the change in the excess partial molar thermodynamic functions of the solute in the given stationary phase.

A plot of the logarithm of the specific retention volume, ln V_g^0, versus reciprocal of absolute temperature, 1/T is linear when the polymer is either glassy or amorphous. Such a plot is called retention diagram and a typical one was shown in Figure 2.1. At temperatures below T_1, retention proceeds by surface adsorption and the corresponding retention diagram is linear. The probe interacts only with the surface because the rate of diffusion of the probe throgh the polymer is too slow to permit significant bulk interaction. Penetration of the solute into the bulk of the polymer begins at the first deviation (T_1) from the linear plot. In IGC studies, T_1 is commonly identified with the glass transition temperature of the polymer, T_g. The region between T_1 and T_2 is called the non-equilibrium region due to the very slow rate of diffusion of the solute into and out of the stationary phase. Both factors contribute to retention. As T increases, the increasing penetrability outweights the effects of increasing vapour pressure, so that retention volume increase with increasing temperature in this region. At T_2, bulk-sorption equilibrium is established and the retention diagram becomes linear at temperatures above T_2 indicating absorption by the bulk polymer. (Romdhane, 1990; Etxeberria et al.,1992) Braun and Guillet stipulate that equilibrium bulk sorption is achieved at least at T_g+50 ^{0}C for most polymers. Linear retention diagram should assume the bulk sorption equilibrium in the column in the above temperature range, that is a fulfilment of the precondition for thermodynamic measurements. (Tyagi et al ,1987)

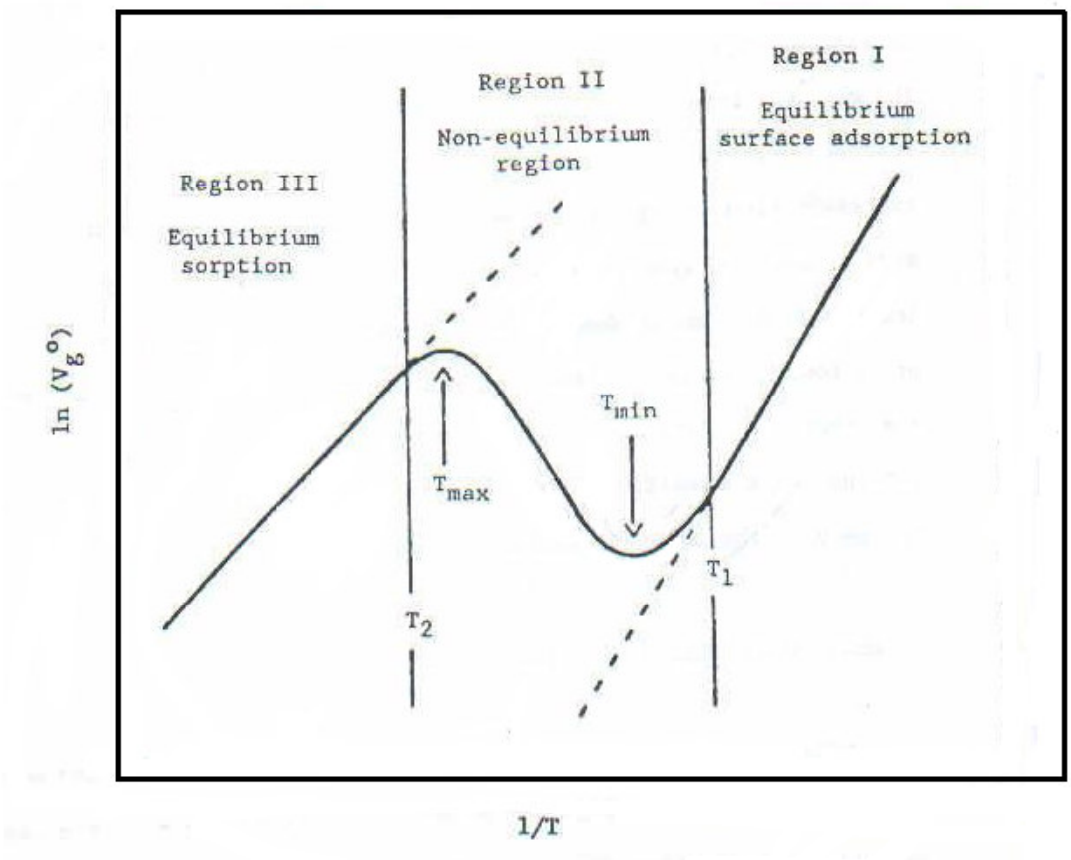

Figure 2.1. Typical retention diagram of polymer stationary phases (Romdhane,1990)

Specific retention volume at 0 ^{0}C (V_g^0) is (Laub and Pecsok, 1978):

$$V_g^{\,0} = \frac{273.2}{T}\left(\frac{V_N}{w_2}\right) = \frac{273.2}{Tw_2}(t_r - t_c)FJ \qquad (2.1)$$

where V_N is the net retention volume at temperature in K, w_2 is the mass of polymer, t_r and t_c are the retention times of solute and marker gas, F is the flow rate of gas and J is the pressure drop correction factor which is negligible for capillary columns.

The specific retention volume is related to the partition coefficient by (Laub and Pecsok,1978):

$$V_g^{\,0} = \frac{273.2}{T}\frac{K}{\rho_p} \qquad (2.2)$$

K is the partition coefficient (ratio of the concentration of solvent in the polymer phase to the concentration of solvent in the gas phase), T is the column temperature and ρ_p is the density of the polymer.

2.2.2 Weight Fraction Activity Coefficient (Ω_1^∞)

The weight fraction activity coefficient may be written as; (Braun and Guillet,1976)

$$\Omega_1^\infty = \frac{RT}{P_1^s V_g^0 M_1} \exp\left(- P_1^s \frac{(B_{11} - V_1)}{RT} \right) \tag{2.3}$$

where Ω_1^∞ is the infinite dilution activity coefficient, R is the ideal constant, T is the system pressure, M_1 is the molecular weight of the solute, B_{11} is the second virial coefficient of the solute, V_1 molar volume and P_1 is the vapor pressure of the solute.

Ω_1^∞ gives an idea of the polymer- solvent compatibility indicating that;

Ω_1^∞<5 good solvents

5<Ω_1^∞<10 moderate solvents

Ω_1^∞>10 bad solvents (Kaya et. al,1999)

2.2.3. Flory Huggins Interaction Parameter (χ)

Flory Huggins interaction parameter (χ) which was used as a measure of the strength of interaction, and therefore as a guide in the prediction of polymer solvent compatibility is ralated to the weight fraction activity coefficient by the following equation; (Gray,1977)

$$\chi = \ln \Omega_1^\infty - \left(1 - \frac{1}{r}\right) + \ln \frac{\rho_1}{\rho_2} \tag{2.4}$$

where r is referred to as number of segments in polymer chain and given as;

$$r = \frac{\rho_1 * M_2}{\rho_2 * M_1} \tag{2.5}$$

Here, ρ_i is the density and M_i is the molecular weight of component i.

The values of χ greater than 0.5 represent unfavourable polymer- solvent interactions, while the values lower than 0.5 indicate favourable interactions. (Demirelli,2001)

2.2.4 Solubility Parameters

The solubility parameter for the volatile solvent (δ_1) and the relation between the polymer solubility parameter (δ_2) is as follows; (Romdhane,1990)

$$\delta_1 = \left[\frac{\Delta H_v - RT}{V_1} \right]^{\frac{1}{2}} \tag{2.6}$$

$$\left(\frac{\delta_1^2}{RT} - \frac{\chi}{V_1} \right) = \frac{2\delta_2^{\infty}}{RT} \delta_1 - \left(\frac{\delta_2^{\infty 2}}{RT} + \frac{\chi}{V_1} \right) \tag{2.7}$$

After χ, $V_1$and δ_1 are known,the polymer solubility parameter at infinite dilution (δ_2^{∞}) can be determined graphically by using the combination of Hildebrand Scatchard and Flory Huggins Eqn. (Romdhane,1999). According to Eqn (2.7.), δ_2^{∞} can be found by drawing, a plot of (δ_1^2/(RT)- χ/V_1) versus δ_1 should yield a straight line with $2\delta_2^{\infty}$/(RT) as the slope and $-(\delta_2^{\infty 2}$/(RT)+ χ/V_1) as the intercept.

2.3 Chromatographic Models

Various mathematical models have been developed by many researchers in order to determine diffusion coefficients for both packed and capillary columns.

2.3.1 Packed column inverse gas chromatography

Gray and Guillet (1973) were the first researchers that used packed column inverse gas chromatography to determine diffusion coefficients of some hydrocarbon penetrants in low-density polyethylene (LDPE). In all of the previous studies, Van Deemter approach was used to obtain diffusion coefficients for packed column IGC.
The general form of Van Deemter model can be represented by;

$$H = A + \frac{B}{V} + CV \tag{2.8}$$

where H is the height equivalent to a theoretical plate and V is the mean velocity of the carrier gas. A, B, C are the constants which represent the contributions of eddy diffusion, gas, -phase molecular diffusion, and stationary phase mass-transfer resistances toward broadening of the peak.

The Van Deemter model is applicable only if the elution profiles are symmetric (Gaussian). In reality, the distribution of the polymer will not be uniform.

So, Romdhane et. al proposed a new mathematical model and developed a moment analysis procedure to analyze the chromatographic peaks eluting from a packed column.

They derived the solvent diffusion equation as;

$$\frac{H_{eff}}{v} = C_p \frac{j}{f} + C_{g0} \tag{2.9}$$

v is the average linear velocity of the carrier gas, C_p and C_{g0} are the resistance to mass transfer in the polymer and the gas phase respectively, j is the James Martin compressibility factor and f is the compressibility factor of Giddings.

$$j = \frac{3\left[\left(\frac{P_i}{P_o}\right)^2 - 1\right]}{2\left[\left(\frac{P_i}{P_o}\right)^3 - 1\right]} \tag{2.10}$$

$$f = \frac{9\left[\left(\frac{P_i}{P_o}\right)^4 - 1\right]\left[\left(\frac{P_i}{P_o}\right)^2 - 1\right]}{8\left[\left(\frac{P_i}{P_o}\right)^3 - 1\right]^2} \tag{2.11}$$

where P_i and P_o are the inlet and outlet pressures of the column respectively.

$$H_{eff} = L\frac{\mu_2^*}{\mu_1^*}\frac{j}{f} - A_j - \frac{B_0}{v}\,j^2 \tag{2.12}$$

A is the multi-path factor; B_0 is the longitudinal diffusion term, L is the length of the column, μ_1 and μ^*_2 are the first temporal moment and the central second moment of the elution curves, respectively, which are defined as;

$$\mu_1 = \frac{\int_0^\infty tC(t)dt}{\int_0^\infty C(t)dt} \tag{2.13}$$

$$\mu_2^* = \frac{\int_0^\infty (t-\mu_1)^2 C(t)dt}{\int_0^\infty C(t)dt} \tag{2.14}$$

C (t) is the eluting concentration of solvent at the moment of t. The values of μ_1 and μ^*_2 at different temperatures and velocities of the carrier gas can be obtained by numerical integration of the data of the elution curves according to the above equations.

As shown in Eq 2.9 the plot of H_{eff}/v versus j/f should yield a straight line with a slope of C_p and an intercept C_{g0}. According to the definitions of Cp and Cg_0,

$$C_p = \frac{2}{3}\frac{k}{(1+k)^2}\frac{d_f^2}{D_p} \tag{2.15}$$

$$C_{g0} = \frac{2}{3}\frac{k}{(1+k)^2}\frac{KR_p}{k_{f0}}\left(\frac{R_p^3 - R_s^3}{R_p^3}\right) \tag{2.16}$$

If the capacity ratio k and the film thickness d_f are determined, the diffusion coefficient of solvent in polymer D_p will be obtained from C_p.

The major disadvantage of the packed column is the difficulty to achieve a uniform polymer film thickness. So, capillary columns are introduced. Since, there is no packing inside the column, stationary phase is coated around the inner wall of the capillary, more uniform polymer thickness can be obtained.

2.3.2 Capillary Column Inverse Gas Chromatography

Early capillary column models, which were developed by Golay, Aris and Khan evolve from the pioneer work of Taylor. He treated the problem of the dispersion in early capillaries. Golay (19589 has considered the effect of solute sorption on dispersion but he used a simplified description of the transport of solute in the stationary phase. Axis (1959) has treated the stationary-phase transport processes in a more rigorous fashion but his method requires numerical solution. Khan's (1962) model leads to temporal moments. He also obtained the Laplace transform of the solution.

Edwards and Newman (1972) presented plug-flow model, which neglects the gas phase transport processes. They examined the effect that increasing stationary-phase transport resistance has upon the shift in the time of peak maximum with respect to the mean residence time of the sample. Although they use Laplace transform to solve the

governing differential equations, they do not generate the moment equations in their analysis. Afterwards, Macris introduced (1979) further simplifications to their model and presented a plug-flow model in which curvature of the polymer coating and axial transport in the stationary phase were neglected. Then Pawlisch (1985) has used this model and developed this model for nonuniform coatings. All these models were developed for infinitely dilute region. In 1998, Tıhmınlıoğlu has introduced a capillary column inverse gas chromatography model for the finite concentration range of the solvent.

In this project, the model developed by Pawlisch et. al (1985) was used for infinitely dilute region.

The capillary column is modeled as straight cylindrical tube with a polymer film deposited on the wall. The following initial assumptions were made;

1) The system is isothermal.
2) The carrier gas is an incompressible fluid.
3) The carrier flow is steady laminar flow.
4) The polymer stationary phase is homogeneous.
5) The polymer film is constant in thickness.
6) The polymer film thickness is much less than the radius of the column.
7) Axial diffusion in the stationary phase is negligible.
8) The carrier gas is insoluble in the polymer.
9) The absorption isotherm is linear.
10) No surface adsorption occurs at the polymer-gas interface or the polymer-column interface.
11) No chemical reaction occurs between the sample gas and the polymer.
12) Diffusion coefficients are concentration independent.
13) The injected sample enters the column as a narrow pulse so that the inlet concentration profile can be modeled as an impulse function.

With these assumptions, the continuity equations for the gas and polymer phase can be written as;

Gas phase:

$$\frac{\partial C}{\partial t} + 2u\ (1 - r/R)^2 \frac{\partial C}{\partial z} = D_g \frac{1}{r}\frac{\partial}{\partial r} r \frac{\partial C}{\partial r} + \frac{\partial^2 C}{\partial z^2} \tag{2.17}$$

Polymer phase:

$$\frac{\partial C'}{\partial t} = D_p \frac{1}{r}\frac{\partial}{\partial r} r \frac{\partial C'}{\partial r} \tag{2.18}$$

where C and C' are the gas and stationary phase solute concentrations, D_g and D_p are the gas and stationary phase diffusion coefficients for the solute, z and r are the axial and radial coordinates, u, is the mean velocity of the carrier gas. Appropriate initial and boundary conditions are;

$$C(r,z,t) = C'(r,z,t) = 0 \qquad \text{at t} = 0 \ \ z > 0 \tag{2.19}$$

$$C(r,z,t) = \delta(t) C_0 \qquad \text{at z} = 0 \tag{2.20}$$

$$C(r,z,t) = C'(r,z,t)/K \qquad \text{at r} = \text{R} \tag{2.21}$$

$$D_g\left(\frac{\partial C}{\partial r}\right) = D_p\left(\frac{\partial C'}{\partial r}\right) \qquad \text{at r} = \text{R} \tag{2.22}$$

$$\frac{\partial C}{\partial r} = 0 \qquad \text{at r} = 0 \tag{2.23}$$

$$\frac{\partial C'}{\partial r} = 0 \qquad \text{at r} = R + \tau \tag{2.24}$$

$\delta(t)$ is the Dirac delta function, C_0 is the strength of the inlet pulse, K is the partition coefficient, R is the radius of the gas polymer interface, and τ is the thickness of the polymer film.

The solution of this model at the exit of the column in the dimensionless Laplace domain is:

$$\frac{CL}{C_0 u} = \exp\left(\frac{1}{2\Gamma}\right)\exp\left[\left(\frac{1}{4\Gamma^2}+\frac{s}{\Gamma}+\frac{2\sqrt{s}}{\alpha\beta\Gamma}\tanh\beta\sqrt{s}\right)^{\frac{1}{2}}\right] \tag{2.25}$$

$$\alpha = \frac{R}{K\tau} \qquad \Gamma = \frac{D_g}{uL} \qquad \beta^2 = \frac{\tau^2 u}{D_p L} \tag{2.26}$$

where C is the outlet concentration of the solute in the gas phase, t_c=L/u, the residence time of the carrier gas, L is the length of the column, τ is the thickness of the polymer film, s is the Laplace operator, α is a thermodynamic parameter where as Γ and β represent the gas and the polymer phase transport properties.

2.4 Evaluation of the Model Parameters

Methods to obtain model parameters are developed and they divide into four main categories, moment fitting, Laplace domain fitting, Fourier domain fitting and time domain fitting.

In this project, time domain fitting method is chosen since it is a direct and reliable method.

2.4.1 Time Domain Fitting Method

Moment generating properties of Laplace transforms can be used to obtain analytical information on the concentration distribution.

$$\mu_k = \left(\frac{L}{V}\right)^k (-1)^k \lim_{s\to\infty}\frac{d^k Y(s)}{ds^k} \tag{2.27}$$

where

$$\mu_k = \frac{\int_0^\infty t^k c(t)dt}{\int_0^\infty c(t)dt} \tag{2.28}$$

$$Y(s) = \exp\left(\frac{1}{2\Gamma}\right)\exp\left[-\left(\frac{1}{2\Gamma}\right)(1+4\psi(s))^{1/2}\right] \tag{2.29}$$

Central moments, usually defined as higher moments than the first, can be calculated using the normalized moments.

The k th central moment is;

$$\mu_k = \frac{\int_0^\infty (t-\mu_1)c(t)dt}{\int_0^\infty c(t)dt} \tag{2.30}$$

By solving these equations;

$$\mu_1 = t_c\left(1+\frac{2\tau}{R}k\right) \tag{2.31}$$

$$\mu_2^* = t_c^2\left[\frac{4\tau^3 K}{3t_c D_p R} + \frac{2D_g}{uL}\left(1+\frac{2\tau}{R}k\right)^2\right] \tag{2.32}$$

μ_1 is the first temporal moment and μ_2 is the second central moment. The first moment depends only on the thermodynamic properties where as second moment depends both on thermodynamic and transport properties of the polymer solvent system.

To obtain the model parameters, the elution curve is integrated numerically to determine first and second moments. Then, these moments are used as initial estimates of partition and diffusion coefficients. By these initial estimates, Laplace transform eqn was then numerically inverted using an algorithm. Experimental data is regressed by the CCIGC model to obtain K and D which best characterize the experimental elution curve.

CHAPTER 3

FREE VOLUME THEORY

3.1 Free Volume Concept

Molecular transport by free volume was first introduced by Cohen and Turnbull (1959). According to their perspective, the hard sphere molecules which constitute an idealized liquid exist in cavities (cages) formed by nearest neighbors. Thus, the total volume of the liquid, therefore, could be divided into two components: occupied volume and free volume. Each sphere was presumed incapable of migration until natural fluctuations caused a hole (or vacancy) to form adjacent to its cage. The hole had to be sufficiently large to permit a significant displacement of a spherical molecule. A single step of the diffusional transport mechanism was successfully completed when the cavity a molecule left behind was occupied by a neighboring molecule. Translational motion, according to Cohen and Turnbull, did not require a molecule to attain a prerequisite energy level to overcome an activation energy barrier. Rather than creating holes by physically displacing nearest neighbors, as suggested by the activation energy approach, molecular transport was presumed to rely on the continuous redistribution of free-volume elements within the liquid. (Duda,1985)

In this manner, two criteria must be satisfied; i) a sufficiently large hole opens up next to the molecule due to a fluctuation in local density and ii) the molecule has sufficient energy to break away from its neighbors. The diffusional transport will be completed only if another molecule jumps into the hole before the next molecule returns to its initial position.

This model provides a relationship between the system free volume and the self-diffusion coefficient, D_1, for a one component liquid. This relation can be extended to describe self-diffusion of a single species in a binary mixture:

$$D_1 = D_{01} \exp\left[\frac{-\gamma \bar{V}^*}{\bar{V}_{FH}}\right] \tag{3.1}$$

V_1 is the critical molar free volume required for a jumping unit of species 1 to migrate, and V_{FH} is the free volume per mole of all individual jumping units.

In solutions of real molecules, particularly in mixtures of macromolecules, however, an individual molecule can be comprised of multiple jumping units, each covalently bonded together. Free volume holes that readily accommodate entire polymer molecules simply do not form. Instead, polymer chain migration is envisioned to result from numerous jumps of small segments along the polymer chain. To complicate matters further, low molecular weight molecules of sufficient size and flexibility are also capable of migrating by a mode, reminiscent of polymers, which involves coordinated motion between several parts of the molecule. To generalize the Cohen and Turnbull theory to describe motion in binary liquids, Vrentas and Duda used the following relationship,

$$\bar{V}_{FH} = \frac{\hat{V}_{FH}}{\left(\frac{\text{moles of jumping units}}{\text{g}}\right)} = \frac{\hat{V}_{FH}}{\left[\frac{w_1}{M_{1j}} + \frac{w_2}{M_{2j}}\right]} \tag{3.2}$$

where V_{FH} is the specific hole free volume of a liquid with a weight fraction, w_1, of species 1, and with jumping unit molecular weights of M_{1j} (ı=1 or 2)

Combining Eqns (3.1) and (3.2) results in an expression for solvent self diffusion in a polymer solution;

$$D_1 = D_{01} \exp\left[\frac{-\gamma(w_1 \hat{V}_1^* + w_2 \hat{V}_2^*)}{\hat{V}_{FH}}\right] \tag{3.3}$$

V_1 is the specific hole free volume of component 1 required for a diffusive step and

$$\varepsilon = \frac{\bar{V}_{1j}^* / \bar{V}_{2j}^*}{V_1^* M_1 / V_2^* M_2} \tag{3.4}$$

$$\hat{V}_{FH} = \hat{V}(T) - \hat{V}^0(0) \tag{3.5}$$

$\hat{V}(T)$ is the specific volume of an equilibrium liquid at any temperature T. $\hat{V}^0$ is the specific volume of the equilibrium liquid at 0 ^{0}K and can be estimated by the group contribution methods.

Vrentas and Duda divided free volume into two types as shown in Figure 3.1. One portion, redistribution energy and, thus, is not implicated in facilitating transport through the mixture. The remaining free volume, which is presumed to dictate molecular transport, is termed the hole free volume, and is redistributed effortlessly.

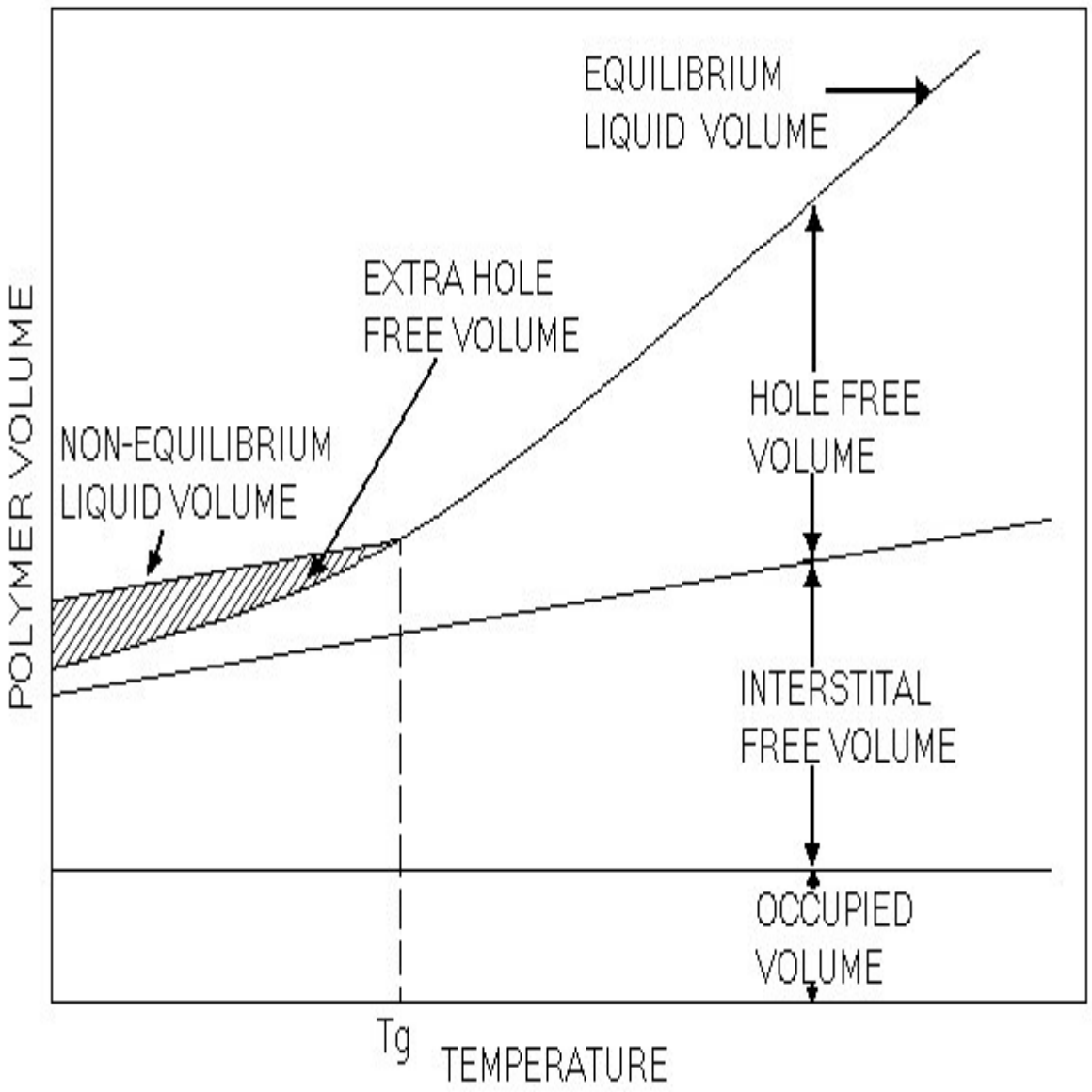

Figure 3.1. Free Volume Concept (Duda,1983)

At low solvent concentrations, a small increase in the solvent weight fraction will cause a very significant increase in available free volume and a correspondingly large increase in the diffusion coefficient. The sensitivity of the diffusion coefficient to the solvent concentration will increase as the temperature approaches the glass transition temperature of the polymer. The diffusivity becomes more independent of concentration as the temperature increases and as the molecular size of the solvent decreases. (Duda,1985)

Vrentas and Duda developed a relationship between the hole free volume and well-defined volumetric characteristics of the pure components in solution:

$$\hat{V}_{FH} = w_1 K_{11}(K_{21} - T_{g1} + T) + w_2 K_{12}(K_{22} - T_{g2} + T) \tag{3.6}$$

For polymer solutions, K_{11} and K_{21} denote free volume parameters for the solvent, while K_{12} and K_{22} are free volume parameters for the polymer. The glass transition temperature of species are given by T_{gi}.

$\frac{\hat{V}_{FH}}{\gamma}$ is the total free volume available for diffusion and defined as;

$$\frac{\hat{V}_{FH}}{\gamma} = w_1 \frac{K_{11}}{\gamma}(K_{21} - T_{g1} + T) + w_2 \frac{K_{12}}{\gamma}(K_{22} - T_{g2} + T) \tag{3.7}$$

In concentrated polymer solutions, the pre-exponential factor D_{01} is often less dependent on temperature than the exponential term related to free volume, in many cases D_{01} can be taken as constant.

With all of these modifications, the self diffusion coefficient of a solvent in a polymer solution becomes as;

$$D_1 = D_0 \exp\left[\frac{-E}{RT}\right] \exp\left[\frac{-\gamma(w_1 \hat{V}_1^* + w_2 \hat{V}_2^*}{\hat{V}_{FH}}\right] \tag{3.8}$$

Combining Eqns (3.6) and (3.8); self diffusion coefficient of solvent in mixture at temperatures above the glass transition temperature of the polymer;

$$D_1 = D_0 \exp\left[\frac{-E}{RT}\right] \exp\left[\frac{-(w_1 \hat{V}_1^* + w_2 \varepsilon \hat{V}_2^*)}{w_1 \frac{K_{11}}{\gamma}(K_{21} - T_{g1} + T) + w_2 \frac{K_{12}}{\gamma}(K_{22} - T_{g2} + T)}\right] \quad (3.9)$$

3.2 Mutual Diffusion Coefficient

Bearman (1961) and Duda et al.(1977) proposed an approximation for low solvent concentrations which couples D, the mutual binary diffusion coefficient, to the self diffusion coefficients for polymer solvent systems:

$$D = \frac{D_1 w_1 w_2}{RT}\left(\frac{\partial \mu_1}{\partial w_1}\right)_{T,P} \quad (3.10)$$

where μ_1 is the chemical potential of the solvent.

Many thermodynamic theories are available to determine the concentration dependence of the solvent chemical potential. The Flory-Huggins theory has provided an adequate representation of polymer solution thermodynamics in many cases.(Flory,1942; Huggins,1942). Eqn (3.10.) is often rewritten as;

$$D = D_1(1-\phi_1)^2(1-2\chi\phi_1) \quad (3.11)$$

where ϕ_1 is the solvent volume fraction in the solution and χ is the polymer-solvent interaction parameter.

3.3 Influence of the Glass Transition

As amorphous rubbers are cooled, the motion of individual polymer chains become so constrained that the cooling rate becomes faster than the rate at which the polymer sample can volumetrically relax. The resulting non-equilibrium condition is referred to as the glassy state and the passage from the rubbery to glassy states is denoted the glass transition.

At $T>T_g$ polymer chains are capable of achieving equilibrium conformations within commonly referenced time scales. So, extra hole free volume becomes trapped within the polymer as it is cooled through the glass transition. It is assumed that this nonequilibrium structure does not change during the self diffusion process and thus the average hole-free volume does not change. (Duda)

The fluctuations in the local density occurs both above and below T_g. So, Vrentas and Duda accomplished that the free volume theory should provide an adequate description of transport in glassy polymers.

Therefore, Eqn (3.8.) can be used to describe the diffusion of a solvent at temperatures below T_{g2} and at conditions approaching zero solvent concentration. The equation could be written as ;

$$D_1 = D_0 \exp\left[\frac{-E}{RT}\right] \exp\left[\frac{-\gamma \hat{V}_2^* \varepsilon}{\hat{V}_{FH2g}}\right] \tag{3.12}$$

where V_{FH2g} is the specific average hole free volume for the non equilibrium liquid and expressed as;

$$\hat{V}_{FH2g} = \hat{V}_{FH2} + (\hat{V}_{2g}^0 - \hat{V}_2^0) = \hat{V}_{2g}^0 - (\hat{V}_2^0(0) + \hat{V}_{F12}) \tag{3.13}$$

V_{2g} is the specific volume of the pure glassy polymer, V_2 and V_{F12} are the specific volume at 0 K and the specific interstitial free volume of the polymer respectively. Vrentas and Duda expressed that α_{2g}, expansion coefficient for the glassy state, can be approximated by an average value over the temperature of interest. They derived the following expression for the average hole free volume.

$$\hat{V}_{FH2g} = K_{12}\left[K_{22} + \lambda(T - T_{g2})\right] \tag{3.14}$$

where λ describes the character of change of the volume contraction which can be attributed to the glass transition temperature and expressed as

$$\lambda = 1 - \frac{\hat{V}^{0}_{2g} - \hat{V}^{0}_{2}}{K_{12}(T_{g2} - T)} = \frac{\alpha_{2g} - (1 - f^{g}_{H2})\alpha_{c2}}{\alpha_{2} - (1 - f^{g}_{H2})\alpha_{c2}} \tag{3.15}$$

Combination of Eqn (3.15.) with Eqn (3.12.) yields the following expression describing the diffusion of a trace amount of solvent in glassy polymers:

$$D_1 = D_0 \exp\left[\frac{-E}{RT}\right]\exp\left[\frac{-\gamma \hat{V}^{*}_{2}\varepsilon}{K_{12}(K_{22} + \lambda(T - T_{g2})}\right] \tag{3.16}$$

λ is evaluated by regressing D_0,E, and ε above the glass transition temperature. Once these parameters are known, λ can be determined by the aid of equation 3.16.

3.4 Estimation of Free Volume Parameters

Ten independent parameters, K_{11}/γ, K_{12}/γ, K_{21}-T_{g1}, K_{22}-T_{g2}, V_1, V_2, χ, D_0, E and ε are regressed from diffusion data. Assuming E zero yields reliable results.

V_1 and V_2 can be calculated by using the group contribution method. (Sugden and Blitz and Haward, 1970)

K_{11}/γ and K_{21}-T_{g1} are determined from the viscosity data for the solvent. The relationship between the viscosity of the solvent and its free volume parameters are given by Vrentas and Duda (1998),

$$\ln \eta_1 = \ln A_1 + \frac{\gamma \hat{V}^{*}_{1} / K_{11}}{K_{21} - T_{g1} + T} \tag{3.17}$$

K_{22}-T_{g2}, K_{12}/γ are calculated from Williams, Landel and Ferry (WLF) constants (c_1, c_2) that can be regressed from viscosity versus temperature data.

$$K_{22} = (c_2^g)_2 \tag{3.18}$$

$$\frac{\gamma \hat{V}_2^*}{K_{12}} = 2.303(c_1^g)_1(c_2^g)_2 \tag{3.19}$$

These constants are published for several polymers, but if the data for the polymer of interest is not available, then they are obtained from the experimental shift factor. Shift factor (a_T) is denoted by the following expression,

$$\log a_T = -\frac{c_1(T - T_{ref})}{c_2 + T - T_{ref}} \tag{3.20}$$

Shift factor can be obtained by superimposing dynamic mechanical measurements (loss modulus, G', and storage modulus, G'' as a function of frequency) at different temperatures.

χ, Flory Huggins interaction parameter can be estimated by using the Flory Huggins equation;

$$Activity = \frac{P_1}{P_1^0}\exp\left(\frac{B_{11}(P_1 - P_1^0)}{RT}\right) = \phi_1 \exp(\phi_2 + \chi\phi_2^2) \tag{3.21}$$

P_1 and P^0_1 are the solvent saturation vapor pressure, respectively. B_{11} is the second virial coefficient of the solvent, ϕ_1, ϕ_2 are the volume fraction of the solvent and the polymer respectively.

CHAPTER 4

EXPERIMENTAL METHODS, PROCEDURE AND ANALYSIS

This chapter deals with the materials used in the experiments, the equipment, the experimental method and procedure. It also focuses on the method of analyzing the data.

4.1 Materials

The capillary columns used in this study were prepared by Restek,Inc by the static polymer coating technique. In this technique, a coating solution was filtered and degassed by boiling under reduced pressure to half its original volume. The final concentration of the solution determines the coating thickness. The solution is cooled rapidly and drawn into the column under reduced pressure to hinder redissolution of gases. Once the column has been filled, sufficient additional liquid is drawn through the column to eliminate axial concentration gradients that may have formed as the column was being filled. One end of the column is sealed with a commercial epoxy. After the seal has hardened, the column is mounted in a cascade of constant temperature baths and connected to a vacuum system via an open end.

The coating solution is evaporated at nearly full vacuum. If the column has been properly cleaned and sealed, spontaneous boiling will be suppressed, and the coating solution will evaporate at a slow steady rate. The steady state drying rate is dependent upon the polymer, solvent, temperature, and solution concentration.

The polymers that were used for the coating of capillary columns were poly D-L lactide co glycolide (PLGA) and polymethyl methacrylate co butylmethacrylate (PMMA co BMA). The detailed information about the capillary columns were given in Table 4.1.

All solvents, supplied by Aldrich Chemicals were used without further purification.

Table 4.1 Characterization of the capillary columns

Polymer	Inner Diameter (mm)	Axial Length (m)	Film Thickness (mm)
PMMA co BMA	0.53	15	6.0
PLGA	0.53	15	5.0

4.2 Characterization Studies

The two copolymers were analyzed by Fourier Transform Infrared Spectroscopy, Differential Scanning Calorimetry and Thermal Gravimetry.

4.2.1 Fourier Transform Infrared Spectroscopy (FTIR)

To determine the functional groups in the two copolymers, a Shimadzu 8601 Fourier Transform Infrared Spectrophotometer in the range of 400-4000 cm^{-1} wavelength was used. Polymer in filmform was used in FTIR analysis.

4.2.2 Differential Scanning Calorimetry (DSC)

Thermal behavior of the copolymers were investigated by a Shimadzu DSC 50. 3.8 mg PLGA sample was placed in an aluminum pan and heated at a constant rate of 10 C^0/min up to 500 C in an nitrogen atmosphere at a rate of 40 ml/min. Also 3.1 mg PMMA co BMA sample was analyzed at the same conditions.

4.2.3 Thermal Gravimetric Analysis (TGA)

The thermal degradation of PLGA and PMMA co BMA was observed by thermal gravimetry (Shimadzu TGA51). A 10.79 mg sample of PLGA was heated continuosly at a rate of 10 C^0/min to 600 C^0 under nitrogen flow at a rate of 40 ml/min. Also, thermal degradation of PMMA co BMA of a 7.33 mg was observed at the same conditions.

4.3 Experimental Set-up

The schematic diagram of chromatographic apparatus used for the experiments is shown in Figure 4.1. The gas chromatograph used was Schimadzu 17A equipped with a thermal conductivity detector (TCD), a flame ionization detector (FID), an electron capture detector (ECD), on column injector, air-circulating oven. Thermal conductivity detector and flame ionization detector were selected as the detector and helium was used as the carrier gas in all experiments. The temperature of the injector and detector was set about 50 C above the normal boiling point to avoid condensation in the detector assembly. Air and methane were used as the marker gas for TCD and FID respectively. Small amounts of solvent were injected through the rubber septum of the injection port into the carrier gas using a Hamilton 1 μl syringe and air by 10 μl syringe. The output signal from the detector was stored and recorded in Hewlett Packard computer.

4.4 Experimental Procedure

The capillary column was installed in the oven and conditioned to remove any residual volatile components that may be still present in the polymer. Then, the temperature of the column oven, injection port, detector and the carrier gas flow rate, split ratio, were set. When GC has reached a stable steady state operation, a drift-baseline was observed. So, gas chromatograph is ready to use. Afterwards, air or methane, used as marker gas, and a small pulse of solvent were injected into the column. The output elution profile was monitored and stored by a computer for the analysis.

4.5 Data Analysis

The raw data stored in the computer were converted into ASCII format. Then the data were corrected for baseline offset. After the baseline correction, the elution curve was integrated using a FORTRAN program to determine first and second moments. These moments were used as initial estimates of the partition and diffusion coefficients, K and Dp. The Laplace transform equation was then numerically inverted using an algorithm. The predicted response curve was then compared with the

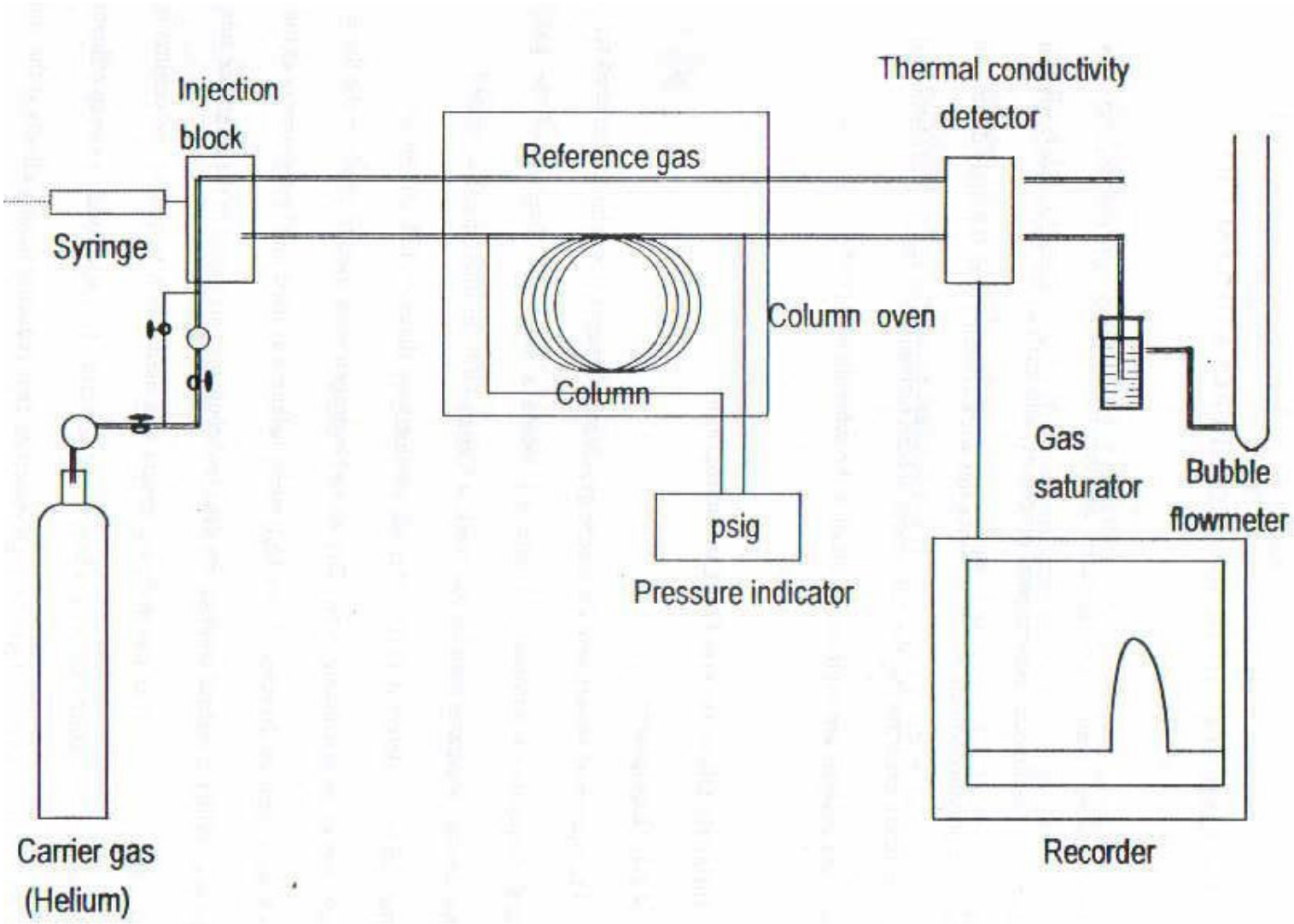

Figure 4.1. Gas chromatographic apparatus

experimental elution curve. The residual was minimized using a nonlinear regression package to find K and D_p that best fit the experimental elution curve. The K and Dp values were the average values of each set that were obtained after at least 5 runs of each set.

CHAPTER 5

RESULTS AND DISCUSSION

5.1 Characterization of the polymers

The characterization of the polymers were performed with Fourier Transform Infrared Spectroscopy, Thermal Gravimetric Analysis and Differential Scanning Calorimetry.

5.1.1 Fourier Transform Infrared Spectroscopy (FTIR) Analysis

FTIR analysis of PMMA co BMA was shown in Figure 5.1. The broad peak ranging from 1500-1000 cm^{-1} is due to the stretching of the C-O (ester) bonds. The sharp intense peak at 1730 is referred to C-O bond. The broad band at 2900-3000 cm^{-1} corresponds to C-H stretching vibrations.

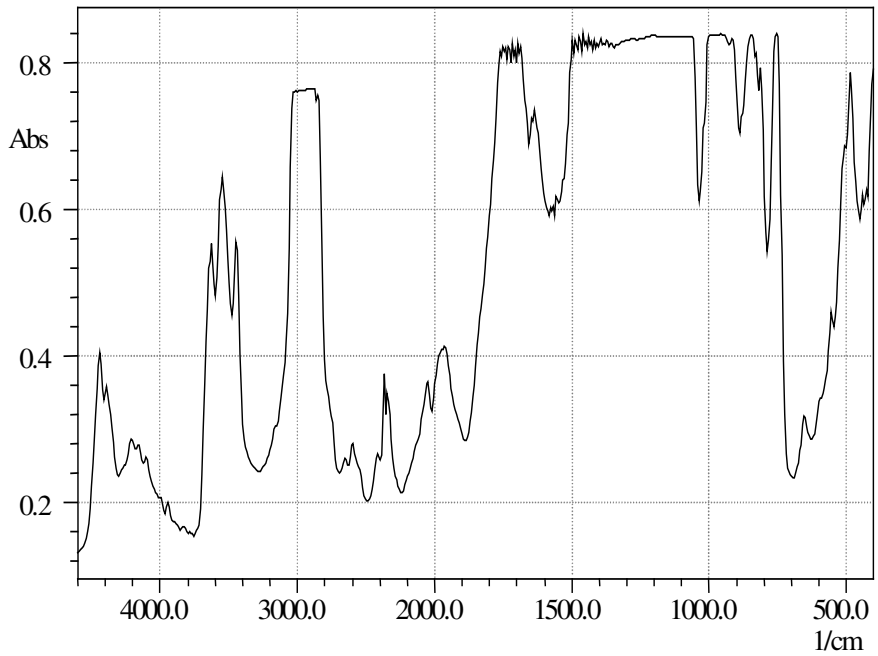

Figure 5.1. Fourier Transform Infrared Spectroscopic Analysis of PMMA-co BMA

FTIR analysis of PLGA was shown in Figure 5.2. The broad peak ranging from 1350-980 cm^{-1} is due to the stretching of the C-O (ester) bonds. The peak at about 1700 cm^{-1} corresponds to C=O bond. The broad band at 2800-3000 cm^{-1} is due to the C-H stretching vibrations.

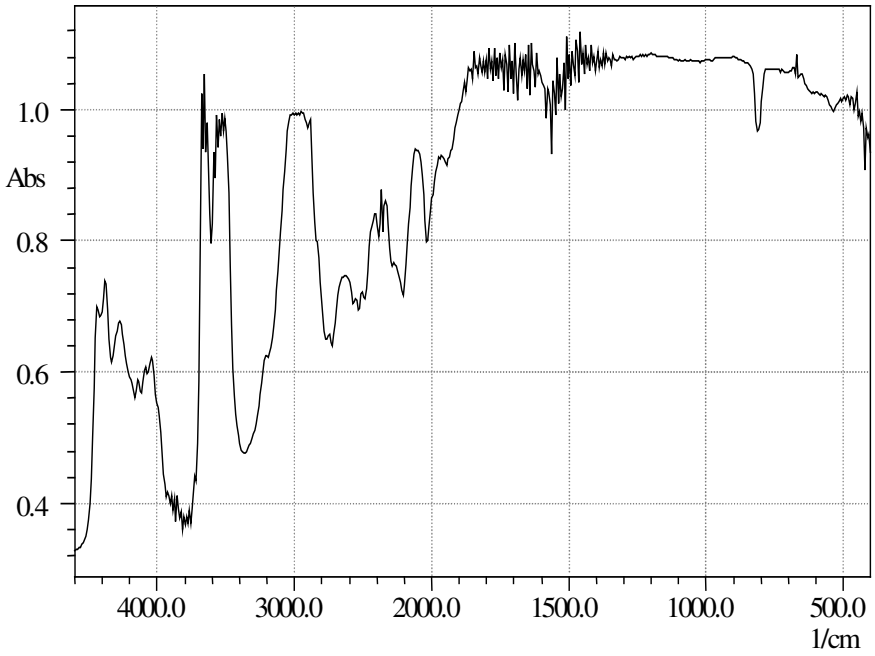

Figure 5.2. Fourier Transform Infrared Spectroscopic Analysis of PLGA

5.1.2 Thermal Gravimetric Analysis (TGA)

Thermal degradation of PMMA co BMA is shown in figure 5.3. It was observed that one step thermal degradation takes place. The weight loss starts at about 250 ^{0}C and significant weight loss continues up to about 375 ^{0}C. When the temperature is above 400 ^{0}C, almost all of the polymer degrades.

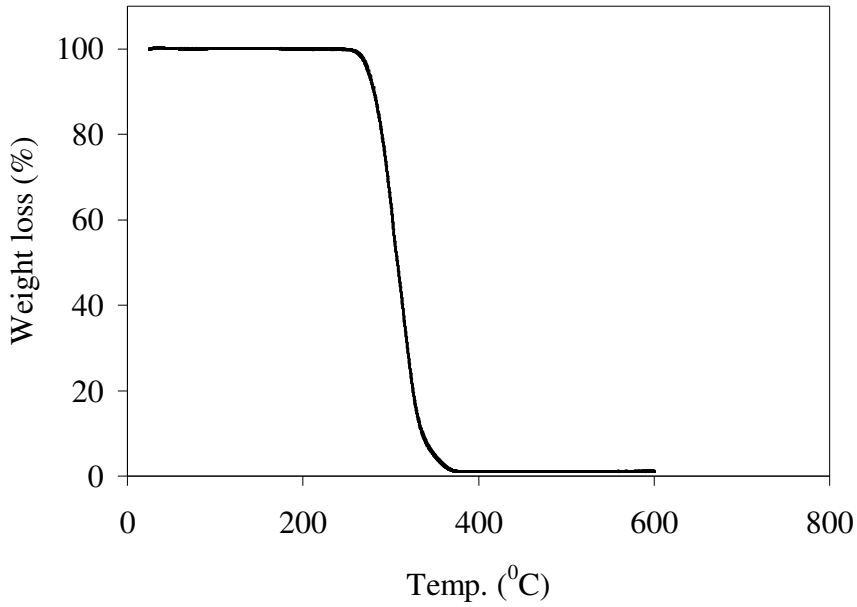

Figure 5.3. Thermal Gravimetric Analysis of PMMA co BMA

Figure 5.4 shows TGA curve of PLGA copolymer. In this figure, weight loss of the sample starts at 240 ^{0}C. After 290 ^{0}C the polymer loses its weight significantly due to the sharp decrease in the figure. When the temperature is above 400 ^{0}C, all of the polymer degrades.

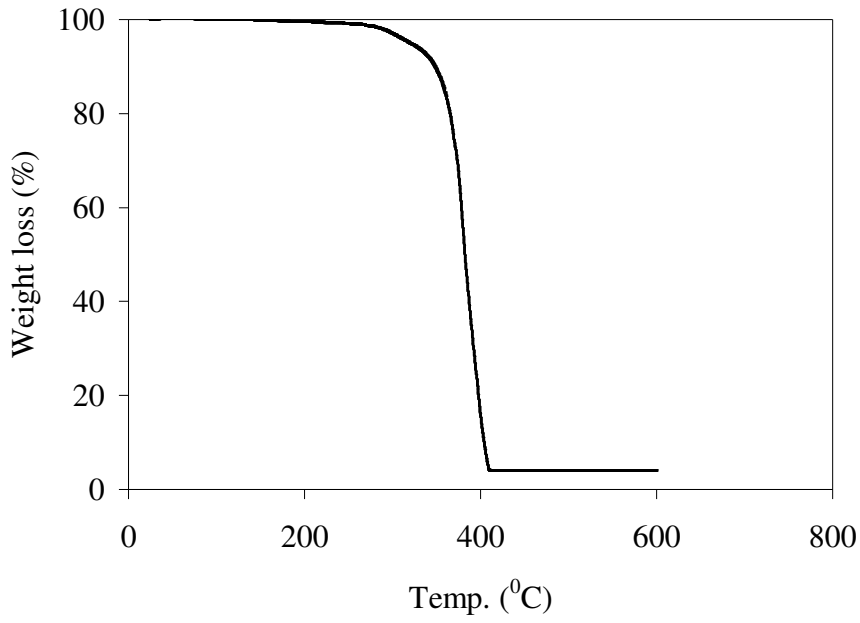

Figure 5.4. Thermal Gravimetric Analysis of PLGA

5.1.3 Differential Scanning Calorimetry (DSC) Analysis

Figure 5.5 and 5.6 show the differential scanning calorimetry analysis of PMMA co BMA and PLGA copolymers respectively. By DSC, the glass transition temperature of the sample can be obtained. The glass transition temperature of pmma co bma was determined as 106.35 ^{o}C from the sharp decrease between 109 ^{o}C and 121 ^{o}C in figure 5.5. Then the heat flow curve remains constant up to 280 ^{o}C and after this temperature a negative peak is observed due to the degradation of the polymer. The heat of degradation was determined as –676.48 kJ/kg from the area under the curve.

In figure 5.6 the differential scanning analysis of plga is shown. The sharp decrease which corresponds to glass transition range was between 45 ^{o}C and 55 ^{o}C and the glass temperature of plga was obtained as 42.53 ^{o}C. The heat flow curve which remains constant to the temperature of 300 ^{o}C indicates that the structure of the polymer does not change. When the temperature exceeds this temperature, a negative peak, corresponding to the degradation of the polymer was observed. The area under the curve gives the heat of degradation as –680.80 kJ/kg.

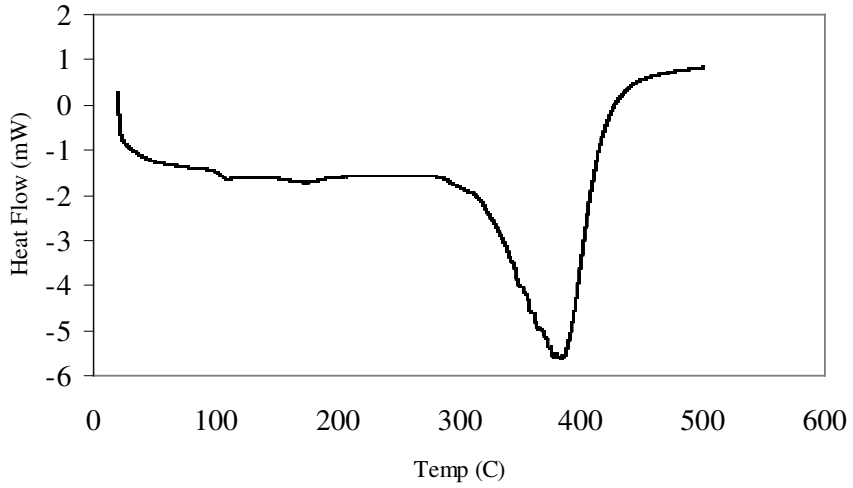

Figure 5.5. Differential Scanning Calorimetry Analysis of PMMA co BMA

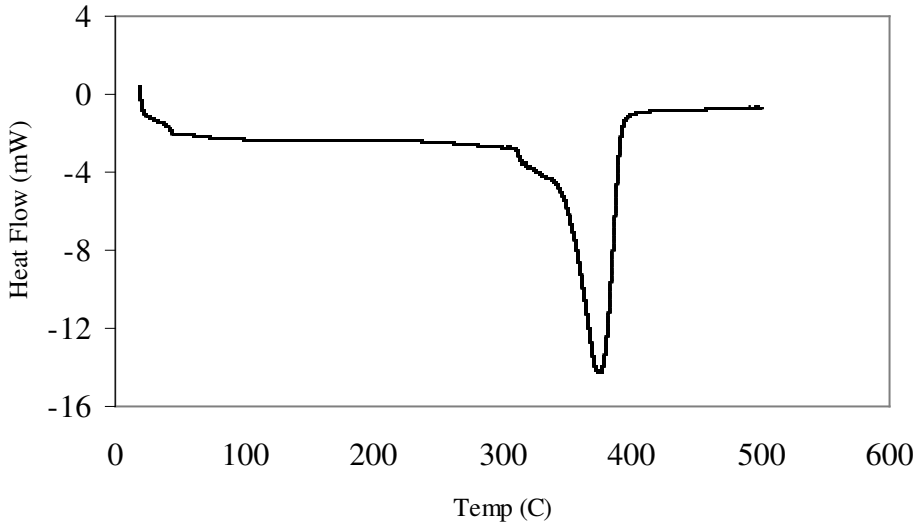

Figure 5.6. Differential Scanning Calorimetry Analysis of PLGA

5.2. Thermodynamic Measurements of PMMA co BMA-solvent systems

Thermodynamic properties (retention volume Vg, infinitely dilute activity coefficient Ω_1^{∞}, polymer solvent interaction parameter χ, solvent and polymer solubility parameters δ_1 δ_2) can be determined using the retention volume by inverse gas chromatography.

5.2.1 Retention Volume

Retention volume (V_g) is a key parameter to obtain the thermodynamic properties of the system by inverse gas chromatography using Equation 2.1. Vg of the solvents for the polymethyl methacrylate co butyl methacrylate at four different temperatures were reported in Table 5.1. Generally V_g decreased as temperature increased. This behavior exhibited that this temperature range was in the equilibrium sorption as explained in section 2.1. Braun and Guillet (1976) stipulate that equilibrium bulk sorption was achieved at temperatures in excess of about T_g+50 ^oC for most common polymers. If temperature decreases near to the glass transition of the polymer non-equilibrium region starts and V_g increases with the temperature. Since the experiments were performed at least 5 runs of each set, an error analysis was applied. The results are given in Appendix B.

Table 5.1.Retention volumes for PMMA co BMA-solvent systems

Solutes	423 K	443 K	453 K	473 K
methanol	4.25	3.03	2.69	1.61
ethanol	5.22	3.86	3.35	2.08
1-propanol	7.72	6.29	5.55	3.36
1-butanol	12.03	10.08	7.37	5.25
methyl acetate	4.12	3.57	2.97	1.99
ethyl acetate	4.93	4.42	3.87	2.39
propyl acetate	6.85	6.12	5.64	3.82
dichloromethane	6.60	4.95	3.94	2.79
trichloromethane	7.58	7.58	6.25	4.30
acetone	4.50	3.65	3.10	2.19
MMA	7.76	7.23	6.33	4.36
BMA	21.35	20.52	16.84	11.10

To investigate the temperature dependence of ln (V_g) on solute molecular weight , ln V_g with respect to 1/T were plotted. In Figure 5.7, ln V_g versus 1/T were plotted for the alcohol series including methanol, ethanol, propanol, butanol in the temperature range of 423-443 K. As temperature increased, ln V_g decreased and linear molecular weight dependence of ln V_g was observed in Figure 5.7 which yielded the highest value for butanol and the lowest for methanol.

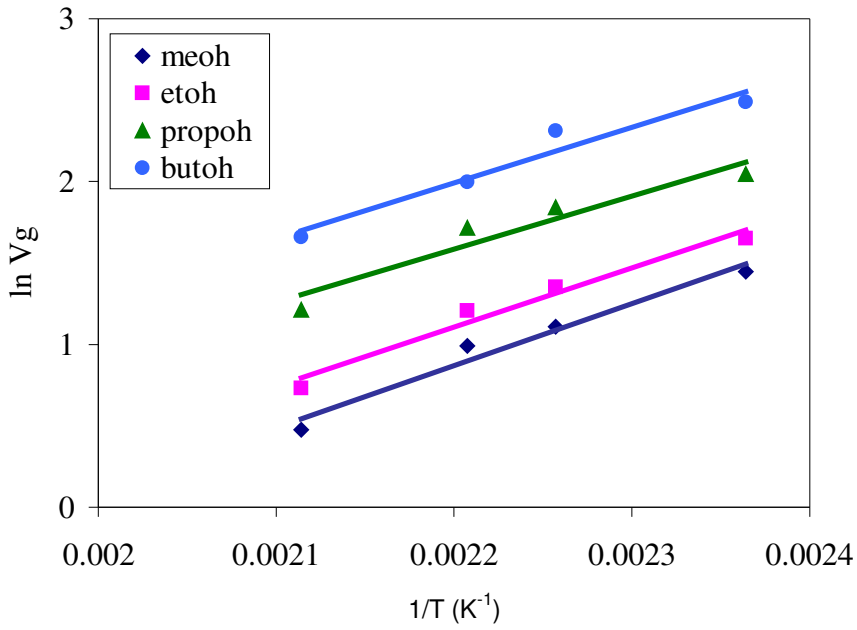

Figure 5.7. Temperature dependence of ln V_g for the alcohols in PMMA co BMA

The same behavior of ln V_g was observed for the other solvents and these behaviors were shown in Figure 5.8 for acetate series (methyl, ethyl, propyl acetate); in Figure 5.9 for dichloromethane, trichloromethane, acetone; in Figure 5.10 for methyl methacrylate and butyl methacrylate which were the monomers of the PMMA co BMA in the temperature range of 423-443 K.

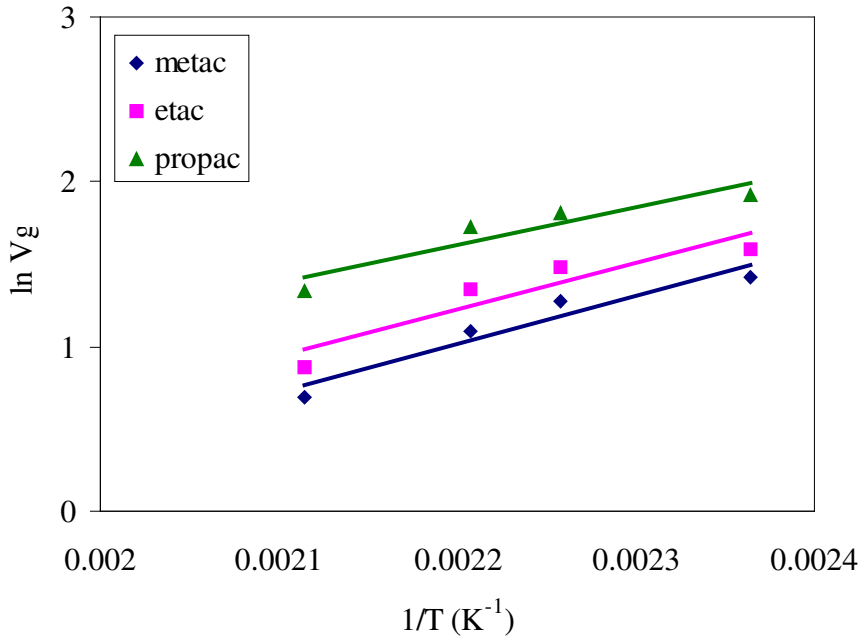

Figure 5.8. Temperature dependence of ln V_g for the acetates in PMMA co BMA

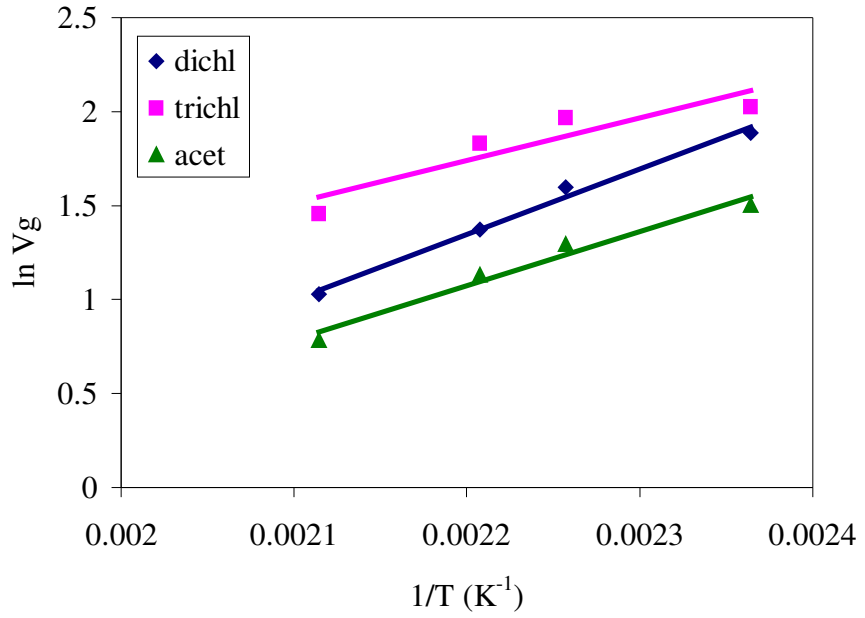

Figure 5.9. Temperature dependence of ln V_g for the dichloromethane, trichloromethane,acetone in PMMA co BMA

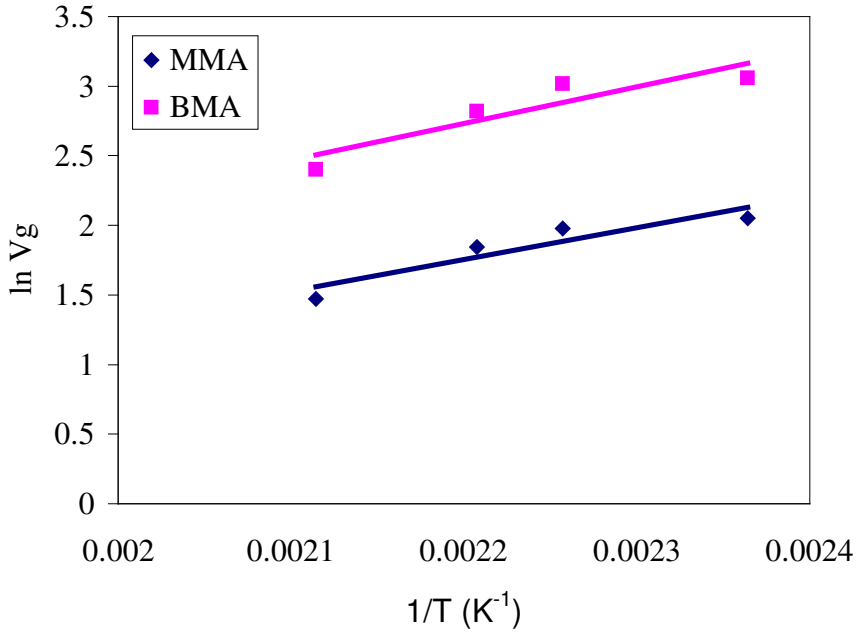

Figure 5.10. Temperature dependence of ln V_g for the MMA,BMA in PMMA co BMA

Retention volumes of water are obtained by thermal conductivity detector using air as the marker gas at temperatures 383, 403, 423 and 443 K. Figure 5.11 shows a perfect linear relationship of ln V_g with respect to reciprocal of temperature.

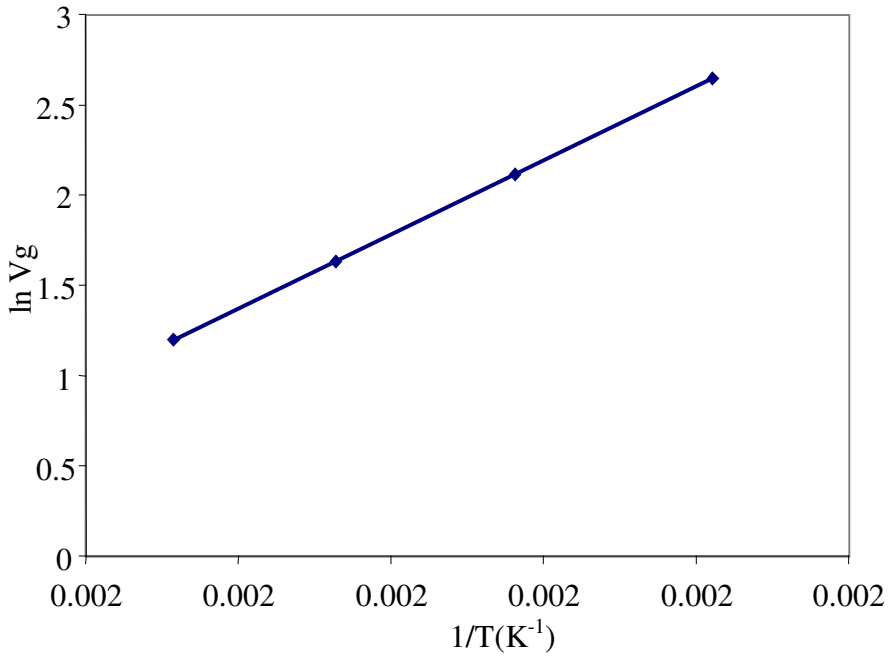

Figure 5.11. Temperature dependence of ln V_g for water in PMMA co BMA

5.2.2 Weight Fraction Activity Coefficient (WFAC)

The weight fraction activity coefficients (Ω_1^{∞}) of the solvents in PMMA co BMA were determined by using Eqn (2.3.) The parameters used for calculation of Ω_1^{∞} were given in Appendix A. Table 5.2 listed the activity coefficients for these solutes at four different temperatures (423, 443, 453, 473 K). Activity results showed that, trichloromethane had the lowest activity coefficient for the same temperature and methanol had the greatest value in a significant manner. According to our findings based on the 13 solvents studied in this polymer, we can say that trichloromethane is the best solvent for this polymer. Although, Ω_1^{∞} exhibited a maximum at 473 K, it was found that Ω_1^{∞} was not a strong function of temperature.

Table 5.2. Weight Fraction Activity coefficients for PMMA co BMA-solvent systems

	Ω_1^{∞}			
Solutes	423 K	443 K	453 K	473 K
methanol	88.31	83.09	77.89	92.54
ethanol	16.88	15.56	15.18	18.29
1-propanol	10.21	8.64	8.33	10.48
1-butanol	11.20	8.75	9.93	10.03
methyl acetate	11.73	10.27	10.93	13.15
ethyl acetate	13.34	10.92	10.86	13.78
propyl acetate	16.79	10.51	10.86	12.07
dichloromethane	4.66	4.86	5.46	6.37
trichloromethane	4.70	3.74	3.78	4.37
acetone	13.70	12.80	13.34	15.32
MMA	14.18	10.82	10.60	11.59
BMA	16.98	10.86	10.61	10.80

Figures 5.12 and 5.13 show the temperature dependence of Ω_1^{∞} of alcohol and acetate series respectively. Ω_1^{∞} decreased as temperature increased from 423 K up to 453 K and when temperature proceeded to 473 K a slight decrease in Ω_1^{∞} was observed. Methanol had farly the greatest value at all temperatures. Propanol and butanol had closer values in the alcohol series and in the acetate series, methyl, ethyl, propyl acetates both had closer values especially at 443 and 453 K.

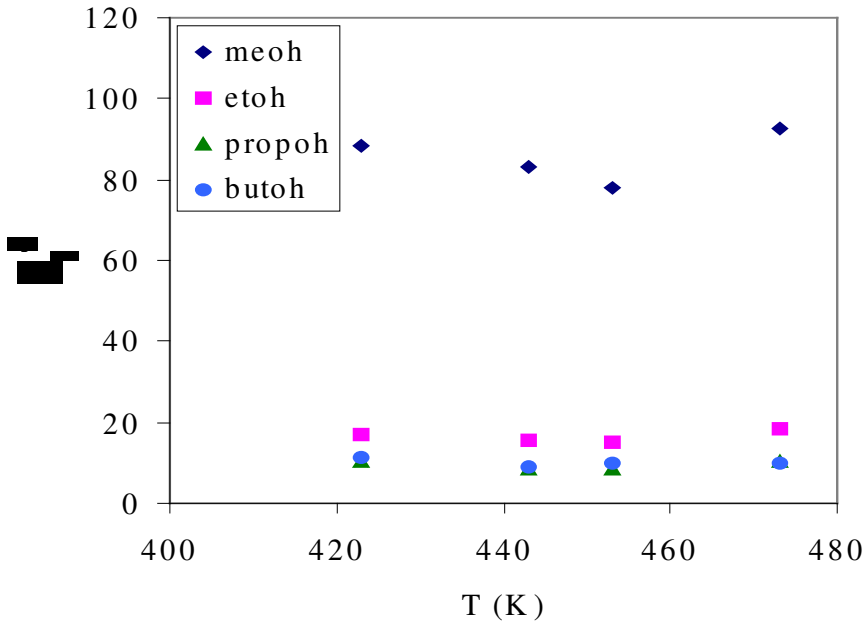

Figure 5.12. Temperature dependence of Ω_1^{∞} for alcohols in PMMA co BMA

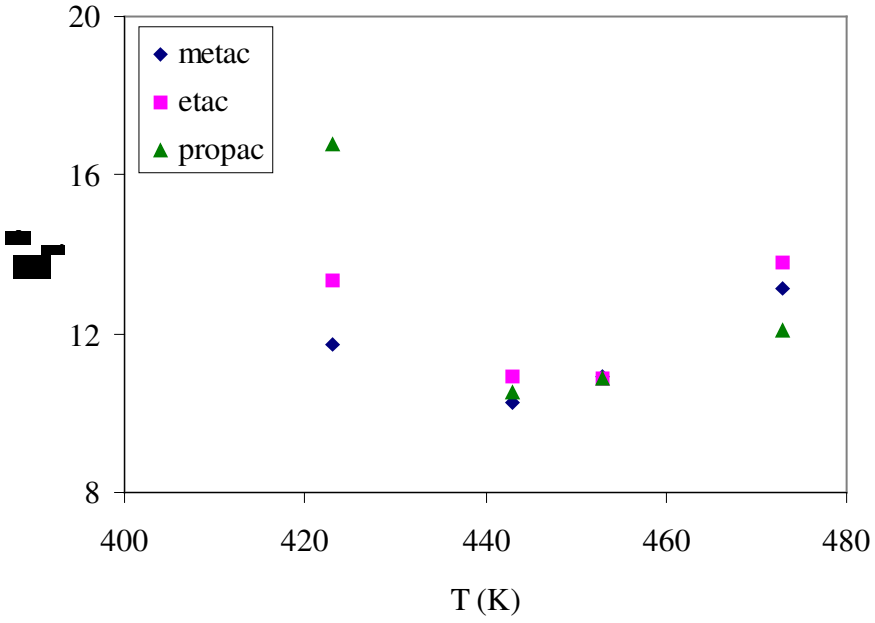

Figure 5.13.Temperature dependence of Ω_1^{∞} for acetates in PMMA co BMA

The activity coefficient behavior with respect to temperature of dichloromethane, trichloromethane, acetone and methyl methacrylate, butyl methacrylate in PMMA co BMA were shown in Figure 5.14 and 5.15, respectively. The Ω_1^{∞} of dichloromethane and trichloromethane depict similar values resulting from their similar structures. Acetone had greater Ω_1^{∞} values when compared with these solvents. Monomers of PMMA co BMA, MMA and BMA have also similar values especially at 443 and 453 K. Generally, the Ω_1^{∞} of all of these solutes decreased as temperature increased from 423 K up to 453 K and then slightly increased at 473 K.

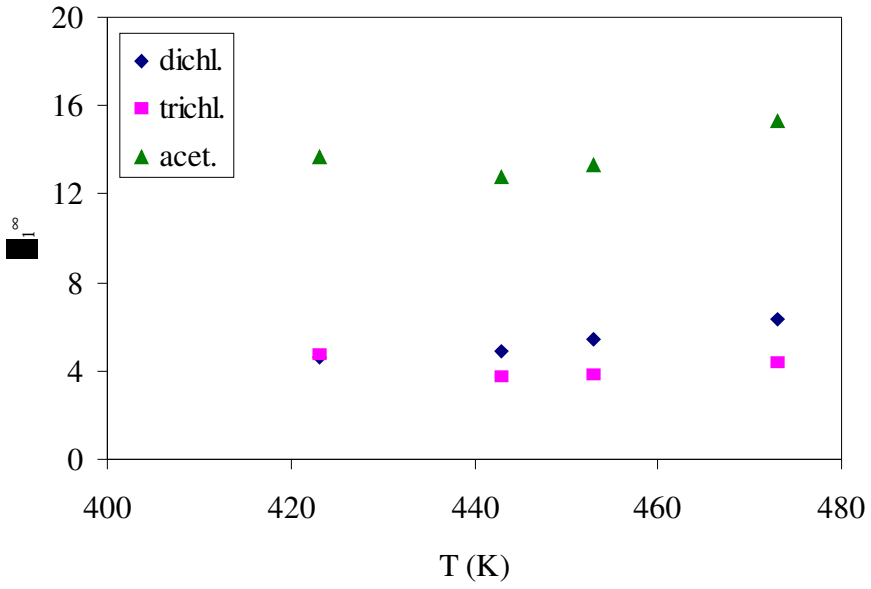

Figure 5.14.Temperature dependence of Ω_1^{∞} for dichl,trichl, acet. in PMMA co BMA

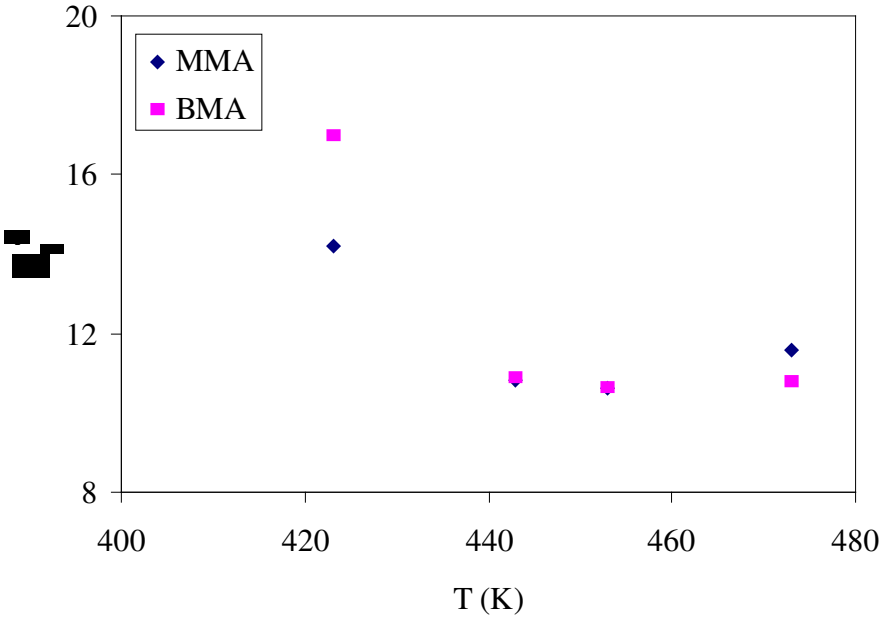

Figure 5.15.Temperature dependence of Ω_1^{∞} for MMA,BMA in PMMA co BMA

The weight fraction activity coefficient of water were determined at four different temperatures (383, 403, 423, 443 K) and was shown in Figure 5.16. The relatively high values indicated very poor solubility characteristic of water.

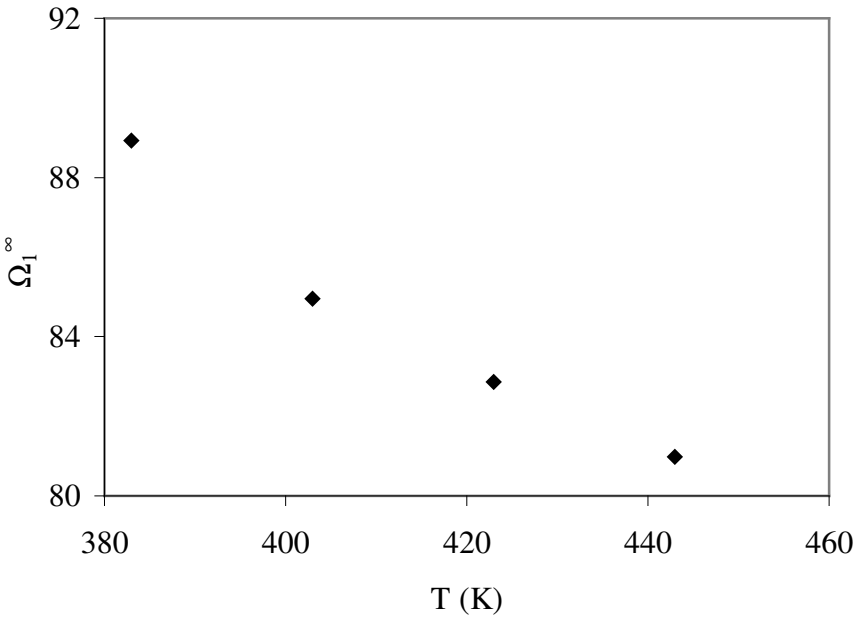

Figure 5.16. Temperature dependence of Ω_1^{∞} for water in PMMA co BMA

5.2.3. Flory Huggins Interaction Parameter (χ)

Flory Huggins interaction parameter values (χ) for 13 solvents with PMMA co BMA were determined by using Eqn (2.4.) at four different temperatures (423, 443, 453, and 473 K). A close inspection of the tabulated interaction data revealed useful information about the degree of compatibility between PMMA co BMA and the various solvents used in this study. When the stability analysis was applied to the Flory Huggins equation, complete polymer solubility exists only when χ is less than 0.5. (Romdhane,1990) If the χ parameters in Table 5.3 were examined, trichloromethane appeared to have the minimum value for χ at all temperatures except 423 K at which dichloromethane had the lowest value. Thus one may predict that trichloromethane is the most suitable solvent for PMMA co BMA. On the other hand, considering all of the solvents studied in this study, methanol had the highest χ value at all temperatures. This indicated that methanol had very poor solubility characteristic among the studied solvents for PMMA co BMA showing no affinity to this polymer as menifested by their relatively high χ values and the decreasing values of Ω_1^{∞} with increasing temperature. Previously the highest Ω_1^{∞} values also proved that methanol was the unsuitable solvent for PMMA co BMA. In the alcohol series, propanol has the minimum value but still all of its values at these temperatures are higher than 0.5. The monomers of PMMA co BMA gave similar interaction parameters and the values were higher than 0.5 at all temperatures. Figures 5.17 to 5.20 show the temperature dependence of interaction parameters in PMMA co BMA for alcohols; acetates; dichloromethane, trichloromethane, acetone and monomers respectively.

Table 5.3. Interaction parameters of PMMA co BMA-solvent systems

	χ			
Solutes	423 K	443 K	453 K	473 K
methanol	3.00	2.88	2.79	2.89
ethanol	1.29	1.16	1.10	1.22
1-propanol	0.76	0.54	0.47	0.62
1-butanol	0.92	0.64	0.74	0.71
methyl acetate	1.05	0.85	0.88	0.98
ethyl acetate	1.16	0.91	0.87	1.04
propyl acetate	1.40	0.890	0.90	0.95
dichloromethane	0.47	0.45	0.54	0.60
trichloromethane	0.64	0.36	0.35	0.44
acetone	1.03	0.90	0.90	0.95
MMA	1.30	0.99	0.95	0.99
BMA	1.47	0.99	0.95	0.94

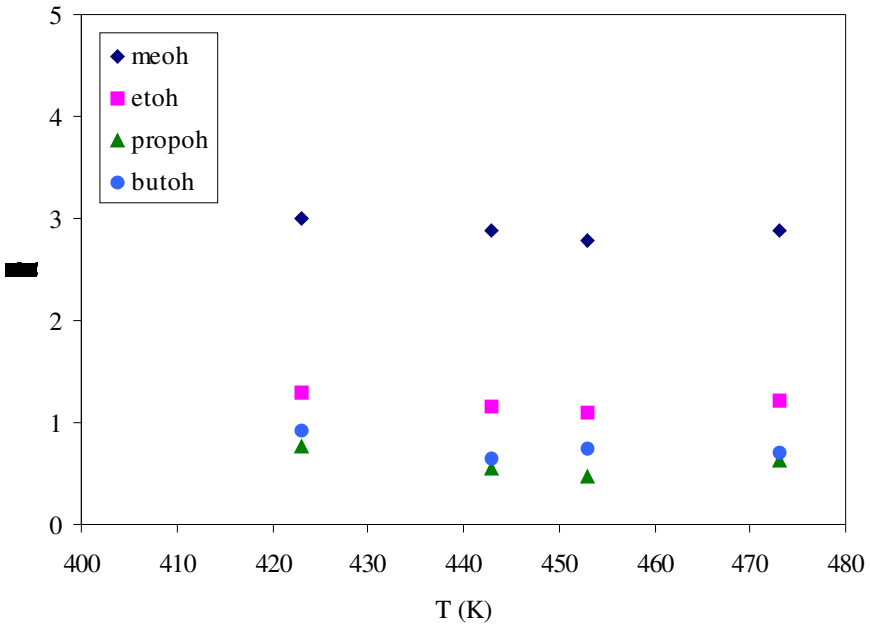

Figure 5.17.Temperature dependence of χ for alcohols in PMMA co BMA

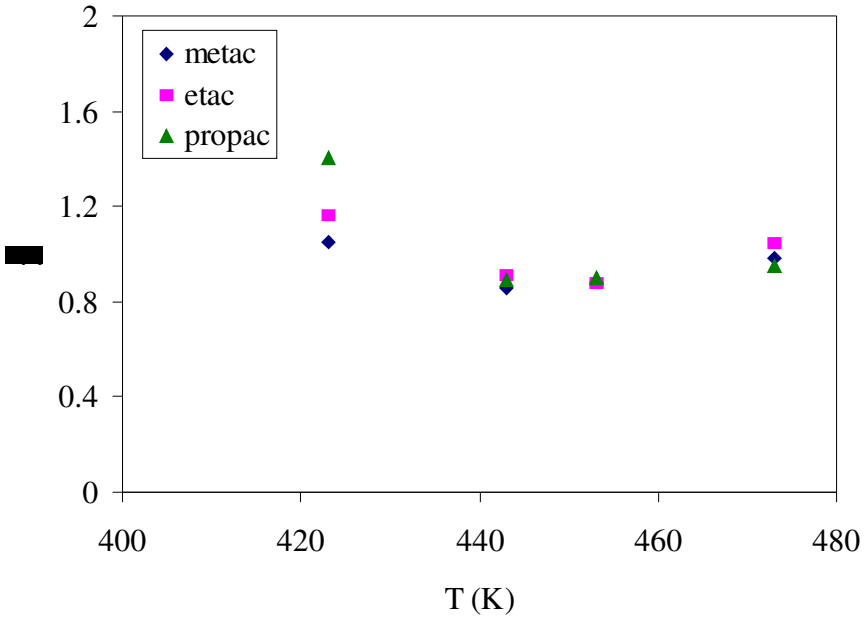

Figure 5.18.Temperature dependence of χ for acetates in PMMA co BMA

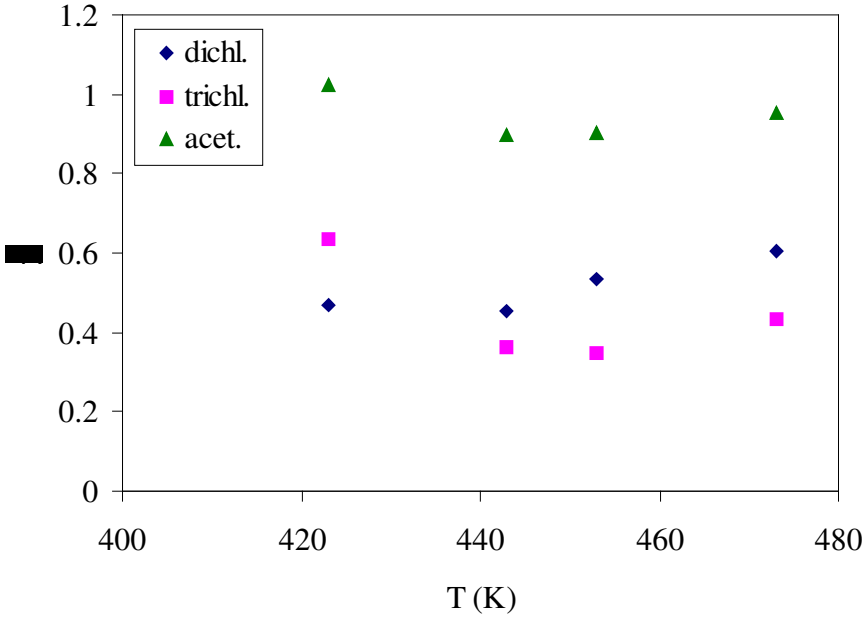

Figure 5.19.Temperature dependence of χ for dichl,trichl, acet. in PMMA co BMA

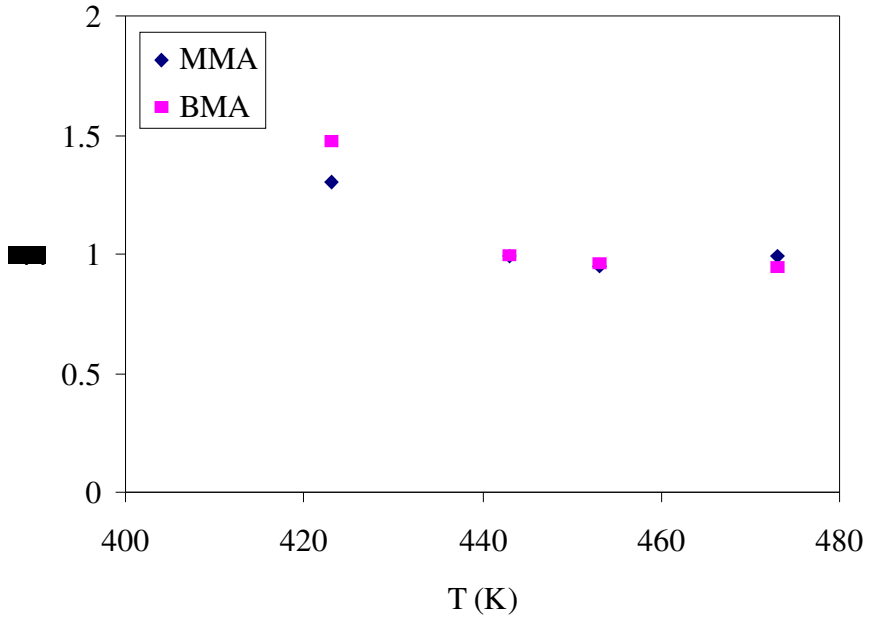

Figure 5.20.Temperature dependence of χ for MMA,BMA in PMMA co BMA

Flory Huggins interaction parameter (χ) of water at four different temperatures, (383, 403,423,443 K) were determined. As temperature increased, solubility parameter of water decreased but all the values at these temperatures were farly higher than 0.5. So, water showed no affinity to this polymer as shown by their high χ values and one may predict that water was not a suitable solute for PMMA co BMA. The temperature dependence was shown in Figure 5.21 in which χ versus temperature was plotted.

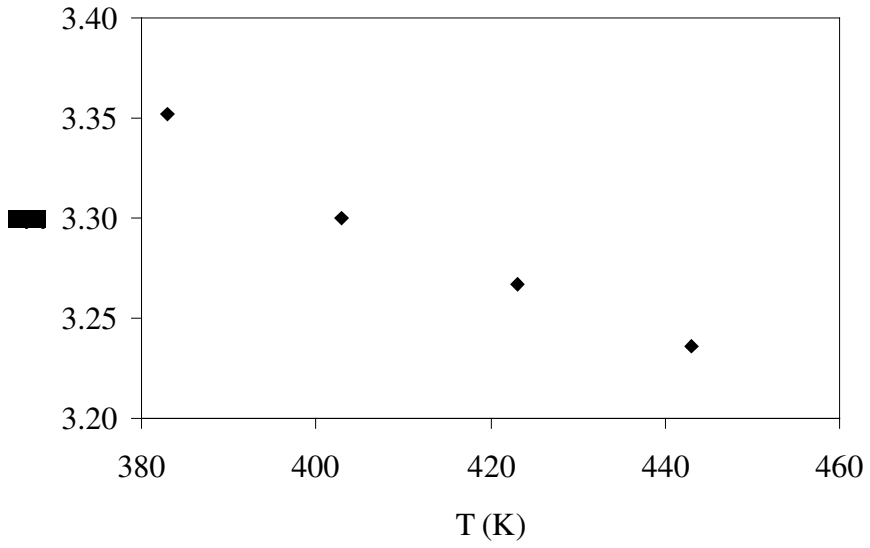

Figure 5.21. Temperature dependence of χ for water in PMMA co BMA

5.2.4. Solubility Parameter (δ)

Solute solubility parameters were computed through Equation 2.6. In this eqn, the molar volume (V_1) and latent heat of vaporization were (ΔH_v) obtained for each solute at appropriate temperatures from Chemcad software and given in Appendix A. The calculated values of δ_1 were compiled in Table 5.4.

Table 5.4 Solute solubility parameters (δ_1)

$\delta_1 (J/cm^3)^{1/2}$				
	423 K	443 K	453 K	473 K
methanol	21.97	20.22	19.22	16.83
ethanol	20.17	18.72	17.90	15.92
1-propanol	18.07	16.75	16.01	14.33
1-butanol	17.69	16.59	16.00	14.71
methyl acetate	13.93	12.67	11.95	10.19
ethyl acetate	13.60	12.56	11.98	10.65
propyl acetate	13.72	12.87	12.41	11.39
dichloromethane	14.31	12.94	12.16	10.29
trichloromethane	14.43	13.48	12.95	11.78
acetone	14.37	13.05	12.29	10.42
MMA	14.39	13.55	13.10	12.13
BMA	14.24	13.68	13.39	12.77

A least- square analysis of plots of ($\delta_1^2/(RT) - \chi/V_1$) versus δ_1 was carried out to obtain the PMMA co BMA solubility parameters at 423, 443, 453, 473 K. As discussed in section 2.2.4, these plots give a slope of $2\delta_2^{\infty}/(RT)$ and an intercept of $-(\delta_2^{\infty 2}/(RT) + \chi V_1)$. Figure 5.22 to 5.25 illustrate plots for various solvents in PMMA co BMA at these temperatures. Derived values of δ_2^{∞} for 423, 443, 453, 473 K were 15.22, 13.81, 13.37, 11.79 $(J/cm^3)^{1/2}$ respectively.

By comparing the solvent solubility parameters δ_1 listed in Table 5.4 with the estimated PMMA co BMA solubility parameter, one could distinguish between solvents and non solvents. Good examples are dichloromethane and trichloromethane which possess the closest solubility parameters to that of PMMA co BMA , indicating their strong solvency power, just as predicted through the other interaction parameters. Alcohols, especially methanol, on the other hand, with their higher solubility parameters were poor solvents of PMMA co BMA, in agreement with the conclusions based on the other parameters.

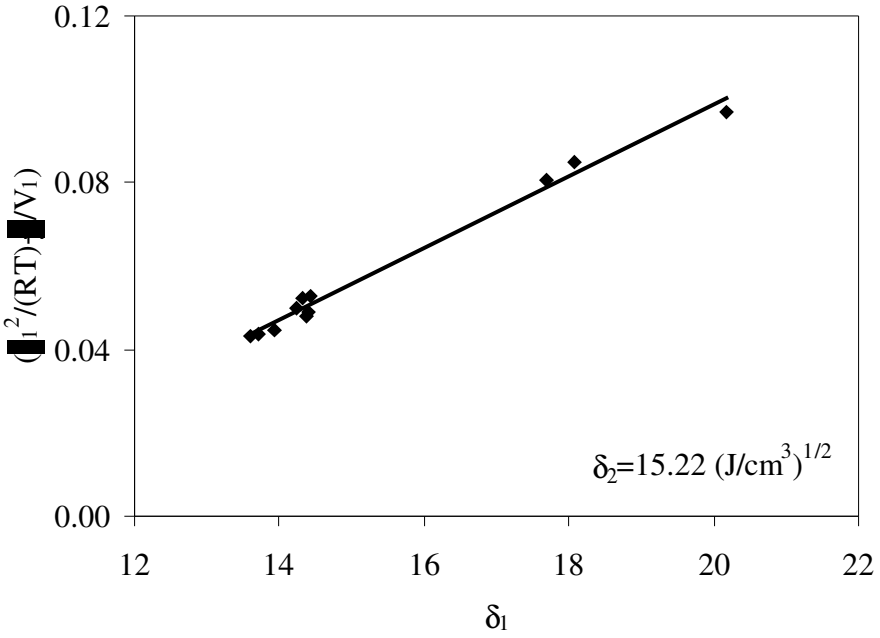

Figure 5.22.Estimation of PMMA co BMA solubility parameter at 423 K

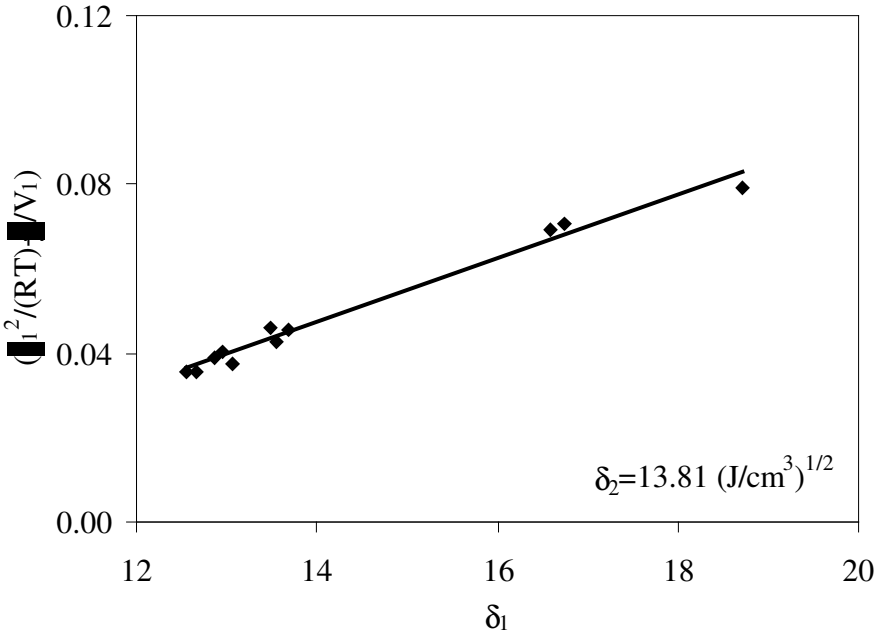

Figure 5.23. Estimation of PMMA co BMA solubility parameter at 443 K

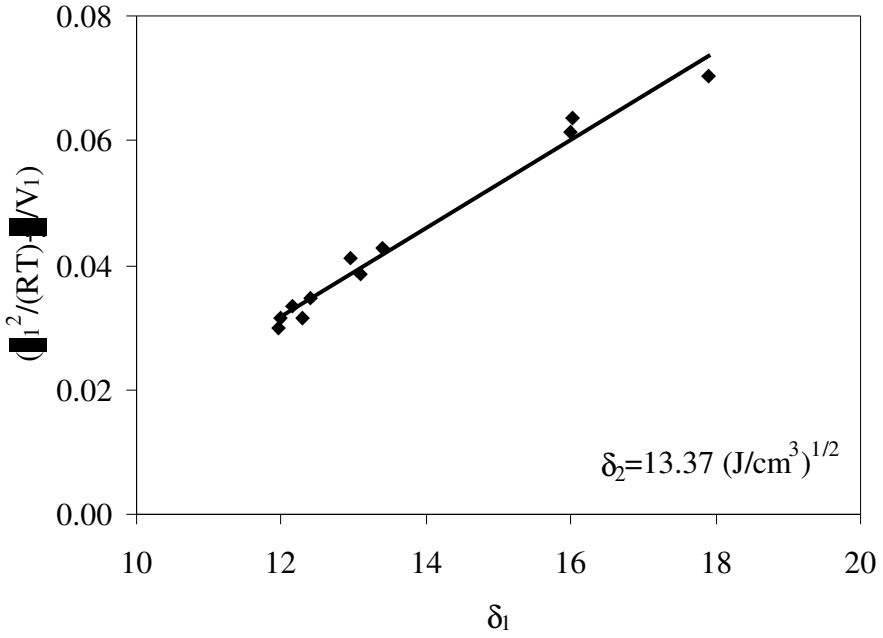

Figure 5.24.Estimation of PMMA co BMA solubility parameter at 453 K

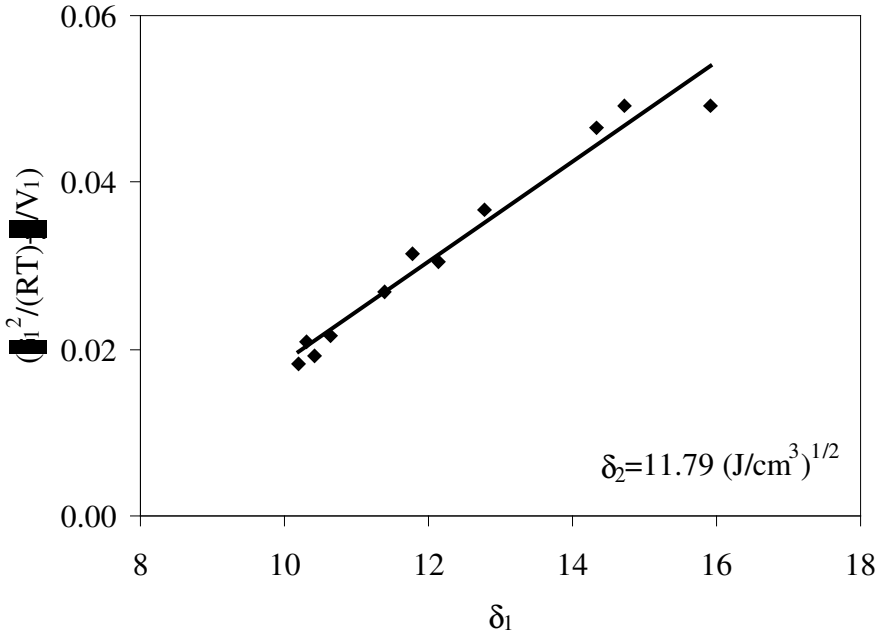

Figure 5.25. Estimation of PMMA co BMA solubility parameter at 473 K

The solubility parameters of water in PMMA co BMA were determined at 383, 403,423, 443 as 44.73, 43.86, 42.91, 41.88 J/cm^3. Since these results were so far to the polymer solubility parameter, water can be considered as a bad solvent for PMMA co BMA. This is in agreement with the interaction parameters results.

In general, the prediction of the degree of compatibility of the various solvents with PMMA co BMA using the solubility concept agreed well with that obtained through the stability analysis approach by using χ parameter.

5.3. Diffusion Measurements of PMMA co BMA-solvent systems

The partition and diffusion measurements of various solvents were performed in PMMA co BMA over a temperature range of 423-473 ^{o}K which was above the glass transition temperature of the polymer (T_g=379 ^{o}K). The diffusion and partition coefficients of methanol, ethanol, propanol, butanol, methyl acetate, ethyl acetate, propyl acetate, dichloromethane, trichloromethane, acetone, methyl methacrylate, butyl methacrylate at 403, 423, 443 and 453 K were determined by flame ionization detector and also water by thermal conductivity detector at 393, 403,423 and 443 K.

Figures 5.26 to 5.30 show the theoretical and experimental elution profiles of methanol, ethyl acetate, dichloromethane and methyl methacrylate and also water at 443 ^{o}K respectively. The points and solid lines in these figures represent the experimental and theoretical data respectively. The partition (K) and diffusion coefficients (D_p) were obtained by regressing these curves. The good agreement between experimental and CCIGC model accurately describes the chromatographic process.

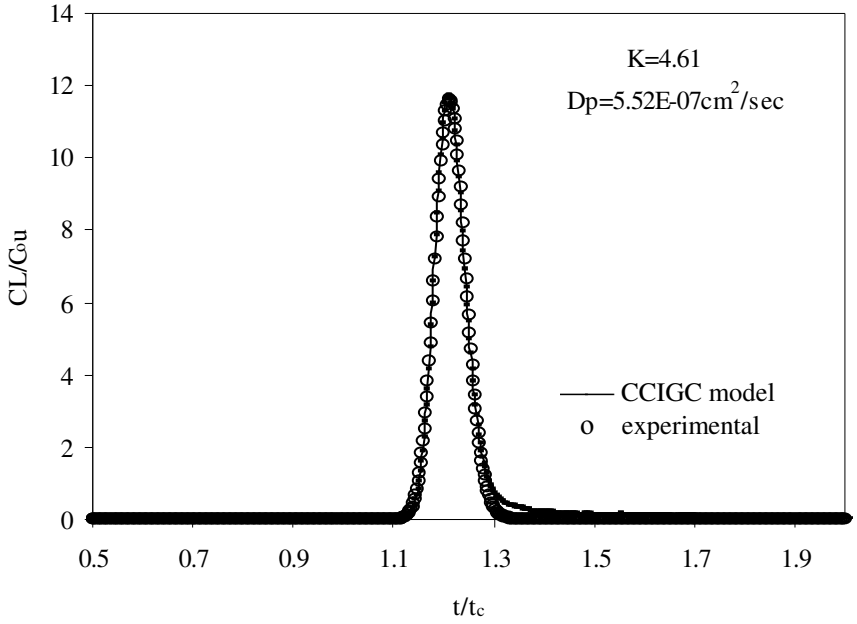

Figure 5.26.Comparison of experimental and theoretical elution profiles for PMMA co BMA- methanol system at 443 ^{o}K

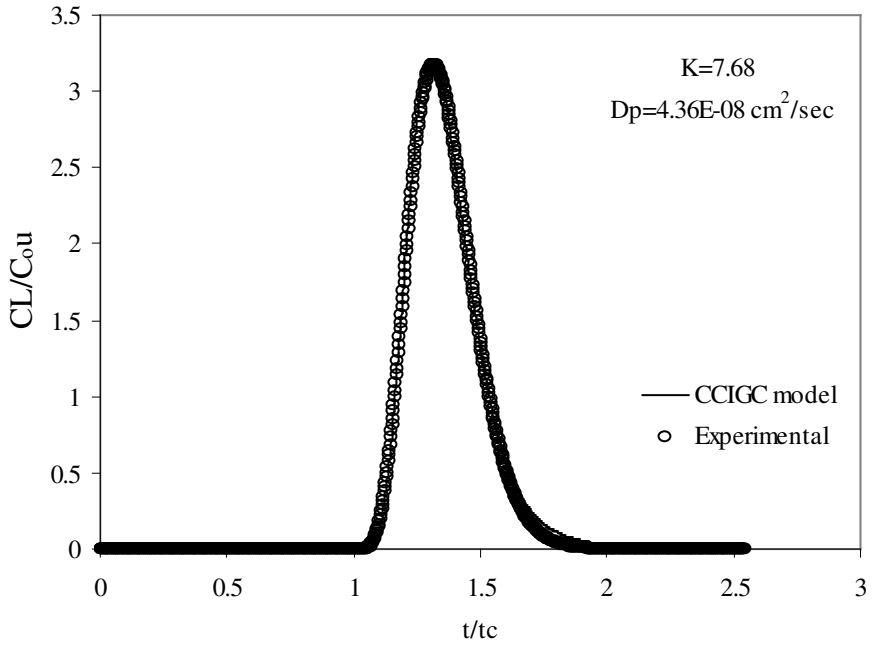

Figure 5.27.Comparison of experimental and theoretical elution profiles for PMMA co BMA- ethyl acetate system at 443 ^{o}K

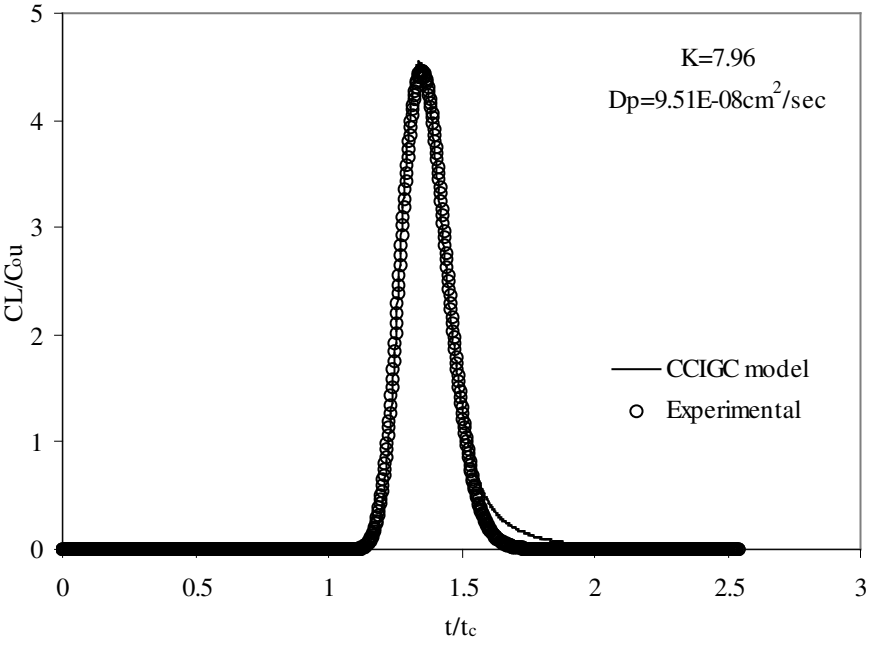

Figure 5.28.Comparison of experimental and theoretical elution profiles for PMMA co BMA- dichloromethane system at 443 ^{o}K

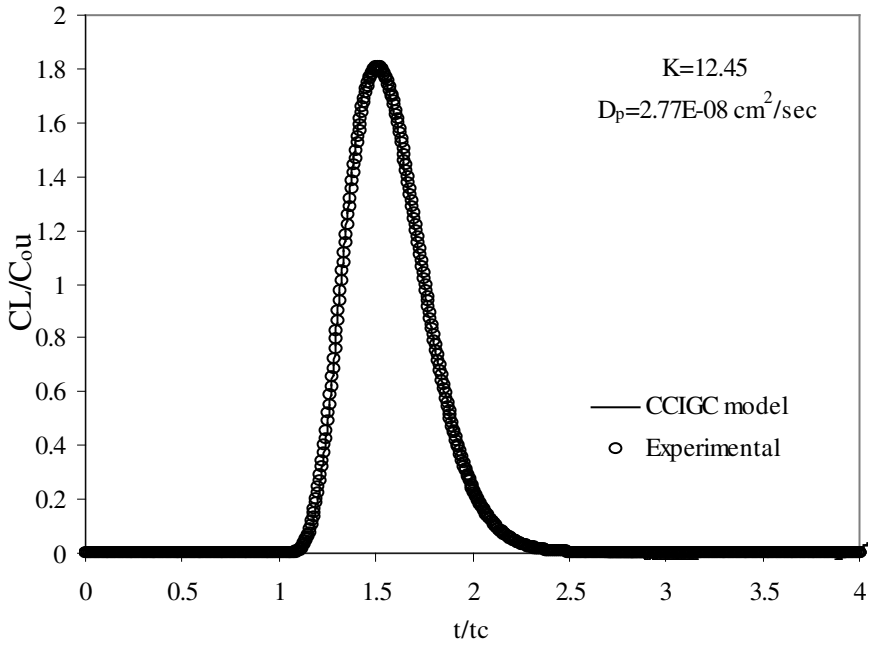

Figure 5.29.Comparison of experimental and theoretical elution profiles for PMMA co BMA-methyl methacrylate system at 443 ^{o}K

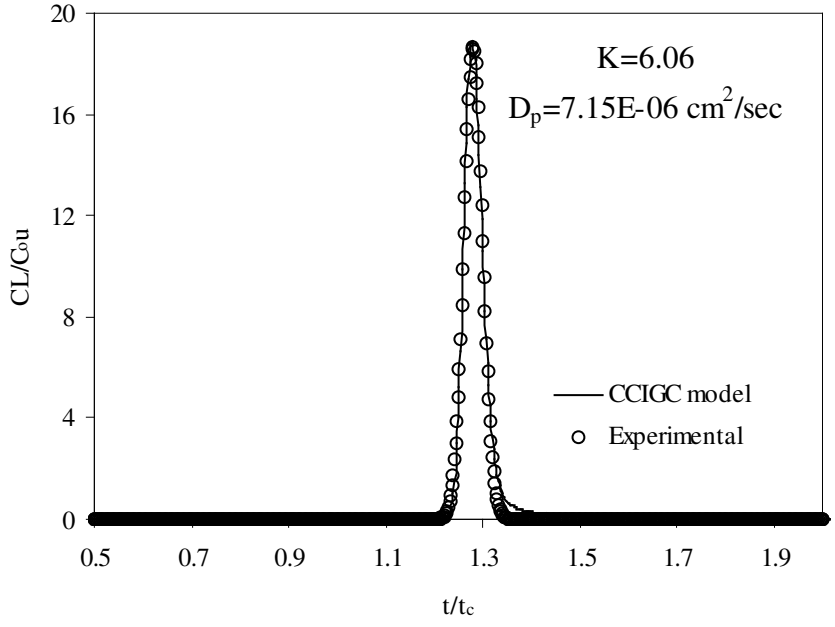

Figure 5.30.Comparison of experimental and theoretical elution profiles for PMMA co BMA-water system at 443 ^{o}K

The values of infinitely dilute partition coefficients (K) of methanol, ethanol, propanol, butanol, methyl acetate, ethyl acetate, propyl acetate, dichloromethane, trichloromethane, acetone, methyl methacrylate, butyl methacrylate at 423, 443, 453 and 473 K and also water at 383, 403, 423 and 443 K at infinite dilution were tabulated in Tables 5.5 and 5.6. respectively. These table exhibited that partition coefficient increased as temperature decreased indicating that the solvent solubility was inversely related to the temperature of the system. At the same temperature butyl methacrylate had the highest partition coefficient where as methanol had the minimum value among all the solvents. The change in partition coefficient was greater at lower temperatures. The standard deviation in K were calculated and are given in Appendix B.

Table 5.5. Partition coefficients for solvent- PMMA co BMA system

	K			
	423 K	443 K	453 K	473 K
Methanol	6.34	4.60	3.96	2.96
Ethanol	8.47	6.12	5.10	3.89
1-Propanol	14.41	10.34	8.78	6.31
1-Butanol	24.38	16.73	13.97	9.89
Methyl acetate	7.74	5.66	4.17	3.68
Ethyl acetate	10.40	7.56	6.40	4.79
Propyl acetate	15.70	11.49	9.43	7.24
Dichloromethane	10.55	7.78	6.47	5.07
Chloroform	15.75	12.93	10.20	7.96
Acetone	7.90	6.08	5.01	3.89
MMA	17.94	12.68	10.73	7.87
BMA	50.97	35.44	28.82	19.76

Table 5.6. Partition coefficients for water- PMMA co BMA system

T(K)	K
383	12.68
403	10.64
423	8.35
443	6.06

To investigate the dependence of K on temperature, K with respect to 1000/T were plotted. The functionality of log (K) with temperature is linear for all solvents studied at temperatures above the glass transition of the polymer as expected and found by other researchers (Tıhmınlıoğlu, 1998; Romdhane, 1994; Pawlisch 1987). For the alcohols butanol had the highest partition coefficient and methanol had the lowest partition coefficient since the molecular weight of butanol was greater than methanol. Figure 5.31. shows temperature dependence of alcohol series. Acetates reflected the same behavior for the molecular weight dependence of partition coefficient as shown in Figue 5.32. Propyl acetate had the highest K value at all temperatures among the acetates supporting this idea. Figure 5.32 showed the partition coefficient of acetates with respect to inverse temperature.

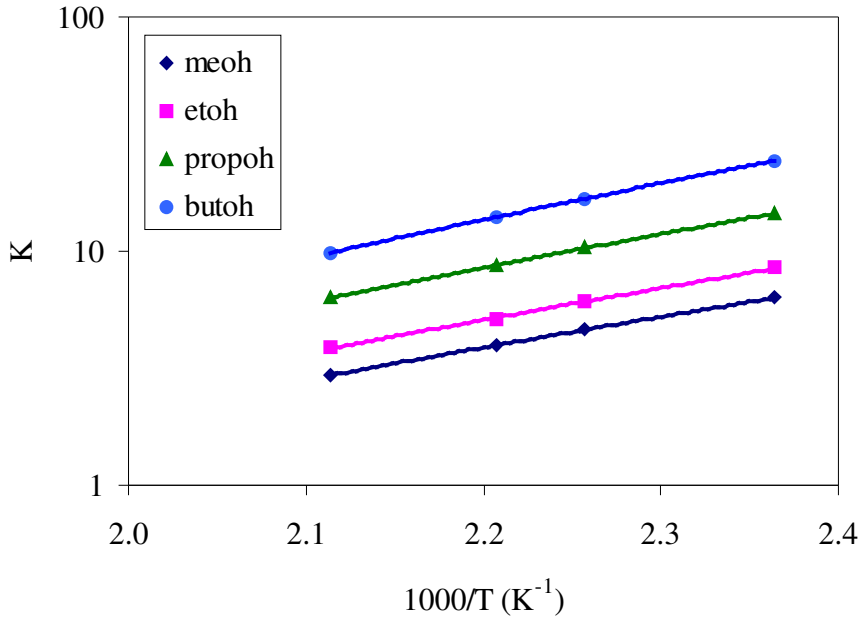

Figure 5.31. Temperature dependence of K for alcohols-PMMA co BMA system

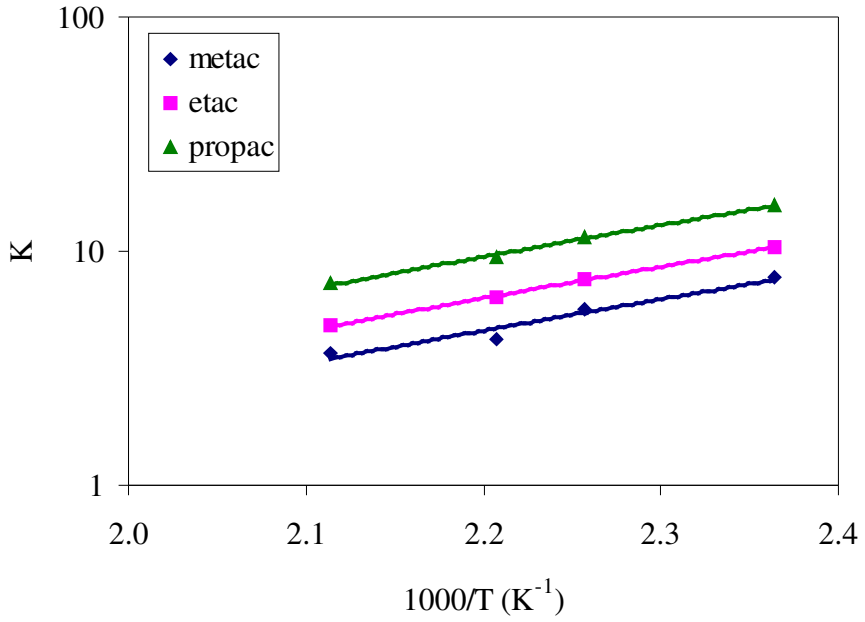

Figure 5.32. Temperature dependence of K for acetates-PMMA co BMA system

Partition coefficients for dichloromethane, trichloromethane and acetone were plotted in Figure 5.33. Among these, trichloromethane had the greatest value and acetone had the lowest at all temperatures. Temperature dependence of K of the monomers of this polymer (MMA and BMA) was shown in Figure 5.34. BMA had farly higher values than MMA. Altough molecular structure of these monomers were similar the molecular weight difference caused K values to differ from each other. Water also depicted a perfectly linear relationship with the inverse temperature supporting the other solute behavior of the system.

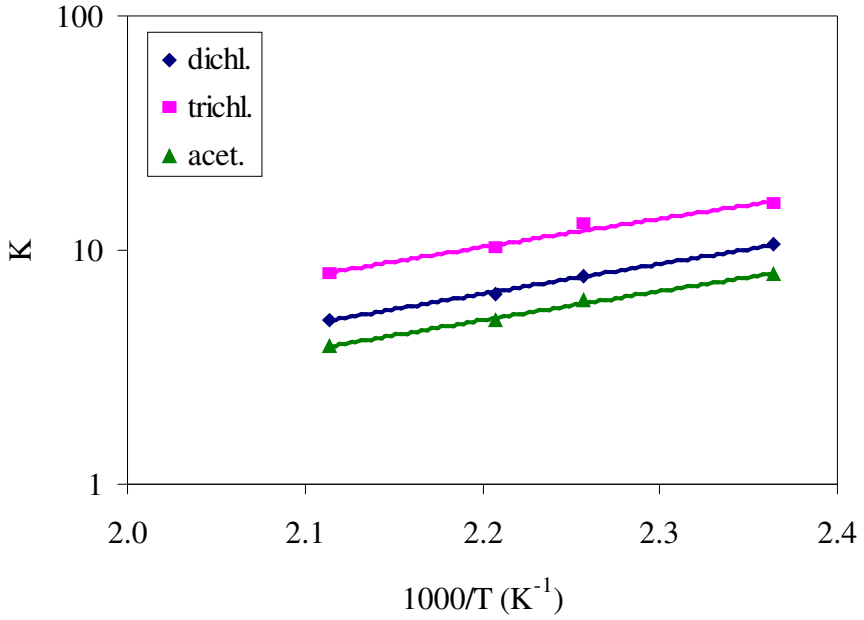

Figure 5.33. Temperature dependence of K for dichloromethane, trichloromethane, acetone-PMMA co BMA system

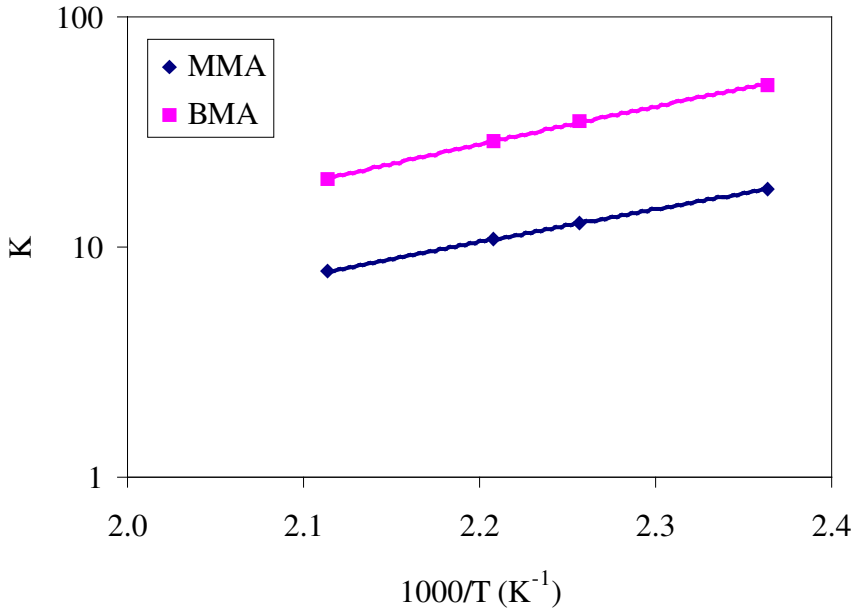

Figure 5.34. Temperature dependence of K for MMA, BMA- PMMA co BMA system

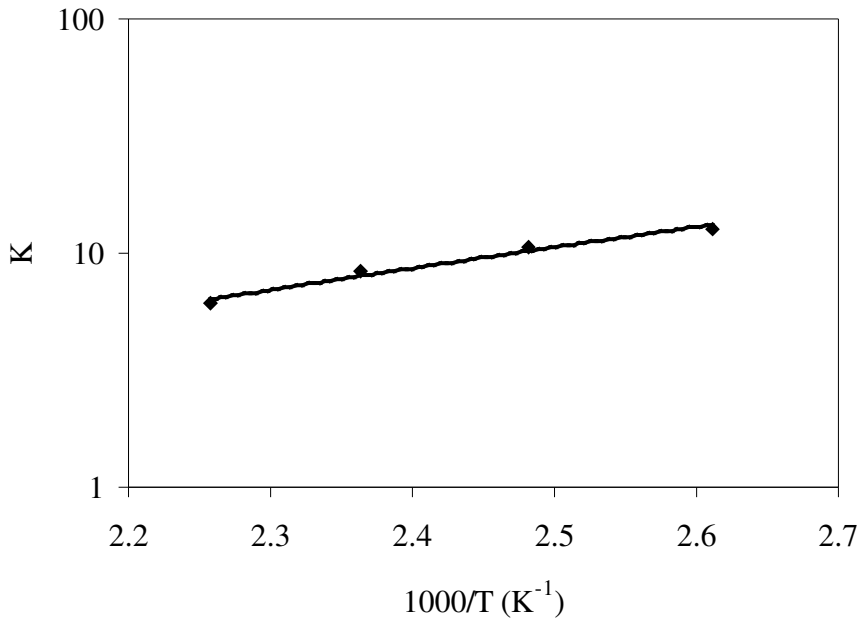

Figure 5.35 Temperature dependence of K for water- PMMA co BMA system

The reported K and Dp values were the average values of each set. So, an error analysis was performed. When standard deviation were calculated, it was in the range of 0.06 –0.4. The analyses of two samples (acetone, methyl acetate) were shown in Figures 5.36 and 5.37. These figures exhibited that the results were reproducible.

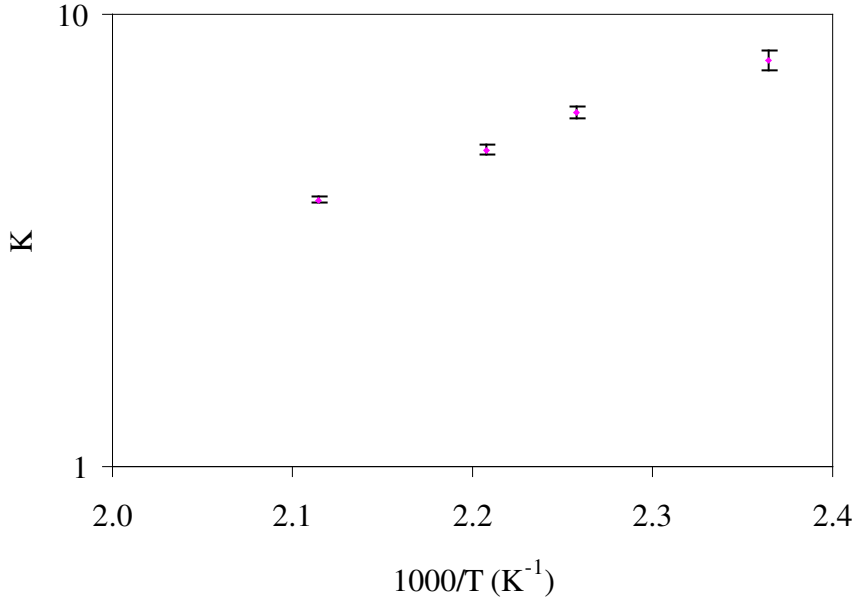

Figure 5.36. Error analysis for acetone- PMMA co BMA system

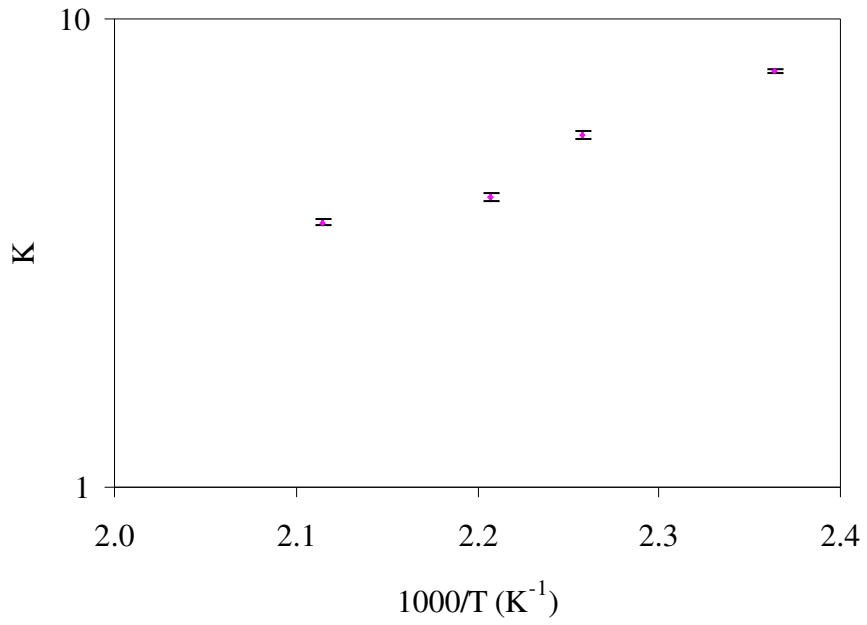

Figure 5.37. Error analysis for methyl acetate- PMMA co BMA system

The diffusion coefficients (D_p) of methanol, ethanol, propanol, butanol, methyl acetate, ethyl acetate, propyl acetate, dichloromethane, trichloromethane, acetone, methyl methacrylate, butyl methacrylate at 423, 443, 453 and 473 K and also water at 383, 403, 423 and 443 K were determined at infinite dilution and tabulated in Table 5.7. The diffusion coefficients were correlated with the free volume theory to analyze the temperature dependence of diffusion coefficients.. The free volume parameters for PMMA co BMA were determined using the data reported by Tonge et. al (2001). Tonge et. al (2001) calculated the pure PMMA and PBMA free volume parameters using viscosity versus temperature data. Free volume parameters of PMMA co BMA were calculated using the mixing rule and found as K_{22}= 93.44 K, K_{12}/γ_2=1.4x10^{-4} cm^3/gK V_2^*=0.7659 cm^3/g (Tonge, 2001). All diffusion data were regressed using two fitting parameters, Do and ξ, using non linear regression analysis.

Table 5.7. Diffusion coefficients for solvent- PMMA co BMA system

	$D_p(cm^2/sec)$			
	423 K	443 K	453 K	473 K
Methanol	2.20×10^{-7}	5.64×10^{-7}	8.05×10^{-7}	1.38×10^{-6}
Ethanol	4.36×10^{-8}	1.34×10^{-7}	2.08×10^{-7}	4.91×10^{-7}
1-Propanol	1.48×10^{-8}	5.25×10^{-8}	8.62×10^{-8}	2.41×10^{-7}
1-Butanol	8.20×10^{-9}	3.38×10^{-8}	6.24×10^{-8}	1.94×10^{-7}
Methyl acetate	2.54×10^{-8}	8.48×10^{-8}	1.39×10^{-7}	3.41×10^{-7}
Ethyl acetate	1.25×10^{-8}	4.53×10^{-8}	8.43×10^{-8}	2.34×10^{-7}
Propyl acetate	7.24×10^{-9}	2.94×10^{-8}	4.64×10^{-8}	1.45×10^{-7}
Dichloromethane	3.34×10^{-8}	9.81×10^{-8}	1.86×10^{-7}	4.42×10^{-7}
Chloroform	8.70×10^{-9}	2.81×10^{-8}	6.12×10^{-8}	1.27×10^{-7}
Acetone	2.37×10^{-8}	7.90×10^{-8}	1.36×10^{-7}	3.49×10^{-7}
MMA	7.01×10^{-9}	2.86×10^{-8}	5.25×10^{-8}	1.63×10^{-7}
BMA	2.55×10^{-9}	1.17×10^{-8}	2.30×10^{-8}	8.68×10^{-8}

The comparison of experimental diffusion coefficients and the correlated values with the free volume theory are shown in Figures 5.38 to 5.42. These figures pointed out that besides temperature effect on D, molecular size had an effect on diffusion coefficient. As molecular size increased, diffusion coefficient decreased.

In literature, to our knowledge, no one studied the diffusion or thermodynamic properties of PMMA co BMA polymer-solvent system. Diffusion data of MMA and BMA in PMMA co BMA were studied using the pulsed field gradient (PFG)- NMR sorption data of MMA and BMA in pure PMMA and PBMA polymers by Tonge et. al (2001). They obtained the diffusion coefficients at 298 K and 313 K. The diffusion coefficients of MMA in PMMA at 298 & 313 K were in the range of 3×10^{-9} m^2/s – 0.5×10^{-9} m^2/s in the polymer weight fraction of 0-0.4. The diffusion coefficients of MMA in PBMA was in the range of 3.5×10^{-9} m^2/s -1×10^{-9} m^2/s at 298 K and 6×10^{-9} m^2/s -1×10^{-9} m^2/s at 313 K in the polymer weight fraction of 0-0.4. In the same polymer weight fraction, D_p of BMA in PBMA was in the range of 1.5×10^{-9} m^2/s -0.4×10^{-9} m^2/s at 298 K and 1.3×10^{-9} m^2/s -0.5×10^{-9} m^2/s at 313 K.

Rodriguez et. al (2003) studied water vapor sorption in PMMA and found water diffusion coefficients in PMMA as 1.6 $x10^{-8}$ cm^2/s – $2.3x10^{-8}$ cm^2/s at high activities at 35 ^0C. This temperature was lower than the temperature range performed and higher values were obtained in this study.

Arnould (1989) studied diffusion of various solvents (methanol, acetone, methyl acetate, ethyl acetate, propyl acetate) in pure PMMA and they have obtained diffusion coefficients in the range of 1.29 $x10^{-7}$-7.22 $x10^{-10}$ cm^2/s at 433-343 K.

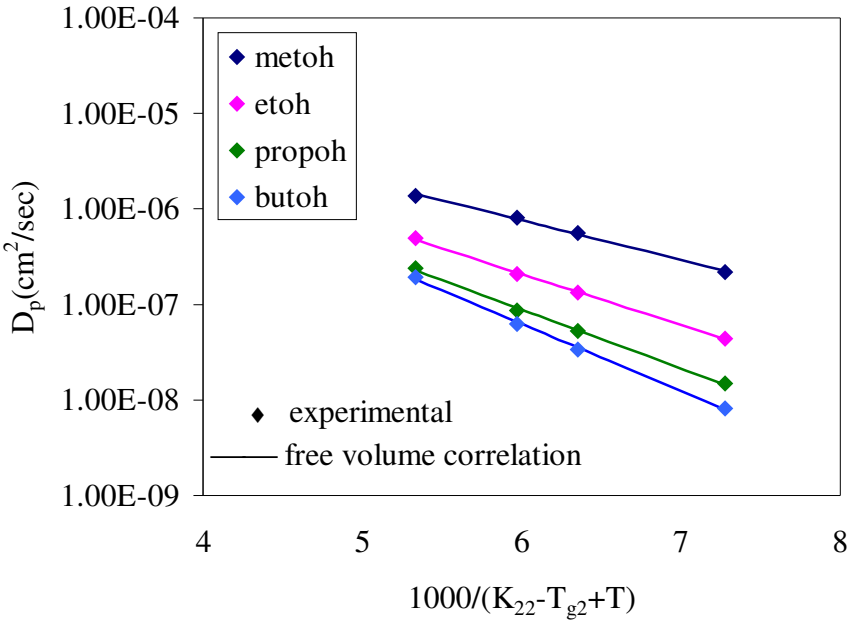

Figure 5.38 Temperature dependence of D_p for alcohols-PMMA co BMA system

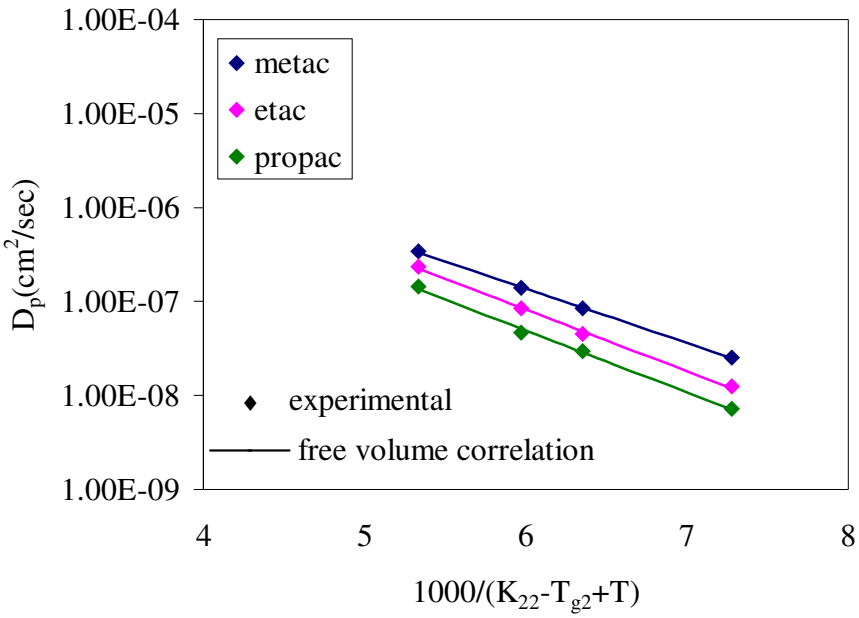

Figure 5.39. Temperature dependence of D_p for acetates-PMMA co BMA system

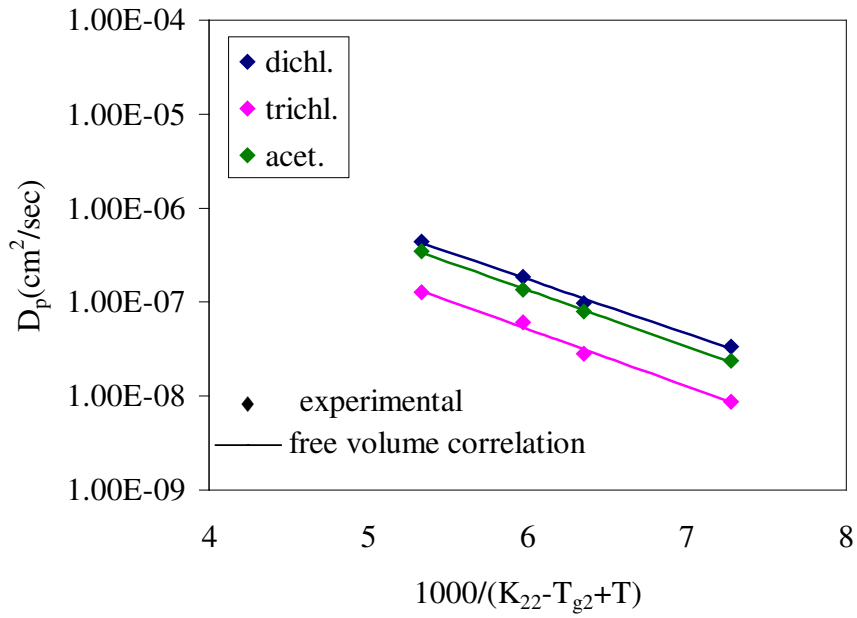

Figure 5.40.Temperature dependence of D_p or dichl.trichl.acet.-PMMA co BMA system

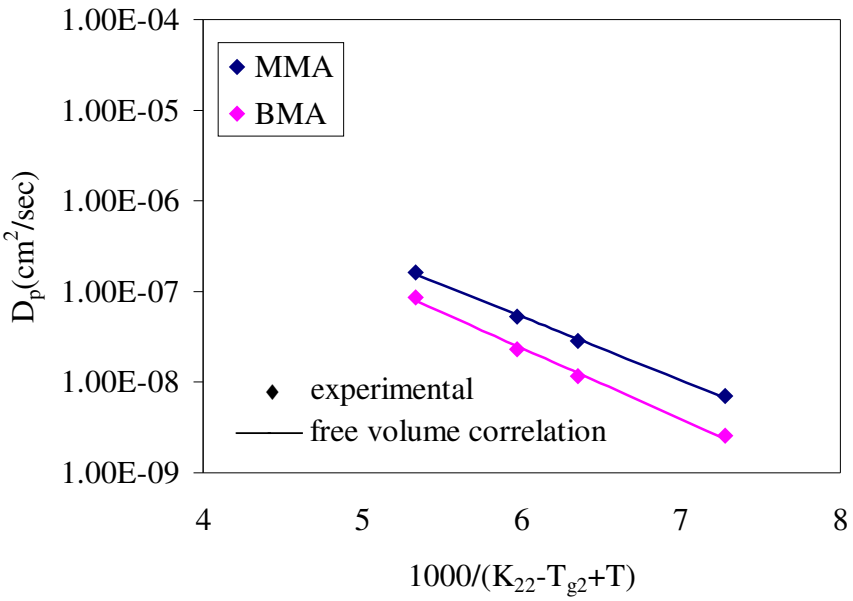

Figure 5.41. Temperature dependence of D_p for MMA, BMA- PMMA co BMA system

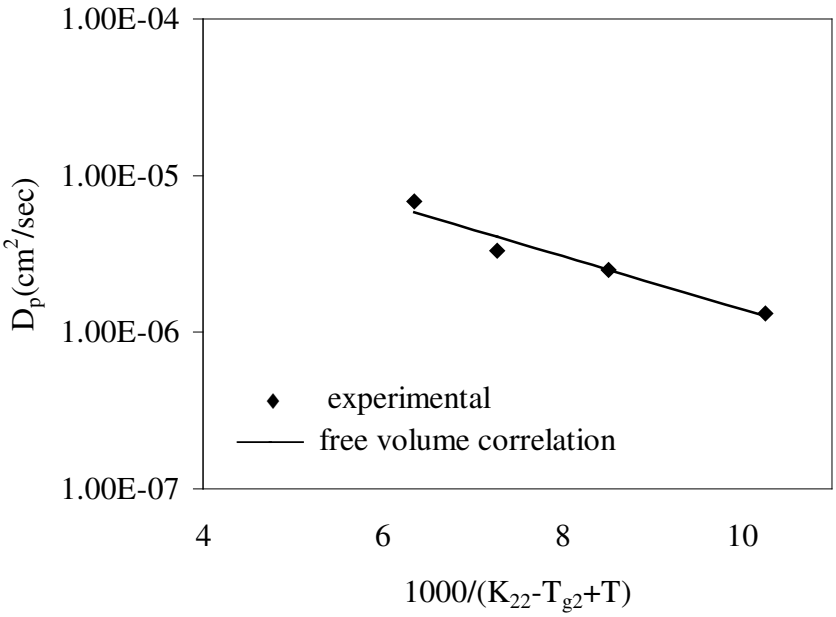

Figure 5.42. Temperature dependence of D_p for water- PMMA co BMA system

The free volume parameters of PMMA co BMA-solvent systems were tabulated in Table 5.8. From Table 5.8., one can also see that with increasing molecular size of the solvent molecule, Do and ξ also increased. The dependence of the parameter ξ on solvent molar volume at 0 ^{0}K for all solvents was presented in Figure 5.43. The data are well described by a straight line. A least squares fitting gives;

$$\xi = m\tilde{V}_1^0(0)$$

the reciprocal of slope corresponds to the critical molar volume of PMMA co BMA jumping unit. The higher the ξ can be attributed to the its geometry or its lower flexibility.

Table 5.8 Free Volume Parameters

Solutes	Do(cm^2/s)	ξ
methanol	2.28x10^{-04}	0.17
ethanol	3.54x10^{-04}	0.23
1-propanol	4.59x10^{-04}	0.26
1-butanol	1.06x10^{-03}	0.29
methyl acetate	4.11x10^{-04}	0.24
ethyl acetate	6.96x10^{-04}	0.27
propyl acetate	4.63x10^{-04}	0.28
dichloromethane	5.35x10^{-04}	0.24
trichloromethane	2.38x10^{-04}	0.26
acetone	5.37x10^{-04}	0.25
MMA	8.44x10^{-04}	0.29
BMA	1.20x10^{-03}	0.33
water	7.01x10^{-05}	0.07

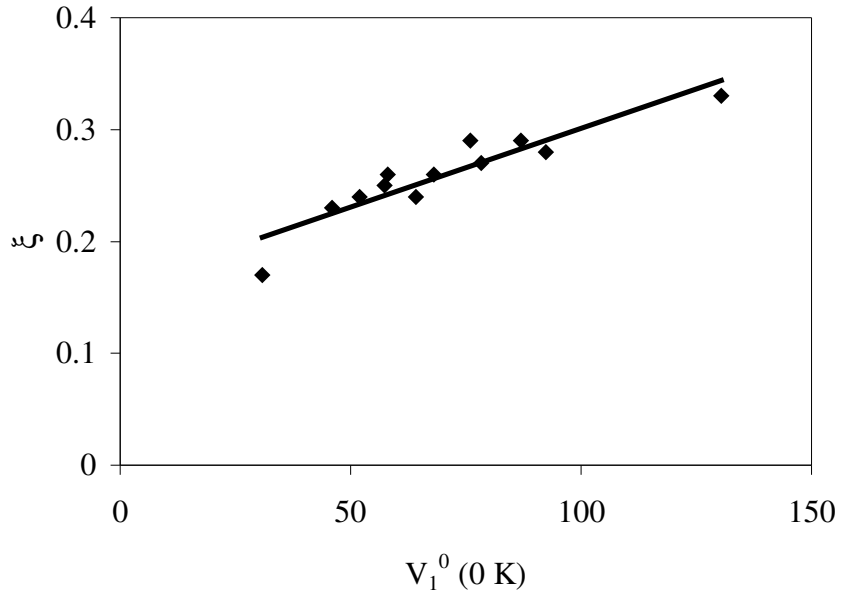

Figure 5.43. ξ versus molar volume V_1^0 (0 K) for PMMA co BMA- solvent system

The predictive capability of the theory was also tested using experimental data measured at 443, 453, 473 K. Diffusion coefficients were predicted using the free volume parameters and were in good agreement with the experimental data at 423 K. The results ($D_{pmethanol(pred)}$=2.52x10^{-7} cm^2/sec , $D_{pmethanol(exp)}$ = 2.20x10^{-7} cm^2/sec; $D_{pethanol(pred)}$=4.83x10^{-8} cm^2/sec, $D_{pethanol(exp)}$=4.36x10^{-8} cm^2/sec; $D_{pacetonel(pred)}$=1.83x10^{-8} cm^2/sec, $D_{pacetone(exp)}$=2.37x10^{-8} cm^2/sec) indicated that correlation obtained from Vrentas and Duda free volume theory can be accurately used to predict diffusivity of solvents in PMMA co BMA.

5.4 Thermodynamic Results of PLGA-Solvent Systems

Thermodynamic measurements (retention volume Vg, infinitely dilute weight fraction activity coefficient Ω_1^{∞}, polymer solvent interaction parameter χ, solvent and polymer solubility parameters δ_1 δ_2), partition coefficients (K) and diffusion coefficients (D_p) of solvents were determined for PLGA –solvent systems by inverse gas chromatography. The measurements were performed at four different temperatures (353, 363, 373, 393 K) for acetone, dichloromethane, trichloromethane, ethyl acetate, ethyl alcohol, tetrahydrofuran and water.

5.4.1 Retention Volume (V_g)

Retention volume (V_g) of the solvents which is a key parameter and basic step for thermodynamic properties were determined according to Eqn. (2.1.). The values were tabulated in Table 5.9. As temperature increased retention volume decreased exhibiting the equilibrium sorption occured in this temperature range as explained in Section 2.2.1. Trichloromethane had the highest value and tetrahydrofuran had the lowest value for all temperatures. Ln V_g versus 1/T was plotted for all the solvents and the results were shown in Figures 5.44. and 5.45. Retention volume depicted linear behavior with the inverse temperature which again showed that V_g for acetone and dichloromethane were similar to each other.

Table 5.9. Retention volumes for PLGA -solvent systems

	Vg (cm^3/g)			
Solutes	353 K	363 K	373 K	393 K
acetone	19.79	16.07	12.25	7.06
dichloromethane	19.73	14.69	11.52	7.00
trichloromethane	34.39	22.33	18.10	10.12
ethyl acetate	15.15	14.63	12.36	6.90
ethyl alcohol	17.22	13.51	10.76	4.13
THF	13.52	12.08	10.20	6.88
water	25.58	18.33	13.47	7.72

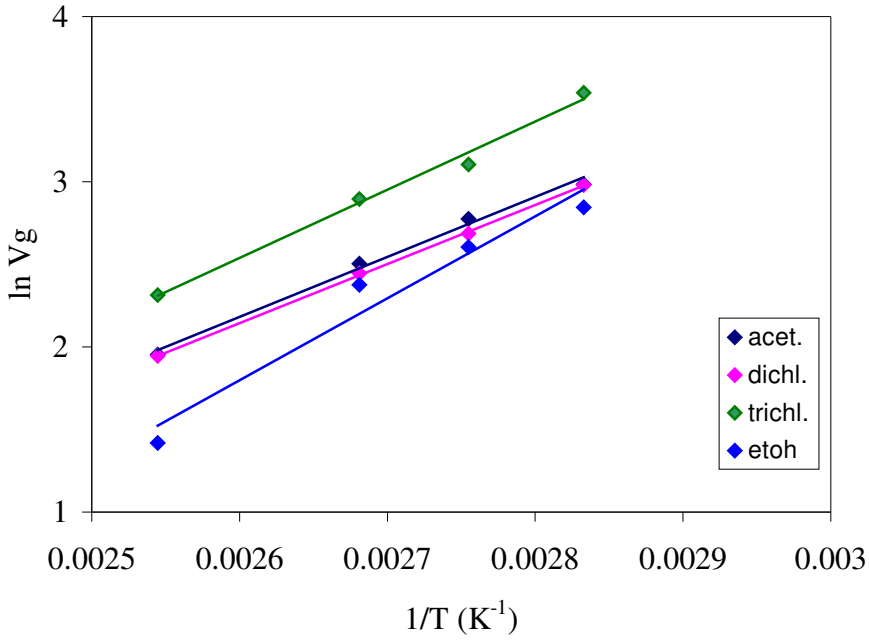

Figure 5.44. Temperature dependence of ln V_g for the acet., dichl., trichl., etoh in PLGA

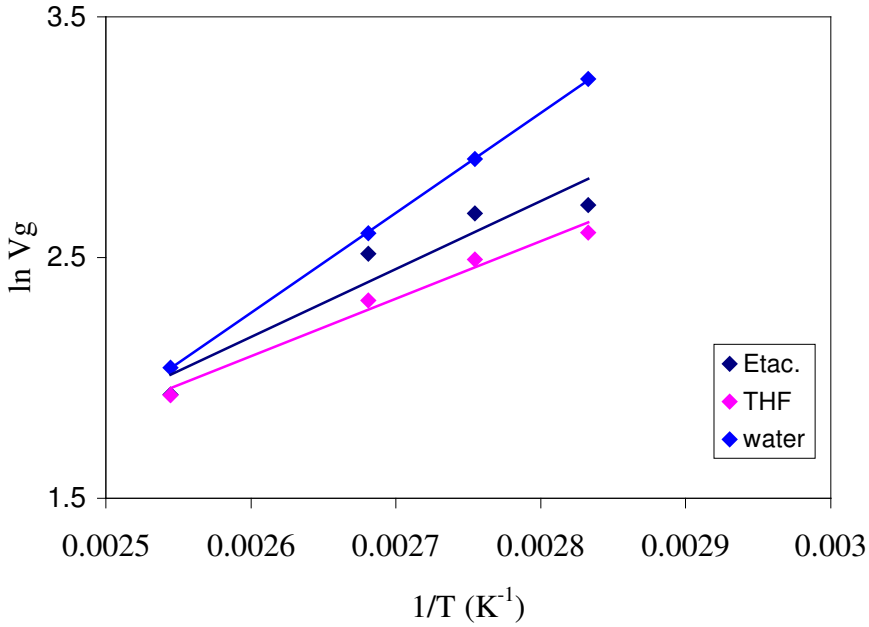

Figure 5.45. Temperature dependence of ln V_g for the Etac., THF, water in PLGA

5.4.2 Weight Fraction Activity Coefficient (WFAC) (Ω_1^∞)

The weight fraction activity coefficient of the solvents which were determined from Eqn (2.3.) were listed in Table 5.10. Water had the highest value among all the solvents with very high values again showing the poor solvent property for this polymer. Since $\Omega_1^\infty<5$ for good solvents which was indicated in Section 2.2.2., trichloromethane was found to be the most suitable solvent for this polymer. Also, dichloromethane had close values to 5 and may be considered a suitable solute for this polymer after trichloromethane. Ω_1^∞ showed weak dependence to temperature except for water which exhibited a decrease in Ω_1^∞ as temperature increased. The temperature dependence of the weight fraction activity coefficient of the solvents were shown in Figures 5.46 to 5.48.

Table 5.10. Weight Fraction Activity coefficients for PLGA-solvent systems

	Ω_1^∞			
Solutes	353 K	363 K	373 K	393 K
acetone	12.43	11.98	12.52	14.47
dichloromethane	5.31	5.73	5.98	6.87
trichloromethane	4.11	4.97	4.89	5.85
ethyl acetate	20.54	16.12	14.76	16.76
ethyl alcohol	35.18	31.86	29.15	43.06
THF	19.94	17.40	16.34	16.01
water	135.46	131.53	127.52	120.36

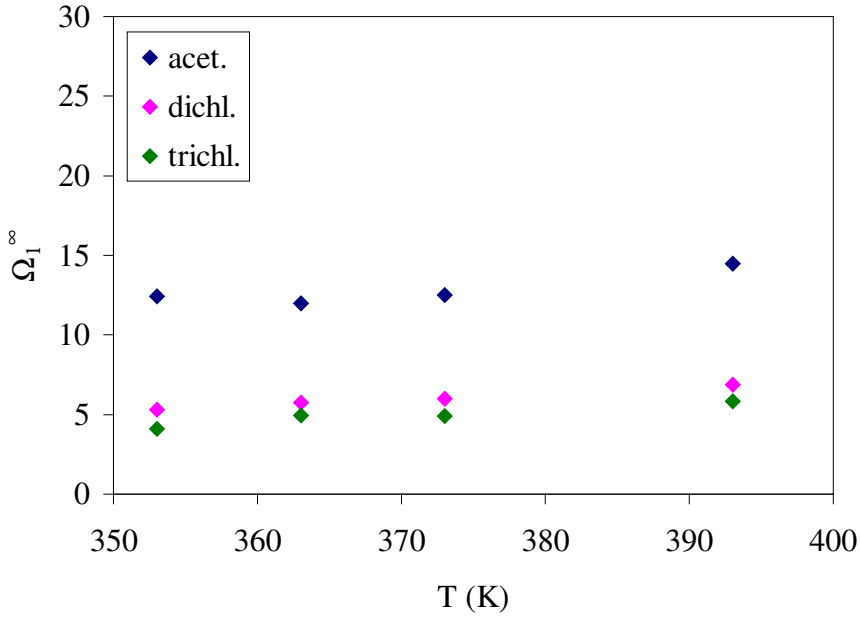

Figure 5.46. Temperature dependence of Ω_1^∞ for acet., dichl., trichl. in PLGA

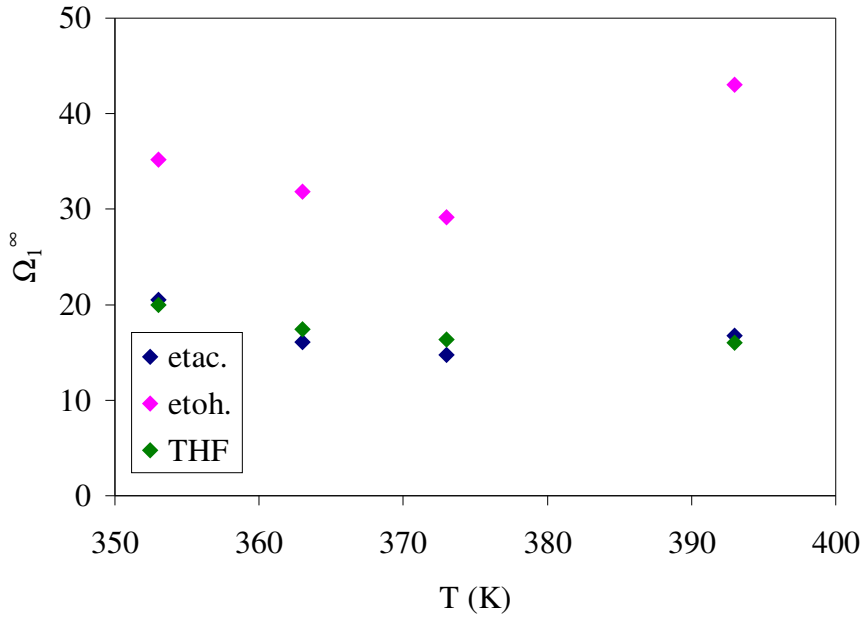

Figure 5.47. Temperature dependence of Ω_1^∞ for etac., etoh, thf in PLGA

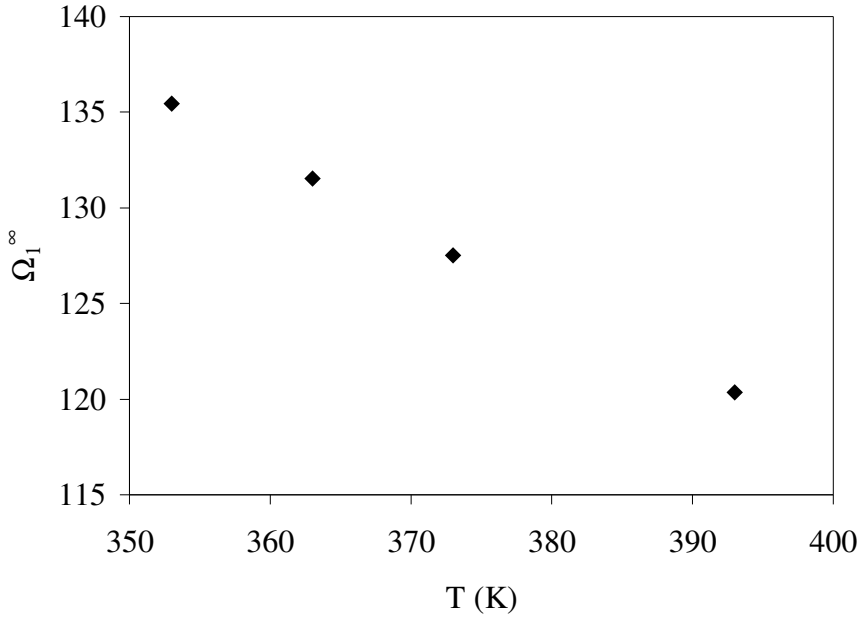

Figure 5.48. Temperature dependence of Ω_1^∞ for water in PLGA

5.4.3. Flory Huggins Interaction Parameter (χ)

Flory Huggins interaction parameter of 7 solvents at four different temperatures (353, 363, 373, 393 K) were determined by using Eqn (2.4.) and the values were tabulated in Table 5.11. Since χ of a solute should be less than 0.5 to be a good solvent for the polymer according to this criteria, it can be expressed as none of the solvents were good solvents for this polymer. But, among them, trichloromethane can be considered as the most suitable one with its close values to 0.5. After trichloromethane, dichloromethane can also be considered a suitable solvent for PLGA. On the other hand, considering all of the solvents studied in this study, water had the highest χ value at all temperatures. This indicated again and confirmed with the other thermodynamic results and water was found the worst solvent among the studied solvents for PLGA showing no affinity to this polymer. Figures 5.49. and 5.50. show the temperature dependence of interaction parameters in PLGA for acetone, dichloromethane, trichloromethane; ethyl acetate, ethyl alcohol, tetrahydrofuran, water respectively.

Table 5.11. Interaction parameters of PLGA-solvent systems

	χ			
Solutes	353 K	363 K	373 K	393 K
acetone	0.98	0.92	0.94	1.05
dichloromethane	0.64	0.70	0.73	0.82
trichloromethane	0.52	0.69	0.66	0.81
ethyl acetate	1.62	1.36	1.25	1.34
ethyl alcohol	2.04	1.92	1.82	2.18
THF	1.58	1.43	1.35	1.30
water	3.68	3.64	3.61	3.54

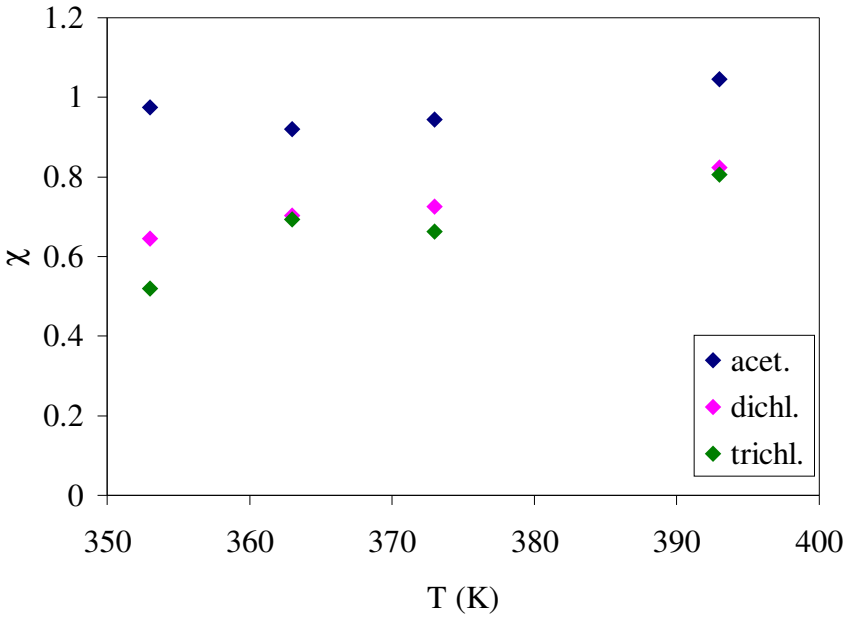

Figure 5.49.Temperature dependence of χ for acetone, dichl., trichl. in PLGA

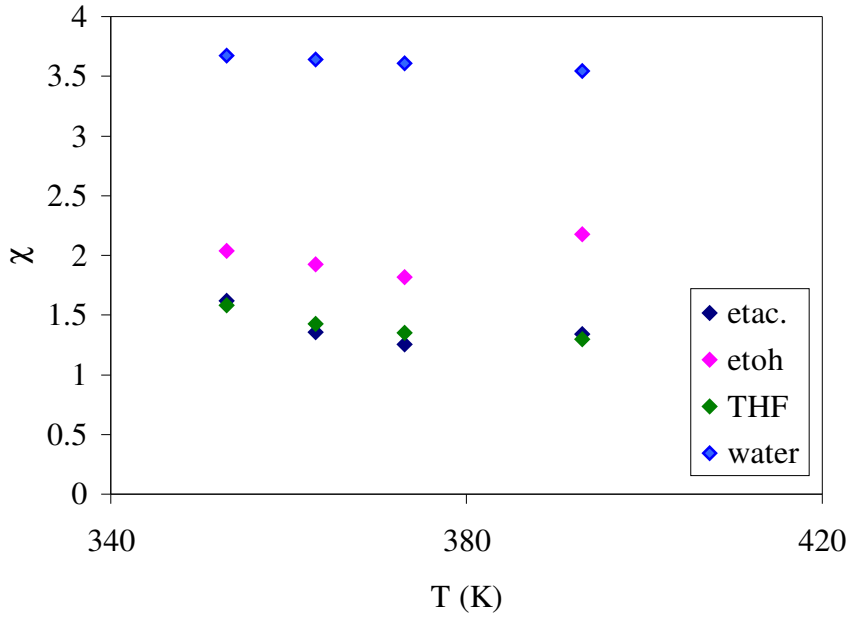

Figure 5.50.Temperature dependence of χ for etac, etoh, THF, water in PLGA

5.4.4. Solubility Parameter (δ)

Solute solubility parameters were computed through Equation 2.4. In this eqn, the molar volume and latent heat of vaporization were obtained for each solute at appropriate temperatures from Chemcad. The calculated values of δ_1 were compiled in Table 5.12.

Table 5.12. Solute solubility parameters (δ_1)

solutes	δ_1 $(J/cm^3)^{1/2}$			
	353 K	363 K	373 K	393 K
acetone	17.76	17.35	16.92	15.99
dichloromethane	18.05	17.58	17.10	16.07
trichloromethane	17.16	16.81	16.45	15.69
ethylacetate	16.50	16.14	15.75	14.95
ethylalcohol	24.06	23.58	23.08	22.01
thf	17.32	16.96	16.59	15.81
water	45.92	45.53	45.14	44.30

A least- square analysis of plots of $(\delta_1^2/(RT)- \chi/V_1)$ versus δ_1 was carried out to obtain the PLGA solubility parameters at 353, 363, 373, 393 K. These plots give a slope of $2\delta_2^{\infty}/(RT)$ and an intercept of $-(\delta_2^{\infty 2}/(RT) + \chi V_1)$. Figures 5.51. to 5.54. show solubility parameters for different solvents at four temperatures (353, 363, 373, 393 K) respectively. Solubility of PLGA at four different temperatures were determined and the values were 21.86, 21.28, 20.78, 19.77 $(J/cm^3)^{1/2}$ respectively.

If solvent solubility parameters, δ_1 listed in Table 5.12. were compared with the estimated PLGA solubility parameter, dichloromethane and trichloromethane possessed the closest solubility parameters to that of PLGA, indicating their strong solvency power, just as predicted through the other interaction parameters. Water, on the other hand, with its higher solubility parameters was a poor solvent of PLGA, in agreement with the conclusions based on the other parameters.

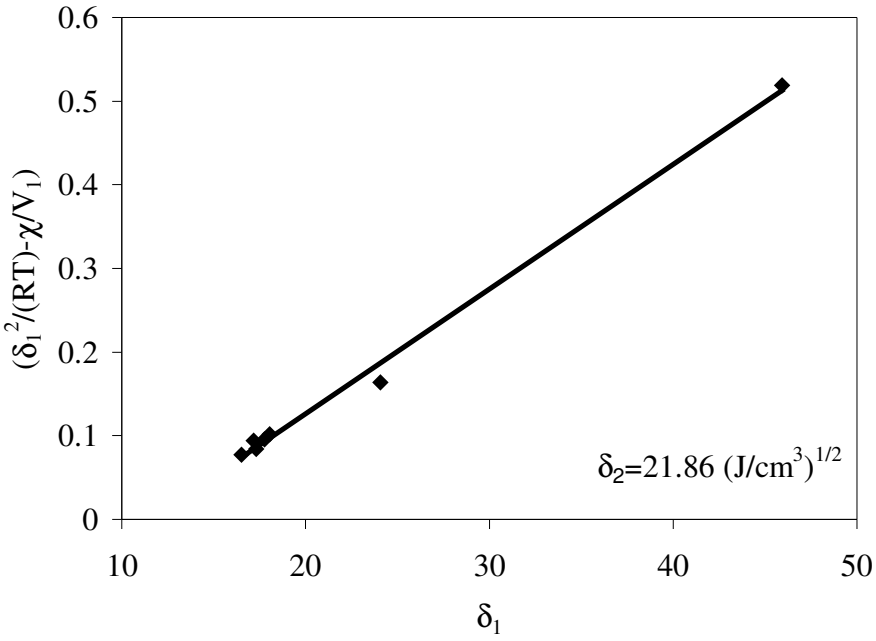

Figure 5.51.Estimation of PLGA solubility parameter at 353 K

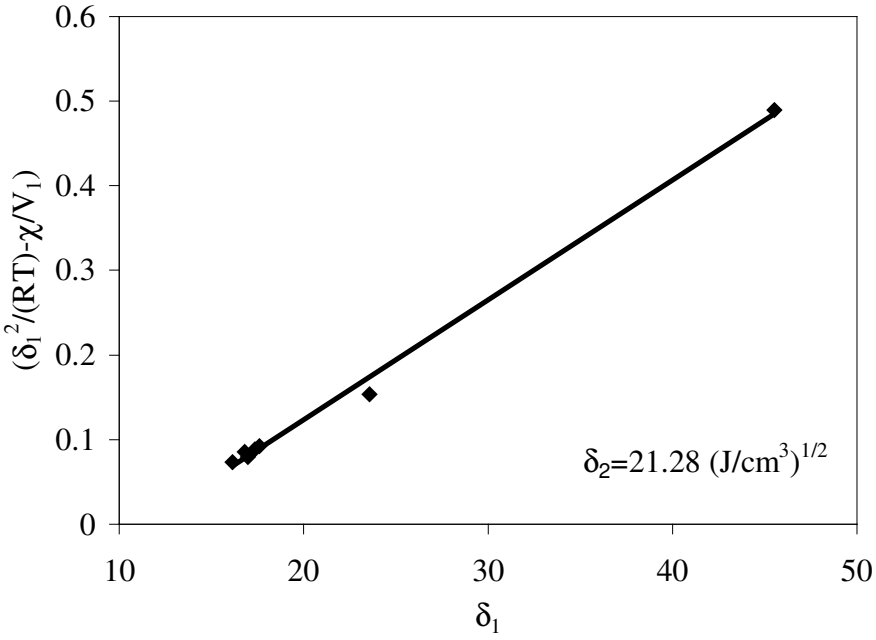

Figure 5.52. Estimation of PLGA solubility parameter at 363 K

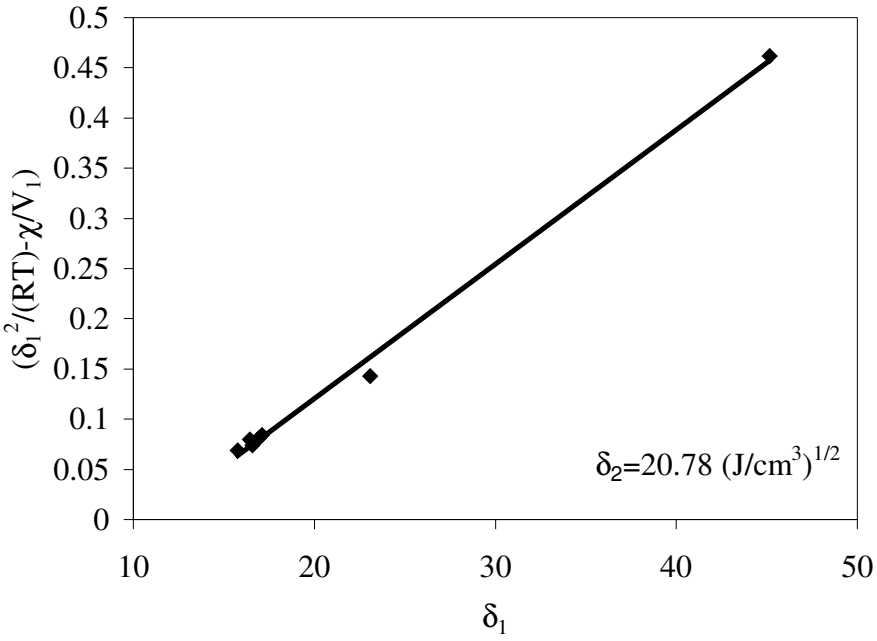

Figure 5.53. Estimation of PLGA solubility parameter at 373 K

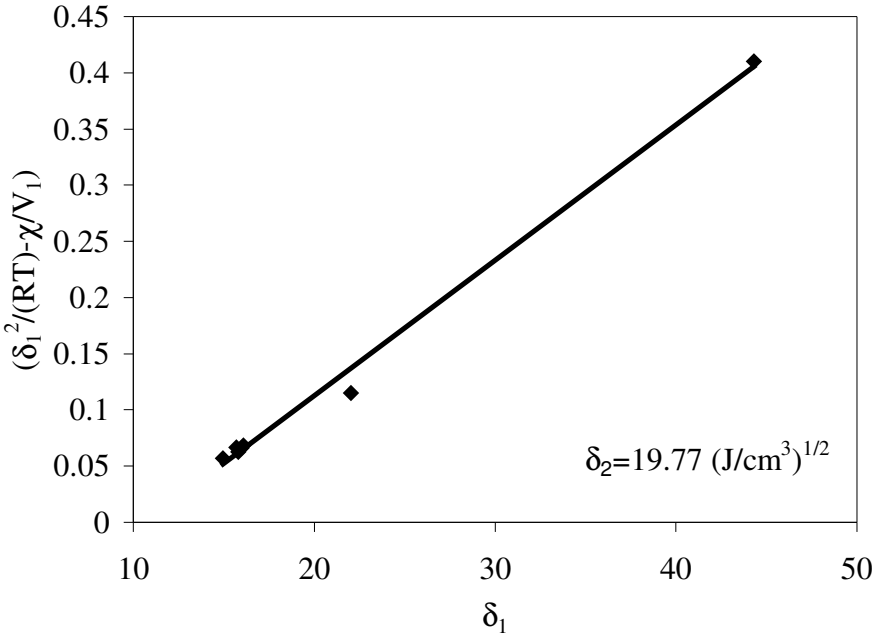

Figure 5.54. Estimation of PLGA solubility parameter at 393 K

The solvents studied in this study were used by many researchers. Liu et. al (2003) prepared PLGA microspheres using dichloromethane as the solvent. Engelberg et. al (1991) prepared PLGA films and films were cast in dichloromethane at room temperature. Price at. al (1996) used PLGA as the biodegradable carrier and gentamicin as the antiobiotic. They mixed PLGA with gentamicin sulfate in a dichloromethane solution. Karp et. al (2002) prepared PLGA films and they dissolved PLGA in trichloroform solution. So, the literature studies supported our results indicating that trichlot,romethane and dichloromethane are the most suitable solvents for PLGA.

5.5. Diffusion Measurements of PLGA-solvent systems

The partition and diffusion measurements of acetone, dichloromethane, trichloromethane, ethyl acetate, ethyl alcohol, tetrahydrofuran and water were performed in PLGA by thermal conductivity detector over a temperature range of 353-393 ^{o}K which was above the glass transition temperature of the polymer (T_g= 315 ^{o}K).

Figures 5.55 and 5.56 show the theoretical and experimental elution profiles of ethyl alcohol at 373 K and ethyl acetate at 363 K respectively. The points and solid lines in these figures represent the experimental and theoretical data respectively. The partition (K) and diffusion coefficients (D_p) were obtained by regressing these curves. These curves exhibited that the model described the data well.

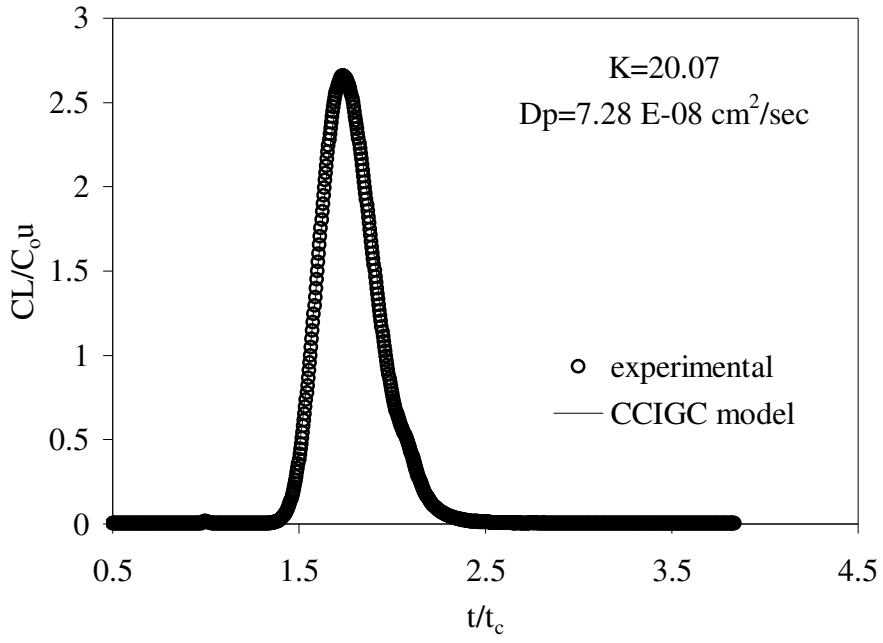

Figure 5.55. Comparison of experimental and theoretical elution profiles for PLGA ethyl alcohol system at 373 K

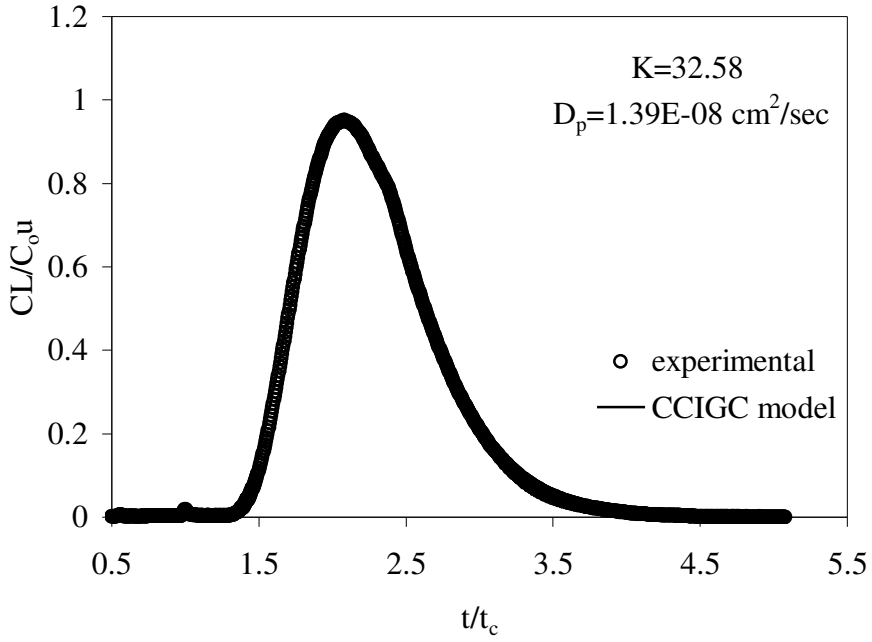

Figure 5.56. Comparison of experimental and theoretical elution profiles for PLGA-ethyl acetate system at 363 K

The values of infinitely dilute partition coefficients (K) of acetone, dichloromethane, trichloromethane, ethyl acetate, ethyl alcohol, tetrahydrofuran and water at 353, 363, 373, 393 K were tabulated in Table 5.13. This table exhibited that partition coefficient increased as temperature decreased indicating that the solvent solubility was inversely related to the temperature of the system. Among all the solvents, trichloromethane had the highest partition coefficient value where as ethyl alcohol had the lowest one.

Table 5.13. Partition coefficients for PLGA- solvent systems

Solutes	353 K	363 K	373 K	393 K
Acetone	38.22	30.12	23.49	15.28
Dichloromethane	33.30	25.73	21.90	13.51
Trichloromethane	53.62	39.95	31.72	20.48
Ethyl acetate	39.37	32.58	25.79	16.45
Ethyl alcohol	32.07	25.41	20.19	12.71
Tetrahydrofuran	35.03	28.98	24.22	16.42
Water	46.46	35.55	28.09	18.04

Temperature dependence of the partition coefficients for the solvents were plotted in Figure 5.57 and 5.58. The functionality of log (K) with temperature was linear for all the solvents studied at temperatures higher than the glass transition of the polymer as expected and found by other researchers. (Tıhmınlıoğlu, 1998; Romdhane, 1994; Pawlisch 1987)

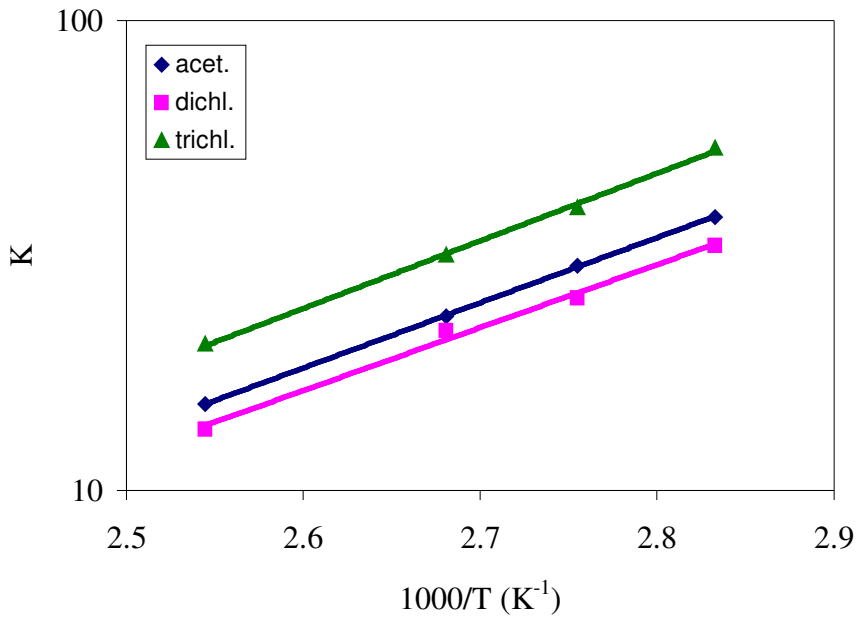

Figure 5.57. Temperature dependence of K for acet., dichl., trichl. – PLGA system

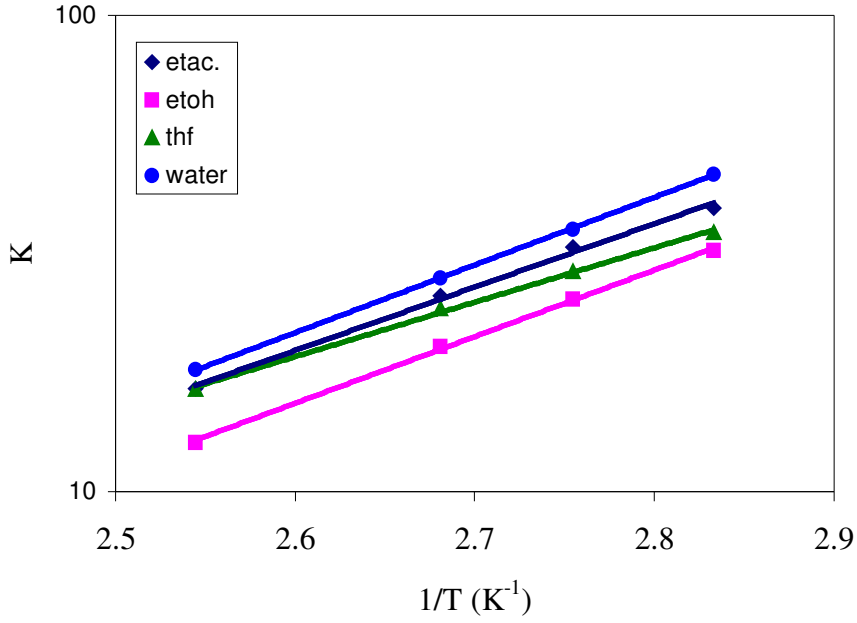

Figure 5.58. Temperature dependence of K for etac., etoh., thf, water. – PLGA system

The infinitely dilute diffusion coefficients of acetone, dichloromethane, trichloromethane, ethyl acetate, ethyl alcohol, tetrahydrofuran and water at 353, 363, 373, 393 D_p were tabulated in Table 5.14. Water had the highest diffusion coefficient values ($5.3x10^{-7}$-$2.1x10^{-6}$ cm^2/s) at all temperatures and tetrahydrofuran had the lowest D_p value ($4.4\ x10^{-9}$-$1.2x10^{-7}$ cm^2/s). The temperature dependence of D_p were plotted for these solvents and shown in Figure 5.59. and 5.60. These figures pointed out that diffusion coefficient was dependent on temperature since D_p increased as temperature increased.

Table 5.14. Diffusion coefficients of PLGA- solvent system

	D_p (cm^2/sec)			
Solutes	353 K	363 K	373 K	393 K
Acetone	$7.01x10^{-9}$	$2.23x10^{-8}$	$6.83x10^{-8}$	$2.57x10^{-7}$
Dichloromethane	$1.09x10^{-8}$	$3.08x10^{-8}$	$9.11x10^{-8}$	$3.49x10^{-7}$
Trichloromethane	$6.02x10^{-9}$	$1.42x10^{-8}$	$3.72x10^{-8}$	$1.76x10^{-7}$
Ethyl acetate	$5.10x10^{-9}$	$1.39x10^{-8}$	$3.71x10^{-8}$	$1.59x10^{-7}$
Ethyl alcohol	$1.03x10^{-8}$	$1.39x10^{-8}$	$7.28x10^{-8}$	$3.08x10^{-7}$
Tetrahydrofuran	$4.40x10^{-9}$	$1.02x10^{-8}$	$2.78x10^{-8}$	$1.19x10^{-7}$
Water	$5.31x10^{-7}$	$8.43x10^{-7}$	$1.25x10^{-6}$	$2.09x10^{-6}$

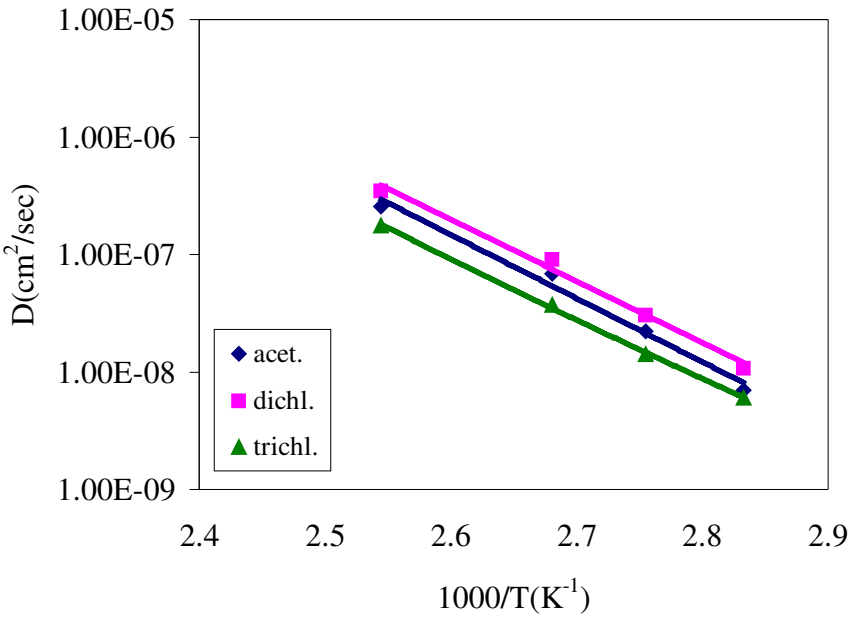

Figure 5.59. Temperature dependence of D_p for various solvents in PLGA

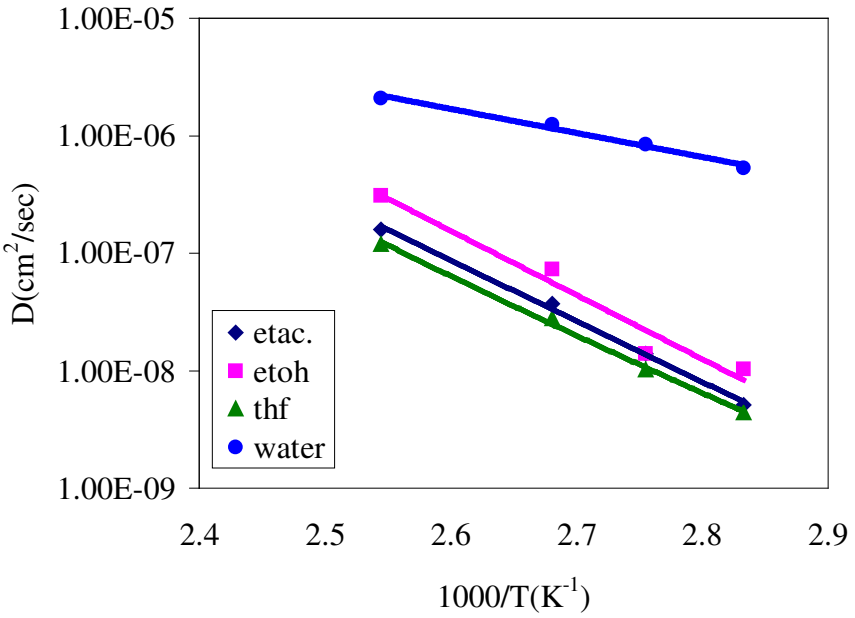

Figure 5.60. Temperature dependence of D_p for various solvents in PLGA

CHAPTER 6

CONCLUSIONS AND SUGGESTIONS FOR FUTURE STUDIES

Polymer- solvent interactions, partition and diffusion coefficients at infinite dilution of solvent were obtained for various solvents in two different polymers by inverse gas chromatography (IGC). Since IGC technique is rapid, simple, reliable; this tecnique has been preferred by many authors to obtain polymer- solvent interactions. In this study, both thermodynamic and diffusion measurements were performed by this technique.

The polymers used in this study were poly (methyl methacrylate co butyl methacrylate) (PMMA co BMA) and poly (lactide co glycolide) (PLGA). PMMA co BMA had a composition of 85% (by weight) MMA, 15% BMA and PLGA had a composition of 65% (by weight) D-L lactic acid, 35% glycolic acid. The characterization results showed that the PMMA co BMA had glass transition temperature of 106 ^{0}C, degradation temperature of 250 ^{0}C and PLGA had glass transition temperature of 42 ^{0}C, degradation temperature of 240 ^{0}C. Since the equilibrium bulk sorption was achieved at temperatures in excess of about T_g+50 ^{o}C for most common polymers, the experiments were performed in the range of 150-200 ^{0}C for PMMA co BMA and 80-120 ^{0}C for PLGA which are above the glass transition temperature and below the degradation temperature of the polymer.

Thermodynamic results obtained in this study were used revealed useful information about the degree of compatibility between the polymers and the various solvents used. The weight fraction activity coefficient Ω_1^∞, Flory Huggins interaction parameters χ of various solvents in PMMA co BMA and in PLGA were determined and trichloromethane and dichloromethane were obtained as the most suitable solvents for both of the polymers. Water showed no affinity for these polymers at all with its high Ω_1^∞ and χ values. The solubility parameters of both solvents (δ_1) and polymers (δ_2) were also estimated. The prediction of the degree of compatibility of the various solvents with PMMA co BMA and PLGA using the solubility concept agreed well with that obtained through the stability analysis approach by using χ parameter.

The mathematical model derived by Pawlisch et al. (1987) for calculating the partition and diffusion coefficients of solvents in polymers at infinite dilute of solvent

was used. The optimum K and D_p values that best fit the data were well found and the model predicted the experimental data well. The effect of temperature on partition and diffusion coefficients was investigated and it was observed that as temperature increased partition coefficient decreased where as diffusion coefficient increased. Vrentas –Duda free volume theory was used to correlate the diffusion coefficients and free volume parameters of various solvents in PMMA co BMA polymer were calculated by regression method. The results indicated that the diffusion data were correlated by the free volume theory.

Investigations done in this thesis have led to some suggestions for future work. For instance, other applications of inverse gas chromatography can be considered. The laboratory equipment could be modified to extend finite concentration of the solute in the stationary phase or conventional techniques (sorption) could be applied to these polymers to measure diffusion coefficients. Vrentas – Duda free volume theory can be used to correlate the diffusion data in finite concentration range. So, both temperature and concentration effect on diffusion and partition coefficients could be observed. Also, the free volume parameters of PLGA polymer could be calculated and the diffusion data of solvents in this polymer could be investigated.

REFERENCES

- Aris, R., "On the dispersion of a solute in a fluid flowing through a tube", *Proc. R. Soc.* London, A235, **67**, (1959)

- Arnould, D., D., "Capillary column inverse gas chromatography for the study of diffusion in polymer solvent systems, "Ph D. University of Massachusetts," (1989)

- Bearman, R.,J., "On the molecular basis of some current theories of diffusion, "*J of Phys., Chem.*, **65**, (1961)

- Braun, J.,M.; Guillet, J.,E., "Study of polymers by inverse gas chromatography" *Adv. Poly. Sci.,***21**, 107 (1976)

- Cohen, M.,H.; Turnbull, D., J. " Molecular transport in liquids and glasses", *Chem. Phy.* , **31**, 1164 (1959)

- Demirelli,K.; Kaya, İ.; Coşkun M., "3,4-dichlorobenzyl methacrylate and ethyl methacrylate system: monomer reactivity ratios and determination of thermodynamic properties at infinite diluton by using gas chromatography," *Polymer*, **42**, 5181-5188, (2001)

- Duda, J., L., "Molecular diffusion in polymeric systems," *Pure&Appl. Chem.*, **57**, 1681-1690, (1985)

- Edwards, T.J.; Newman, J., "Effect of diffusional resistance upon gas chromatography in capillary columns", *Macromolecules*, **10**, 609, (1977)

- Engelberg, I.; Kohn, J., Physico-mechanical properties of degradable polymers used in medical applications: a comparative study," *Biomaterials*, **12**, (1993)

- Etxeberria, A.; Alfageme, J.; Uriarte, C.; Iruin J.J., "Inverse gas chromatography in the characterization of polymeric materials," *J., of Chromatography*, **607**, 227-237 (1992)

- Golay, M., J. E., In gas chromatography, Desty, D.H., Ed; Butterworths: Washington, D.C.(1958)

- Grant, D.,W., "Capillary Gas chromatography", John Wiley&Sons (1995)

- Gray , D.G.;Guillet, J.E., "Studies of diffusion in polymers by gas chromatography", *Macromolecules*, **6**, 223, (1973)

- Huang, R.,Y.,M.; Shao, G.,N.; Feng, X.; Burns., C.,M., "Measurements of partition, diffusion coefficients of solvents in polymer membranes using rectangular thin channel column inverse gas chromatography," *J. of Membrane Science*, **188**, 205-218 (2001)

- Karp, J.,M.; Shoichet, M.; Davies, J.,E., "Bone formation on two dimensional poly (D-L-lactide co glycolide) (PLGA) films and three dimensional PLGA tissue engineering scaffolds in vitro," *Wiley Periodicals, Inc.* (2002)

- Kaya, İ.; Özdemir. E., "Thermodynamic interactions and characterisation of poly(isobornyl methacrylate) by inverse gas chromatography at various temperatures," *Polymer*, **42**, 2405-2410, (1999)

- Khan, M.A., "Non-equilibrium theory of capillary columns and the effect of interfacial resistance on column efficiency", Gas chromatography, Ed. by van Swaay, Butterworths, Washington, (1962)

- Laub, R.,L., "Physicochemical applications of gas chromatography," Wiley, (1978)

- Liu, F.,I.; Kuo, J.,H.; Sung, K., C.; Hu, O.,Y.,P., "Biodegradable polymeric microspheres for nalbuphine prodrug controlled delivery: in vitro characterization and in vivo pharmacokinetic studies," *International J. of Pharmaceutics*, 23-31, (2003)

- Macris , A., "Measurement of diffusion and thermodynamic interactions in polymer-solvent systems using capillary column inverse gas chromatography", M.S. Thesis, University of Massachusetts, Amherst, MA (1979)

- Pawlisch, C.,A.; Macris, A.; Laurence, R.L., "Solute diffusion in polymers.1. the use of capillary column inverse gas chromatography," *Macromolecules*, **20**, 1564-1578, (1987)

- Rodriguez, O.; Fornasiero F.; Arce, A.; Radke, C.,J.; Praustnitz J.M., "Solubilities and diffusivities of water vapor in poly(methyl methacylate), poly(2-hydroxyethylmethacrylate), poly(N-vinyl-2-pyrrolidone) and poly(acrylonitrile)," *Polymer*,**42**, 6323-6333 (2003)

- Romdhane, I.,H.; Danner, R.,P.; Duda, J.,L., "Influence of the glass transition on solute diffusion in polymers by inverse gas chromatography," *Ind.Eng.Chem.Res*., **34**, 2833-2840, (1995)

- Romdhane, I.H., "Polymer solvent interactions by inverse gas chromatography," M.S. Thesis Pennsylvania State University (1990)

- Schreiber, H., P.; Lloyd. D., R.; "Overwiew of inverse gas chromatography," *American Chemical Society*, (1989)

- Skoog, D.,A., "Principles of gas chromatography" Saunders College Publishing," (1991)

- Surana, R.,K.; Danner, R.,P.; Tıhmınlıoğlu F.; Duda, J.L., "Evaluation of inverse gas chromatography for prediction and measurement of diffusion coefficients," *J.,Poly., Sci., Part B.*, **35**, (1997)

- Tıhmınlıoğlu, F., " Finite concentration applications for inverse gas chromatography in polymer solvent systems" Ph. D. Pennsylvania State University (1998)

- Tıhmınlıoğlu, F.; Surana, R.,K.; Danner, R.D.; Duda, J.,L., "Finite concentration inverse gas chromatography: diffusion and partition measurements," *J. of Poly. Sci. Part B.*, **35**, (1997)

- Tonge, M.,P.; Gilbert, R.,G., "Testing free volume theory for penerrant diffusion in rubbery polymers," *Polymer*, **42**, 1393-1405, (2001)

- Tyagi, O.S.; Deshpande, D.,D., "Thermodynamic studies on poly(n-butyl methcrylate)- solute systems using gas chromatography," *Polymer Journal*, **19**. 1231-1239 (1987)

- Vrentas, J., S.; Vrentas, C.,M., "Predictive methods for self diffusion and mutual diffusion coefficients in polymer solvent systems", *Eur. Poly. J.*, **34**, 797, (1998)

- Zhao, L.; Choi, P., "Determination of solvent independent polymer-polymer interaction parameter by an improved inverse gas chromatographic approach," *Polymer* **42**, 1075-1081, (2001)

APPENDIX A

RAW DATA

Table A.1. Saturation Pressure (P_1) of solvents for PMMA co BMA

	P_1 sat (atm)			
Solutes	423 K	443 K	453 K	473 K
methanol	2.78	4.39	5.43	8.09
ethanol	9.62	15.55	19.41	29.25
1-propanol	8.43	13.61	16.95	25.38
1-butanol	3.78	6.28	7.91	12.09
methyl acetate	11.33	16.53	19.72	27.55
ethyl acetate	6.78	10.13	12.21	17.33
propyl acetate	3.61	5.58	6.82	9.95
dichloromethane	15.64	22.10	26.01	35.44
trichloromethane	9.19	13.32	15.85	22.01
acetone	11.33	16.50	19.67	27.35
MMA	3.39	5.14	6.23	8.97
BMA	0.69	1.20	1.55	2.47

Table A.2. Second Virial Coefficient (B_{11}) of solvents for PMMA co BMA

	$B_{11}(cm^3/mol)$			
Solutes	423 K	443 K	453 K	473 K
methanol	-258.82	-236.88	-227.60	-211.73
ethanol	-357.58	-324.46	-310.47	-286.59
1-propanol	-483.50	-436.34	-416.44	-382.52
1-butanol	-652.84	-585.83	-557.60	-509.52
methyl acetate	-378.89	-356.94	-347.58	-331.45
ethyl acetate	-512.69	-478.50	-463.98	-439.03
propyl acetate	-686.74	-633.90	-611.53	-573.24
dichloromethane	-278.81	-267.24	-262.26	-253.59
trichloromethane	-349.40	-331.78	-324.24	-311.20
acetone	-380.69	-359.60	-350.59	-335.06
MMA	-634.39	-589.12	-569.93	-537.03
BMA	-1339.14	-1201.31	-1143.29	-1044.56

Table A.3. Molar Volume (V_1) of solvents for PMMA co BMA

	V_1(cm^3/mol)			
Solutes	423 K	443 K	453 K	473 K
methanol	49.79	52.42	54.02	58.17
ethanol	69.49	72.93	75.02	80.40
1-propanol	94.82	100.09	103.34	111.96
1-butanol	109.46	113.58	115.93	121.47
methyl acetate	101.04	107.26	111.10	121.31
ethyl acetate	122.32	128.75	132.56	142.00
propyl acetate	140.05	146.10	149.55	157.62
dichloromethane	81.89	86.90	89.96	97.92
trichloromethane	98.29	102.90	105.57	111.98
acetone	94.58	100.54	104.19	113.76
MMA	128.90	134.20	137.18	143.96
BMA	184.50	189.93	192.88	199.33

Table A.4. Heat of Vaporization (H_v) of solvents for PMMA co BMA

	H_v (J/kmol)			
Solutes	423 K	443 K	453 K	473 K
methanol	27564348	25116357	23722125	20407006
ethanol	31798728	29252313	27795922	24316776
1-propanol	34473493	31754485	30260637	26925349
1-butanol	37755896	34931949	33432397	30215310
methyl acetate	23126166	20909545	19632149	16528242
ethyl acetate	26128121	23985666	22789323	20035534
propyl acetate	29898323	27879662	26785410	24375624
dichloromethane	20300783	18242792	17075188	14307694
trichloromethane	23984119	22372925	21483071	19472389
acetone	23038600	20814066	19505495	16291008
MMA	30209644	28323362	27311949	25117347
BMA	40926549	39226276	38331950	36439853

Table A.5. Thermodynamic data of water for PMMA co BMA

	P_1 sat (atm)	$B_{11}(cm^3/mol)$	$V_1(cm^3/mol)$	H_v (J/kmol)
383 K	1.41	-211.40	18.57	40327315
403 K	2.65	-185.23	18.70	39312637
423 K	4.67	-164.87	18.84	38209578
443 K	7.78	-148.80	19.00	37005892

Table A.6. Saturation Pressure (P_1)of solvents for PLGA

	P_1 sat (atm)			
Solutes	353 K	363 K	373 K	393 K
acetone	2.12	2.81	3.67	5.98
dichloromethane	3.42	4.42	5.63	8.75
trichloromethane	1.78	2.34	3.04	4.91
ethyl acetate	1.09	1.49	2.00	3.41
ethyl alcohol	1.06	1.55	2.20	4.19
THF	1.54	2.04	2.67	4.35
water	0.47	0.69	0.99	1.95

Table A.7. Second Virial Coefficient (B_{11}) of solvents for PLGA

	$B_{11}(cm^3/mol)$			
Solutes	353 K	363 K	373 K	393 K
acetone	-509.37	-483.22	-460.37	-422.64
dichloromethane	-347.68	-333.83	-321.69	-301.51
trichloromethane	-456.37	-434.69	-415.72	-384.37
ethyl acetate	-724.01	-680.83	-643.18	-581.20
ethyl alcohol	-565.54	-522.77	-485.55	-424.53
THF	-494.00	-469.93	-448.89	-414.11
water	-266.46	-245.50	-227.29	-197.48

Table A.8. Molar Volume (V_1) of solvents for PLGA

	$V_1(cm^3/mol)$			
Solutes	353 K	363 K	373 K	393 K
acetone	80.90	82.43	84.07	87.74
dichloromethane	70.34	71.63	73.02	76.12
trichloromethane	86.78	88.12	89.55	92.68
ethyl acetate	106.82	108.60	110.50	114.68
ethyl alcohol	61.49	62.39	63.36	65.50
THF	88.08	89.39	90.78	93.82
water	18.39	18.45	18.51	18.63

Table A.9. Heat of Vaporization (H_v) of solvents for PLGA

	H_v(J/kmol)			
Solutes	353 K	363 K	373 K	393 K
acetone	28445350	27821620	27159706	25697514
dichloromethane	25847804	25160992	24445986	22917285
trichloromethane	28493957	27927087	27338834	26089014
ethyl acetate	32029930	31292887	30526979	28895274
ethyl alcohol	38522132	37700738	36842351	34995736
THF	29355706	28731929	28086293	26720492
water	41706175	41264098	40804845	39830332

APPENDIX B
ERROR ANALYSIS

Table B.1. Error Analysis of V_g for PMMA co BMA

	Standard deviation			
Solutes	423 K	443 K	453 K	473 K
methanol	0.07	0.03	0.06	0.03
ethanol	0.09	0.08	0.04	0.05
1-propanol	0.14	0.09	0.07	0.06
1-butanol	0.43	0.18	0.06	0.08
methyl acetate	0.09	0.08	0.01	0.02
ethyl acetate	0.17	0.06	0.03	0.09
propyl acetate	0.29	0.07	0.18	0.06
dichloromethane	0.23	0.07	0.11	0.03
trichloromethane	0.38	0.58	0.11	0.12
acetone	0.29	0.05	0.07	0.05
MMA	0.40	0.13	0.08	0.02
BMA	0.88	0.80	0.29	0.12

Table B.2. Error Analysis of K for PMMA co BMA

	Standard deviation			
Solutes	423 K	443 K	453 K	473 K
methanol	0.07	0.03	0.09	0.06
ethanol	0.29	0.12	0.09	0.08
1-propanol	0.24	0.06	0.17	0.14
1-butanol	0.24	0.07	0.09	0.16
methyl acetate	0.08	0.08	0.02	0.19
ethyl acetate	0.61	0.21	0.06	0.06
propyl acetate	0.24	0.13	0.36	0.04
dichloromethane	0.26	0.18	0.17	0.04
trichloromethane	0.93	0.30	0.14	0.37
acetone	0.47	0.18	0.13	0.04
MMA	0.52	0.24	0.08	0.03
BMA	2.19	0.43	0.23	0.19

Table B.3. Error Analysis of water of V_g & K for PLGA

	Standard deviation	
	V_g	K
383 K	0.07	0.08
403 K	0.05	0.12
423 K	0.02	0.28
443 K	0.04	0.04

Table B.4. Error Analysis of V_g for PLGA

	Standard deviation			
Solutes	353 K	363 K	373 K	393 K
acetone	0.49	0.23	0.05	0.21
dichloromethane	0.32	0.06	0.56	0.16
trichloromethane	0.46	0.34	0.04	0.05
ethyl acetate	0.14	0.15	0.87	0.17
ethyl alcohol	0.05	0.18	0.46	0.11
THF	0.99	0.09	0.40	0.05
water	0.04	0.03	0.02	0.05

Table B.5. Error Analysis of K for PLGA

	Standard deviation			
Solutes	353 K	363 K	373 K	393 K
acetone	0.25	0.32	0.26	0.39
dichloromethane	0.34	0.15	0.58	0.46
trichloromethane	0.15	0.23	0.12	0.19
ethyl acetate	0.14	0.11	0.04	0.36
ethyl alcohol	0.69	0.04	0.11	0.15
THF	0.57	1.05	0.1	0.12
water	0.24	0.09	0.06	0.02